Condition Assessment of Power Transformer Winding Insulation Based on Partial Discharge Detection

by

Sally Daif

A thesis
presented to the University of Waterloo
in fulfillment of the
thesis requirement for the degree of
Doctor of Philosophy
in
Electrical and Computer Engineering

Waterloo, Ontario, Canada, 2016

AUTHOR'S DECLARATION

I hereby declare that I am the sole author of this thesis. This is a true copy of the thesis, including any required final revisions, as accepted by my examiners.

I understand that my thesis may be made electronically available to the public.

Abstract

Power transformers are important components of power systems, as their failure can result in major losses to electric utilities. Transformer windings are responsible for approximately 30% of transformer failures. A principal cause of these failures is winding insulation failure due to partial discharge (PD). When PD occurs in power transformers, the insulation system is damaged in two ways: by gases created from the oil and paper, and by degradation of its solid insulation. Solid insulation degradation is correlated with the PD apparent charge value, which is usually measured by conventional PD detectors. However, conventional PD detectors are not suitable for use in a transformer environment due to noise interference and the transformer's complex internal design. In addition to PD apparent charge, identifying the nature of the PD is essential for assessing the transformer winding insulation condition. Due to the difficulties associated with PD measurement in a transformer environment, PD severity assessment is still performed by dissolved gas analysis, which does not provide enough details about the PD's crucial characteristics and hence the transformer insulation condition. To address these shortcomings, this research develops two distinct modules: PD detection and PD severity assessment. Using the leakage current measured at the transformer neutral, the detection module determines the PD charge, PD location, and PD source type in the transformer winding insulation. The severity assessment module then uses this information to assess the transformer winding insulation condition.

In the PD detection module, the leakage current measured at the transformer neutral undergoes three modules: PD source classification, PD localization, and PD charge determination. The techniques used for PD source classification and localization are based on designing feedforward neural network classifiers using the statistical features extracted from leakage current signals, corresponding to different origins, sources or locations. The developed modules are tested on a three-phase transformer. The selection of the proper feature combination to in designing the neural networks results in better recognition of PD source type and location. In the PD charge determination module, the PD charge is calculated from the PD current injected into the transformer winding during a PD event, using both the corresponding leakage current and the winding transfer function. For the transformer under test, a bank of transfer functions from all possible locations along the winding to the transformer neutral is developed and used in the charge calculation module. The error between the measured and calculated charges is 10% or less.

In the PD severity assessment module, a fuzzy logic system maps the PD characteristics, charge and source, into a quantitative index called the partial discharge index (PDI). Based on the damage caused to the insulation system by the PD charge and source, the PDI is used to classify the transformer condition into one of five categories: normal, questionable, harmed, critical, and dangerous. This PDI can also be used in transformer health index calculations.

Acknowledgements

First of all, I would like to thank God for granting me this opportunity and giving me the strength and capabilities to finish it.

I would like to offer my sincere thanks to my supervisor, Professor Magdy Salama, whose unfailing and patient support have guided my studies to their successful completion. I have benefited greatly from his immense knowledge and experience, both professionally and personally.

I would like to thank Professor Ray Bartnikas, Dr. Ayman El-Hag, Dr. Albert Wasef, Dr. Michael Ibrahim, and Mary McPherson, for providing technical support and advice at various point of my research.

I would like to thank my thesis committee, Professor Medhat Morcos, Professor Sheshakamal Jayaram, Professor Gordon Stubley, and Dr. Ahmed Mohamed, for taking time to read my thesis and give me the benefit of their insights and thought-provoking questions.

Finally, I would like to thank my husband, my son, my brother, my sister and my cousin for their endless support and encouragement.

Dedication

To the memory of my father, Rotby, and my mother, Nadia, who devoted their lives to me;

To my husband and soulmate, Michael, who I am truly thankful to have in my life;

To my wonderful son, Timothy, who fills my life with love and joy;

To my brother, Wael, and my sister, Randa, who are like parents to me;

To my cousin, Samar, who has been my best friend all my life…

Thank you all for your love, support, encouragement, and prayers

Table of Contents

List of Figures

List of Tables

Chapter 1
Introduction

1.1 General Overview

Power transformers are integral components of transmission and distribution systems. However, they are expensive, and their outages can result in major losses for electric utilities. To avoid unnecessary costs and prevent unplanned outages, power companies generally rely on condition-based maintenance, which monitors certain operational parameters to detect transformer faults before they become failures [1].

The integrity and reliability of power transformers depend mainly on the correct operation of their insulation system, which is always electrically, mechanically, and thermally stressed [2]. A serious problem that may arise due to electrical stresses is partial discharge (PD) [3]. PD deteriorates the insulation system materials, resulting in a reduction of their dielectric strength and subsequently of the transformer's lifetime. It may even lead to a complete failure. According to IEC standard 60270, "partial discharge is a localized electrical discharge that only partially bridges the insulation system between the conductors and may or may not occur adjacent to a conductor". PD occurs in high voltage insulation systems as a consequence of a field increase in the weak portions of the insulation materials. The existence of cracks, voids, irregularities, and contamination in the insulation system increases the probability of PD [4].

Power transformer windings are responsible for approximately 30% of transformer failures, so they are the main target of this research [5]. One of the primary causes of these failures is PD. Research into several techniques for PD detection and severity assessment in power equipment using multiple electrical and non-electrical detection methods (e.g., high frequency antennas, acoustic sensors, and conventional PD detectors) has shown that not all methods are suitable for detecting PD in transformer windings or can be used in a transformer environment [6, 7]. Moreover, most research is performed using controlled experiments on transformer insulation components and not actual transformers. Therefore, the applicability of these experiments' conclusions to the evaluation of real transformers' condition is debatable.

The transformer health index (THI) is an assessment technique used to estimate the condition of the whole transformer by combining various transformer test results, including dissolved gas analysis (DGA), furfural analysis (FFA), oil quality analysis (OQA), dielectric dissipation factor, frequency

response analysis (FRA), insulation resistance, and polarization index (PI) [8]. Despite the importance of PD testing in power transformers, it is only implicitly considered in THI calculations using the dissolved gas analysis test, due to the difficulties associated with the PD detection [9].

This thesis is designed to address the shortcomings discussed above. In the present chapter, I discuss the incentives that motivated me to conduct the research and the objectives established to achieve these motivations. This chapter also describes the organization of the thesis chapters.

1.2 Research Motivation

Partial discharge continuously degrades transformer winding insulation systems, and without detection and treatment ultimately leads to catastrophic failures. Historically, monitoring PD in transformers has been very limited since utilities depend mainly on DGA tests. DGA is an offline technique that does not provide any details about PD type, location, apparent charge, or severity. The availability of these details may assist in the detection of up to 21% of transformer vessel problems and up to 14% of high voltage bushings problems [10]. Therefore, the main motivation for this thesis is the need for reliable online PD detection and severity assessment modules for transformer winding insulation. The aim is to provide a solid understanding of the PD phenomena inside winding insulation systems and help determine optimum maintenance solutions. Hopefully, this knowledge base will lead to better transformer designs that avoid or reduce PD.

When PD occurs in power transformers, the insulation system is damaged in two ways: by gases created from the oil and paper, and by degradation of the solid insulation [11]. The amount of gas generated in the oil is investigated by the DGA test. The erosion of the solid insulation resulting from the treeing or tracking of paper requires visual inspection of the solid insulation, which is not possible. However, the solid insulation degradation is related directly to the PD apparent charge value. Conventional PD detectors are usually used for measuring the PD apparent charge, as in IEC 60270, but they are not convenient in a transformer environment due to noise interference and the heavy weight of the equipment [6, 7]. A few studies ([12, 13]) have attempted to relate PD charge to other sensor outputs, but these investigations mostly use the terminal PD signal received by the sensor and are greatly affected, attenuated, and suppressed by the propagation path from the PD location to the measuring terminals. Another motivation for this research is to develop a technique for measuring the internal PD charge injected into the winding during the PD event. The PD charge determination technique depends mainly on modeling the transformer windings by transfer functions. The PD

current and charge injected into the transformer winding during the PD event can be calculated using these transfer functions and the leakage current measured at the transformer neutral.

Power transformer winding insulation has a very complex structure that may contain multiple PD sources that degrade the transformer insulation system in different ways. Hence, identifying the PD source is important for evaluating the insulation system's condition. Thus, another motivation for this research is to develop a PD source identification module for the transformer winding insulation system.

For years, researchers have relied on the PD apparent charge to evaluate the destructive effects of PD inside a power transformer. A threshold of 500 pC is suggested by the IEC standard as an acceptable criterion for PD detected in a power transformer, but the techniques for choosing this number are not clearly stated [14]. Therefore, multiple studies have comprehensively investigated the effects of different PD sources with various PD charge ranges on the transformer insulation components, using controlled experiments outside the transformer [11, 14]. However, because the relationship between these experiments and the actual transformer insulation condition is unclear, the PD charge thresholds suggested by these studies cannot be used to assess the transformer insulation condition. Yet another motivation for this thesis is to develop a PD severity assessment module based on the comprehensive studies of PD's damaging effects on the insulation system and to use the output of this assessment module to evaluate the transformer condition directly. Instead of relying solely on the PD charge in the transformer condition assessment, the PD source is also considered in the severity assessment module. The output of this module is a numeric index that is used to classify the transform condition based on the PD features. Additionally, this index can be used in the transformer health index calculations.

Simultaneous measurement of multiple PD characteristics requires different equipment and methods, making such measurements complicated, expensive and time-consuming; in some cases, they are not even possible. These difficulties motivated me to design an easy on-line PD detection and severity assessment modules that require only one PD signal. In the transformer manufacturing company, these PD modules can be developed and a microcontroller can be programmed with these modules and integrated with the transformer. This microcontroller will only need the leakage current measured at the transformer neutral and will produce multiple PD details, such as the PD charge, source, and location. This microcontroller will also enable power transformer winding condition

assessment based on PD activity; and ultimately provide easy, reliable, inexpensive and fast PD detection and severity assessment.

1.3 Research Objectives

There are two main goals for this research: designing and developing PD detections module and a condition assessment technique based on PD for transformer winding insulation. Various objectives to achieve each goal are summarized in the following sections.

1.3.1 Objectives for PD Detection Modules

The PD detection module has three different modules: PD source classification, PD localization, and PD charge determination. These three modules are developed using the following steps:

1.3.1.1 PD Source Classification and Localization Modules

- Design experiments for injecting different PD sources into tap locations of the transformer windings and measuring the related output signals.
- Design neural network classifiers that are trained and tested by the statistical features extracted from the measured signals.

1.3.1.2 PD Charge Determination Module

- Design experiments to measure the winding frequency response from each tap of the transformer winding to the neutral.
- Calculate transfer functions corresponding to each frequency response.
- Perform PD charge calculations using the transfer function and leakage current.
- Verify results by injecting different PD signals with measured charge levels. Then, the PD charges of these signals are calculated using the developed module and compared to their measured values.

1.3.2 Objectives for Transformer Winding Condition Assessment

Transformer winding condition assessment based on PD characteristics has two main steps: developing the PD severity assessment module (partial discharge index (PDI)) and power transformer winding condition evaluation based on the PDI. These steps are addressed using the following steps:

- Designing a fuzzy logic system to calculate the PDI;

- Developing a correlation between the PDI values and the transformer winding insulation condition.

1.4 Thesis organization

This thesis has seven chapters. The remaining six chapters are organized as follows:

- Chapter 2 reviews the literature of transformer maintenance plans, failure modes, different tests, and health condition assessment techniques such as the power transformer health index. Methods for calculating the transformer health index reported in the literature are also discussed in this chapter. A brief overview of PD types, detection methods, and signal processing approaches is provided as well.
- Chapter 3 discusses the research gaps that motivated me to conduct this research. The philosophy behind choosing certain detection, pattern recognition, and modeling techniques is explained in this chapter, and an overview of the entire thesis is given at the end.
- Chapter 4 describes the PD detection and pattern recognition modules, source classification, and localization. Detailed explanations are provided for laboratory experiments, signal processing, and classifier training and testing.
- Chapter 5 develops a module for determining the PD charge in a transformer winding insulation using the leakage current and winding transfer function. This chapter thoroughly explains the experiments conducted to measure the winding frequency response, calculates the corresponding winding transfer functions, and computes the PD charge using these calculated transfer functions and leakage currents measured at transformer neutral.
- Chapter 6 introduces PD severity assessment inside transformer winding insulation via calculating the PDI, using a Mamdani fuzzy logic system. Steps for constructing the fuzzy variables' MFs and rules are described in detail. The transformer winding insulation classification is developed based on this PDI.
- Chapter 7 highlights the conclusions and contributions of the thesis, and offers suggestions for future research directions.

1.5 Summary

In this chapter, I have presented a general overview of PD severity effects on transformer insulation systems and the complications and the shortcomings associated with the present PD detection and assessment techniques. Research motivations, objectives, and thesis organization were also presented.

Chapter 2
Literature Review

2.1 Introduction

Power transformers are considered among the most significant and expensive components in power grids. Failures and forced outages of transformers cause electric utilities and their customers huge losses, so transformer defects need to be detected and treated in order to avoid these failures. In this chapter, transformer failure analysis is presented to highlight transformer windings, which is the component most likely to contribute to transformer failures. Various transformer maintenance plans are discussed, including condition-based maintenance, which depends on applying proper maintenance actions based on monitoring certain transformer operational parameters and diagnostic tests. PD detection in transformer winding insulation is the primary focus of this research; therefore, different insulation condition monitoring diagnostic tests are presented here as well. Comprehensive details about PD-specific phenomena, such as PD types, PD detection techniques, and power transformer condition assessment by the transformer health index (THI) is discussed.

2.2 Transformer Failure Types

Transformer failure means that the transformer is no longer able to perform its function. This failure can be a failure with forced outage that causes transformer immediate removal from service, a failure with scheduled time outages decided by the operator, or defects that be treated without taking the transformer out of service [15]. Although various root causes in the design, manufacturing process, or operation of the transformer can cause the transformer components to fail (Table 2.1) [16], transformers are most likely to fail due to their insulation system breakdown [17]. Power transformer insulation systems are constantly exposed to various stresses, such as:

- Electrical stresses caused by transient or sustained over-voltages, lightning or switching surges, PD caused by defects due to poor design , contaminations or excessive moisture content [17].
- Mechanical stresses caused by the vibration during normal operation or the force during a fault condition, resulting in winding deformation and hence reduction of the electrical clearance, which can eventually breakdown the insulation electrically [17].

- Thermal stresses caused by extended periods of transformer overloading, failure of the cooling system, or excessive ambient temperature, resulting in cellulose degradation until it fails under the mechanical and electrical stresses [17].

Different components of transformers have different deterioration and failure rates. Figure 2.1 shows the failure analysis of transformers, as reported by CIGRE [18]. Other transformer failure surveys are reported in [19]. If the load tap changer and the bushings are considered independent components, transformer windings make the highest contribution to transformer failures by percentage [18].

With proper transformer maintenance, these failure causes can be detected and treated before they become failures, resulting in better transformer performance and longer life.

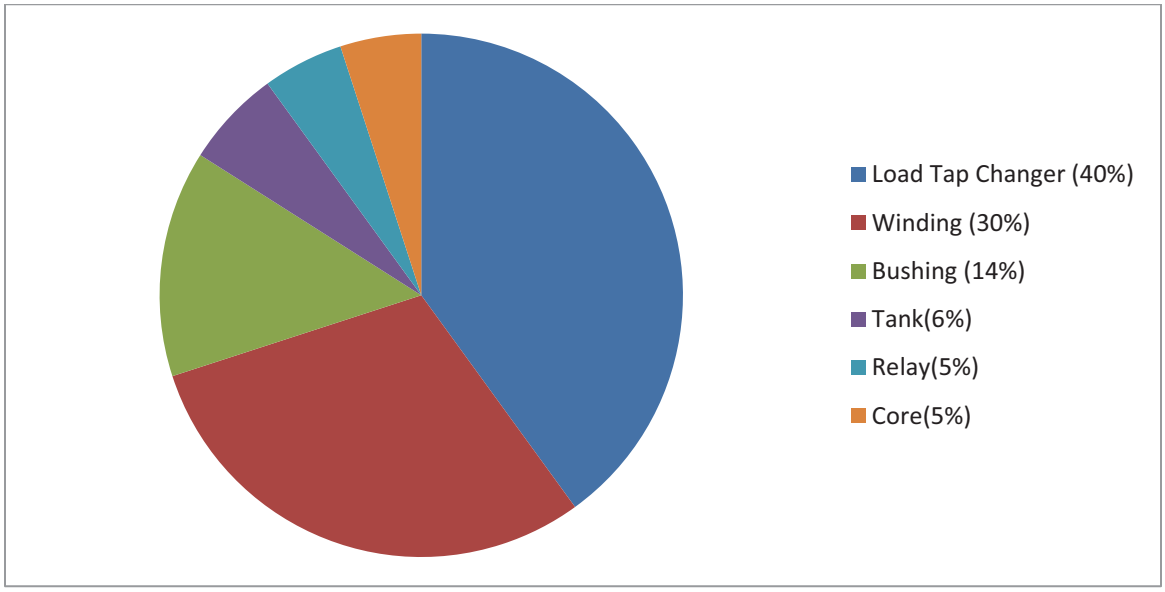

Figure 2.1: Transformer failure as reported by CIGRE [2]

Table 2.1: Transformer failure modes and causes [16]

Component	Function	Failure mode	Failure Event	Failure Causes
Core	Carry magnetic flux	Loss of the transformer's efficiency	Mechanical fault	• DC-magnetism • displacement of the core steel during the construction
Winding	Carry current	Short circuit	Mechanical damage	• Poor design • Transient overvoltage • Movement of the winding
			Insulation breakdown	• Insulation material contamination • Excessive water • Winding deformation • Hot spot
Tank	Contain and protect the transformer materials	Leakage	Tank damage	• Mechanical due bad handling or high pressure by excessive gas generation • Material corrosion
Bushings	Connect the transformer winding to the power system and isolate the winding from the tank	Short Circuit	Insulation damage	• Contamination • Water penetration • Cracks • Bad handling
Tap Changer	Change the voltage level	No voltage regulation	Mechanical	Corrosion

2.3 Power Transformer Maintenance Plans

Power transformers usually remain in service for 25 to 30 years, but suitable maintenance can extend a transformer's life to 60 years [17]. Transformer maintenance plans can be categorized into three types: corrective, preventive, and reliability-centered (Figure 2.2).

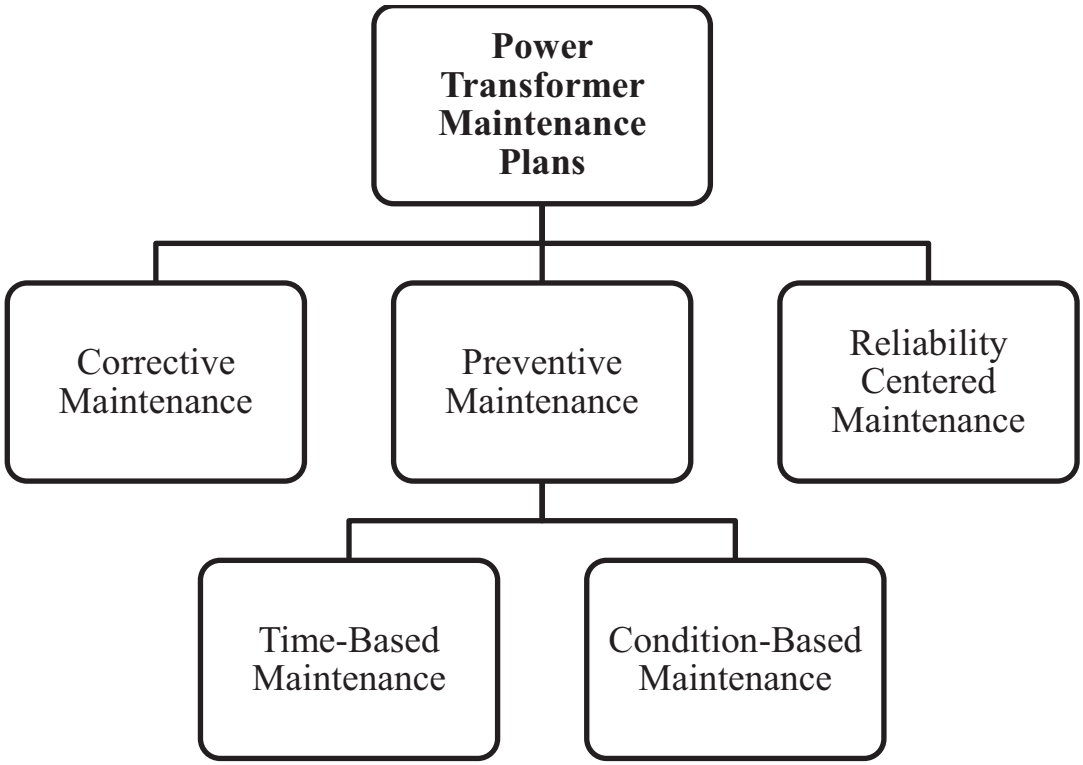

Figure 2.2: Transformer maintenance plans

- Corrective maintenance programs

Corrective maintenance programs are employed after a failure occurs and thus are applied only to certain transformer accessories defects that do not have important impacts on the system. Although corrective maintenance programs are less expensive than other methods and save manpower, they cannot be used as primary maintenance programs for transformers, as some defects may be irreparable or lead to a complete shutdown [17].

- Preventive maintenance programs

Preventive maintenance programs are mainly used to prevent failures and are classified into two categories: time-based and condition-based. Time-based preventive maintenance is applied at regularly scheduled time intervals, regardless of transformer condition. The length of the interval is

crucially important: if it is too long, unexpected events may occur and cause problems; if it is too short, unnecessary outages may occur and result in a waste of manpower, time, and costs [17].

Condition-based preventive maintenance depends on detecting faults before they become failures by monitoring certain parameters in a transformer. These parameters are determined based on a transformer's past history, including working factors, diagnostic test results, and external conditions. Although this method does sometimes save money and manpower, it can be expensive when monitoring a large number of parameters [17].

- Reliability -centered maintenance

The aim of reliability-centered maintenance is to maintain transformer operation at a reasonable cost by optimizing maintenance based on risk analysis, which is performed by classifying the failure modes of the transformers based on their impact on the system. This form of maintenance requires the availability of huge amounts of transformer information and system data [20].

Previously, time-based preventive maintenance was applied to transformers. However, due to the necessity of reducing maintenance costs, the time-based approach was replaced by condition-based preventive maintenance, which depends on transformer condition monitoring [17].

2.4 Transformer Condition Monitoring

Transformer condition assessment is essential for providing transformers with appropriate maintenance actions and thereby preventing their failure. The form of assessment depends on monitoring the parameters that initiate thermal, mechanical, environmental, and electrical transformer aging [21].

The proper operation of transformers depends mainly on the correct operation of their insulation systems [2]. The main diagnostic tests used for monitoring the condition of transformer insulation are presented in this section, including the PD test, which is the main focus of this thesis.

2.4.1 Dissolved Gas Analysis

The dissolved gas analysis (DGA) technique is extensively employed for fault detection in power transformers. Approximately one million DGA are carried out annually by more than four hundred laboratories around the world [22]. DGA is based on detecting certain soluble gas components in oil, resulting from insulation oil and paper degradation, and hence warns about certain corresponding problems [23]. Determining the amount of gases (e.g., hydrogen, methane, acetylene, ethylene,

ethane, carbon monoxide and carbon dioxide) in the insulating oil can effectively and reliably help detect faults such as PD, thermal heating, and arcing [24]. Multiple techniques, including the Doernenburg Ratio, Roger's Ratio, Key Gas and Duval Triangle, are applied to interpret transformer faults from the measured dissolved gases [24]. In each of these techniques, concentrations of the stated combustible gases or relations between certain gas concentrations are compared to the threshold values that correspond to a healthy transformer [25].

2.4.2 Degree of Polymerization (DP)

The life of a transformer relies on its solid insulation life, paper, pressboard [26]. Insulation papers are sheets manufactured from wood pulp that contains 90% cellulose, 6-7% lignin, 3-4% hemicelluloses, small amounts of metallic particles, and absorbed water. The average number of glucose monomer elements in the cellulose is called the degree of polymerization (DP), and the DP of papers in new transformers ranges between 1000 and 1500. During their service lifetime, insulation papers degrade and their DP decreases [24]. DP can be used as an indication of a transformer's end of life, since a DP less than 200 implies that the paper tensile strength is halved [27]. Unfortunately, DP testing is destructive, as it requires an insulation paper sample from the transformer, thus damaging the insulation [20]. For this reason, DP testing is generally avoided in favor of furan testing.

2.4.3 Furan Analysis

Although insulation paper degradation cannot be measured by direct inspection, it can be assessed by measuring its deterioration by-products. Under high temperatures and in the existence of oxygen, acid and moisture, insulation papers degrade, producing glucose or degraded products of glucose. These, in turn, deteriorate, producing furan products, water, and gases. In furan testing, the oil is sampled and the amounts of soluble furan products are investigated. There are multiple furan products, including 2-furaldehyde, 5-methyl-2-furaldehyde, 5-hydroxymethyl-2-furaldehyde, 2-acetyl furan, and 2-furfurol, but the dominant component of furan products is 2-furaldehyde (2FAL). Furan analysis has gained significant attention since its introduction 20 years ago, as it can be used as an indication of the condition of transformer solid insulation [28]. The direct relationship between furan products and DP has been thoroughly investigated [29, 30]. In ASTM D5837 and IEC 61198, an oil sample is analyzed using one of three methods. Each method describes a relationship between DP and furan products, and compares the furan by-product levels to known threshold level values.

2.4.4 Insulation Power Factor

Insulation power factor, or dissipation factor, testing provides a strong indication of the losses in transformer insulation materials [8]. Insulation materials can be represented by a capacitance in parallel with a resistance, as a simulation of the ideal insulation behavior and electrical losses, respectively (Figure 2.3). The ratio of the resistive current to the capacitive current (tan δ) is called the dissipation factor, whereas, the ratio of the resistive current to the total leakage current (cos ϕ) is the insulation power factor [17]. Good insulation materials have very low resistive current, and hence, the dissipation factor and power factor have the same values, which should be very low. Transformer arm or shearing bridges are usually used to measure power factor of the between the [31]:

- high voltage winding and ground,
- high voltage and low voltage windings,
- high voltage and tertiary voltage windings,
- low voltage and ground ,
- low voltage and tertiary voltage windings, and
- tertiary voltage winding to ground [31].

According to [17], a good insulation power factor should be less than 1%; a questionable insulation power factor is between 1-2 %; an action should be taken if the insulation power factor exceeds 2%.

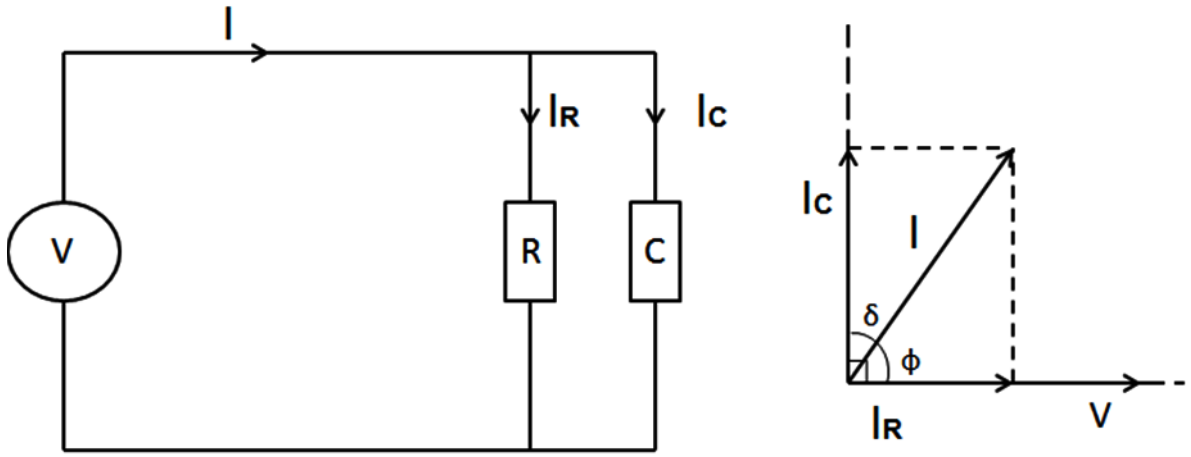

Figure 2.3: Insulation material modeling and the corresponding phasor diagram

2.4.5 Water Content

Increased water content in power transformers results in increased insulation conductivity, which can lead to several problems. Water in transformer insulation systems reduces PD inception voltage and may even form bubbles, thus deteriorating the insulation system and increasing the transformer aging rate [24]. In [32], the researchers concluded that the transformer thermal aging rate is directly proportional to the insulation water content, such that when the water content is doubled, the mechanical strength of the transformer solid insulation is halved. Several methods are reported in the literature for measuring the dissolved or non-dissolved water content in transformers, the most common of which is the Karl Fischer method, as explained in ASTM D1744. In Karl Fischer methods, Volumetric Method or Coulometric Method, a reagent of known concertation is added to the insulating oil to react with the water content, resulting in a non-conductive chemical material. Water content determination using Volumetric Method or Coulometric Method depends on the determination of the quantities of the added reagent or the current required converting the water into the non-conductive chemical material, respectively. According to IEC 60814, the limit of the water content in transformer oil is 25ppm [33].

2.4.6 Acidity

Acids are formed in transformer oil either internally by oxidation or externally by contamination. Increased acid content hastens the rate of insulation degradation, especially in the presence of water, as together they can cause iron rusting. The acidity problem should be treated because otherwise sludge is formed. Oil acidity is represented by a number that expresses the number of milligrams of potassium hydroxide (KOH) in the oil. For safe oil acidity levels, the acidity number should not exceed 0.25mg KOH/g. Various methods can be used to interpret the acidity level in the insulating oil, as stated in ASTM D1902, ASTM D 1534, and IEC 296 [34].

2.4.7 Partial Discharge

According to IEC standard 60270 [35], "Partial discharge is a localized electrical discharge that only partially bridges the insulation system between the conductors and may or may not occur adjacent to a conductor." PD occurs in high voltage insulation systems as a result of field enhancement in weak zones in the insulation materials, such as fractures, bubbles, irregularities, and contaminations [4].

PD constantly degrades the insulation systems, influencing their dielectric strength and may eventually lead to their breakdown [4]. Oil-filled power transformers have immensely complex

insulation structures that can experience various PD defects, such as internal discharges, surface discharges, coronas, and electrical trees [4]. This section presents a brief overview of PD types and their detection techniques inside transformer insulation.

2.4.7.1 Types of Partial Discharge

Various PD may occur in the transformer insulation system, including internal, surface, and PD due to sharp edges and floating particles [36]. Internal PD occurs at the location of insulation system contaminations, such as gas voids, papers, textile fibers, and other particles, which are created during the manufacturing process or normal transformer operation. The dielectric strength of these contaminants is less than that of the surrounding insulating substance, resulting in electric field localized enhancement [4], which depends on the contaminant type, dimensions, and shape. If this localized enhanced field exceeds the withstand electric field of the contaminant, a localized breakdown, PD, occurs. After a PD, the voltage builds up again and the process is repeated, as in the case of a gas void. Multiple discharges release heat that carbonizes the surrounding material insulations, reducing its thickness. The remaining insulation material will be electrically and mechanically over-stressed, increasing the probability of more discharges that potentially lead to a complete breakdown [37].

At weak locations (e.g., irregularities and cracks) of the insulation surface, the tangential electric field is enhanced, causing ionization of the surroundings and resulting in discharge. The presence of contamination and moisture increases the probability of this process. Repeated discharges create lower-resistance tracks in which leakage currents flow, dehumidifying the surface and forming tiny islands. The ‘islands’ stop the flow of leakage currents, resulting in discharge due to the concentration of the voltage drop across the formations. These discharges burn the insulation surface, producing conductive carbonized tracks that become the new weak points on the insulation surface, thereby guaranteeing surface discharge continuity until the whole surface is bridged [37].

Around high voltage conductors in gases or fluids, especially around sharp edges, the electric field enhancement and distortion cause PDs [38]. These PDs cause power loss, insulation deterioration, and toxic by-products. Their polarity can be either positive or negative based on the polarity of the high voltage conductor [39]. Researchers in [38] use a point-plane electrode arrangement to study positive and negative PDs around sharp edges. In both types, the electric field is enhanced around the sharp-point high voltage electrode, accelerating the surrounding free electrons, which then start an avalanche process. In positive PD, the free electrons are attracted to the electrode and the positive

ions are repelled. Thus, the density of the free electrons in a positive PD is less than that of a negative one. The production of secondary electrons in the positive PD is mainly dependent on the photon emission that results from recombination processes and liberates electrons from the fluid. In a negative PD, the free electrons are repelled from the active electrode and the positive ions are attracted to it. The secondary process depends on the photoelectric effects that cause electron emissions from the electrode surface.

2.4.7.2 PD Detection Methods

PD effects, such as gases (ozone and nitrogen), light, heat, and electromagnetic and mechanical waves, can be detected using electrical and non-electrical methods [40]. Electrical PD detection methods, including conventional PD detectors, radio frequency (RF) antennas and high frequency current transformers (HFCTs), are used to measure electrical PD pulses [40]. The conventional PD detection method is described in IEC 60270 [35]. In [35], different circuit configurations are employed to detect multiple PD features, such as the apparent charge, pulse repetition rate, pulse repetition frequency, phase angle, time of occurrence within the voltage cycle, inception voltage, and extinction voltage. The components common in all configurations are the coupling capacitor, measuring system, high voltage supply, data storage oscilloscope, and connections. Due to the weight of the equipment and background noise sensitivity, the use of conventional PD detectors in transformer environments may not be appropriate [6, 7]. HFCTs are ring-shaped ferrite core current transformers whose frequencies range from a few tens of kilohertz to several hundreds of megahertz [41]. HFCTs are lightweight, portable, and low-cost devices. However, when the rise time of PD current is very short, multiple HFCTs may be required [41, 42]. RF antennas are used to detect electromagnetic waves emitted from a PD source. Due to a transformer's complex structure, PD electromagnetic waves attenuate and take more time to migrate from the PD source to the RF antennas, so an RF antenna array may be required [43].

Acoustic sensors are used to detect the mechanical waves resulting from this explosion, converting the waves into electrical signals [44]. Such sensors are inexpensive and immune to electric interference, and thus are suitable for PD detection in a transformer environment [45]. However, due to a transformer's structural complexity, the acoustic PD signals are attenuated, necessitating the use of amplifiers.

2.5 Power Transformer Condition Assessments

The objective of performing condition assessments is to provide transformers with the maintenance needed to prevent failures and unwanted outages [46]. Transformer condition is assessed based on multiple factors, such as diagnostic test results, operation and maintenance history, transformer age, and environmental condition. The transformer health index (THI) is a technique used to assess transformer condition by combining multiple operational transformer factors and providing a quantitative value that represents the condition.

The THI calculation is a multi-step process that includes determining, scoring, and weighting a transformer's operational factors, and then combining them into one quantitative value. In [8], multiple test result parameters, such as the DGA, furfural analysis, oil quality, and power factor, plus operational loading and maintenance data are used in the THI calculation. For each parameter, a score from zero to four is given based on the parameter's test analysis or condition, with zero representing a very poor condition and four representing a good one. The weights for the parameters related to the transformer and tap changer are 40% and 60%, respectively. The THI is calculated by adding the normalized weighted scores.

In [47], the parameters are classified into two tiers. The first-tier parameters are the oil quality analysis, DGA and furfural analysis, power factor and excitation current tests, along with load and maintenance history, and transformer in-service age. The second tier parameters are the turns-ratio test and frequency response analysis (FRA). Scores and weights are given to each parameter and the weighted scores of each tier are then summed. The THI is computed by subtracting the results of tier two from those of tier one. The THI ranges between ten and zero, with ten representing a good condition and zero representing a poor one.

Artificial intelligence techniques are also used to calculate the THI. In [1], a feed-forward neural network with four hidden layers is used to calculate the THI for real working transformers. The input variables to the neural networks are the available test results, and the output is the THI. The THI ranges from zero to one, corresponding to a new transformer condition and a very poor transformer condition, respectively. In [48], a Mamdani fuzzy logic system is used to calculate the THI for transformers under 69 kV. The inputs to the fuzzy logic system are the moisture content, acidity number, oil breakdown voltage, dissipation factor, dissolved combustible gases, and 2-furfuraldehyde content. The membership function for the inputs and the THI are developed based on transformer testing standards and previous research results.

Despite the importance of PD effects on transformer health, PD test results are explicitly considered in only a few studies. In [9], transformer operational parameters are classified into three tiers. The first-tier parameters are the DGA, oil quality analysis, furan analysis, physical condition analysis, and operating performance; the second tier parameters are the measurements of turns-ratio, winding resistance, dissipation factor, excitation current, insulation resistance, and polarization index; and the third tier parameters are the frequency response analysis (FRA) and PD measurement. First, the THI is calculated using only the first tier parameters. If the transformer condition is not classified as normal, the second tier parameters are considered in the calculations. The same concept applies to the tier-three parameters. The PD is not considered an essential test, according to [49], despite being a significant indicator of solid insulation condition.

2.6 Summary

In this chapter, a survey of transformer failure analysis and various maintenance plans have been presented. One of the primary maintenance plans is the condition-based maintenance, which relies on applying proper maintenance actions based on monitoring certain transformer operational parameters and diagnostic tests. PD detection in transformer winding insulation is the main focus of this research; hence different insulation condition monitoring diagnostic tests were presented in this chapter. A comprehensive review about PD phenomena such as types, detection techniques, and signal processing was also discussed in this chapter. Assessing a transformer's condition by using the transformer health index (THI) was also presented.

Chapter 3
Power Transformer Winding Insulation Condition Assessment Based on Partial Discharge Detection

3.1 Introduction

Power transformers are critically important components of power systems, as they are expensive and their failure results in major losses to electric utilities. Transformer windings cause approximately 30% of transformer failures [5], the main cause of which is winding insulation failure due to partial discharge (PD) [50]. PD testing provides a good indication of the electrical, thermal, mechanical, and environmental aging of transformer's winding insulation. Therefore, finding effective PD detection techniques has been a subject of interest for more than 80 years [51].

In general, testing high voltage equipment for PD is usually performed for three purposes: design, quality assurance, and diagnostics. These tests are done to guarantee that PD levels are within permitted thresholds, as well as to identify the PD defect type and to ensure that equipment still has the expected lifetime. The design PD testing is performed to guarantee either that the PD levels for new transformers' designs are within the permitted values or do not exist; the quality assurance PD measurements are performed to guarantee that no PD defects were created in the transformer during manufacturing; the diagnostic tests are performed to investigate transformer insulation conditions under various stresses during operation [51].

When PD occurs, a transformer's insulation system can be damaged in two ways: by gases created from the oil and paper, and by the degradation of the systems' solid materials [11]. The amount of gas generated in the oil is investigated by the dissolved gas analysis test. The erosion of solid insulation resulting from the treeing or tracking of paper requires a visual inspection, which is not possible; however, this solid insulation degradation is directly related to the PD apparent charge value.

During complex PD events, energized electrons and ions bombard insulation surfaces, causing permanent damage. The amount of damage caused to an insulation system depends on both the number and the energy of these particles. Measuring the PD charge can indicate the number of energized particles, which can then be used to predict the damage caused to the solid insulation [52]. Conventional PD detectors are usually used, as in IEC 60270, for measuring the PD apparent charge. However, they are not suitable for a transformer environment due to noise interference and the heavy

weight of the equipment [6, 7]. Furthermore, the standardized conventional PD detection method described in IEC 60270 has a limited frequency range of up to 400 kHz. In other words, it can only detect the low frequency components of PD signals but not the high frequency components that carry important information for PD pattern recognition [52]. The conventional method depends mainly on the calibration process, which tends to be influenced by multiple factors, such as calibration charge, pulse wave shape, upper and lower cut-off frequencies, amplifier gain, and test set-up. Recalibration is thus required if one of these parameters is changed. Moreover, these parameters have a high integration error and low sensitivity if the wave shape has an increase in rise time or duration [12].

Due to the importance of measuring the PD charges and the difficulties associated with conventional PD detectors in the transformer environment, considerable research has been invested in finding the correlation between different PD sensors and the PD apparent charge. In [12], the output voltage signal (mV) of HFCT is used to calculate the PD apparent charge by calculating the transfer function of the HFCT, with the mV considered to be the sensor output and the leakage current to be the sensor input. Using the measured output and sensor transfer function, the leakage current (and hence the charge) can be calculated by integrating this PD current. Multiple attempts have also been made to correlate the output of high frequency antennas and the PD apparent charge [13, 53]. Most studies use the terminal PD signal received by the sensor at the transformer tank or neutral terminal to calculate the PD charge. However, these terminal PD signals are greatly affected, attenuated, and suppressed by the propagation path from the PD location to the detection terminals [54]. Therefore, the PD charges calculated using these signals are much lower than the original PD charge. In [54], an intensive study was conducted to investigate the attenuation caused to PD signals by the propagation path, mainly through the transformer winding. It was found that the degree of attenuation depends on multiple factors, including the PD location along the winding and the PD wave shape. Specifically, the PD signals injected at the middle and end of the winding are attenuated to a greater degree compared to those injected into other locations.

For years, researchers have relied on the PD apparent charge to evaluate PD destructive effects inside power transformers. Although the PD apparent charge is a powerful indication of the transformer insulation condition, it provides only partial information. Hence, it is essential to identify the nature of the PD in order to evaluate the transformer condition. Oil-filled power transformers have highly complex insulation structures that can have PD defects capable of causing PD phenomena such

as internal discharge, surface discharge, corona, and electrical trees. Various types of defects have different levels of severity [55].

The existing research recognizes the critical role of PD detection inside the transformer winding insulation. The main challenge is the complexity of such insulation systems. Research on PD detection inside transformer winding insulation has been mostly limited to conducting controlled PD experiments outside transformers, obtaining data from these experiments, and processing the signal data for PD pattern recognition. Because there is still a considerable level of uncertainty concerning the conclusions drawn from these controlled experiments and their applicability to real working transformers, the relationship is still unclear. For instance, the recommended PD apparent charge by the IEC 60270 standard is 500 pC, whereas the recommended PD apparent charges in are much larger. The authors in have comprehensively investigated the destructive effects of PD on different components of transformer insulation, such as oil, Kraft paper, and pressboard. These destructive effects have been expressed as the length of the carbonized track caused on insulation paper and number of papers damaged. Each one of these studies suggests ranges, with some overlap, for the PD apparent charge based on the level of damage caused to the insulation under test. Correlations between these studies and real transformer insulation structures are indeterminate.

In order to address the research gaps discussed above, the research detailed in this thesis has developed a novel module for partial detection and a module for PD severity assessment inside transformer winding insulation systems. For the same-structured transformers, by using the developed PD detection module, the PD source, location and charge can be identified. These PD characteristics are then used in the developed PD severity assessment in order to evaluate the condition of transformer winding insulation. Moreover, the severity assessment output can be used to represent the PD test in transformer health index calculations. In transformer factory, these modules can be developed for each class of transformer. A microcontroller can be programed with these modules and integrated with each transformer.

3.2 PD Detection Module

The PD detection module uses a detected PD signal from a transformer in order to determine the PD source, PD location and charge inside the transformer winding insulation (Figure 3.1). The PD localization module is also used in the PD charge calculation module, as shown in the next section.

The PD source classification and PD localization depend mainly on PD signal pattern recognition. The steps for developing both modules are introduced together in the following section.

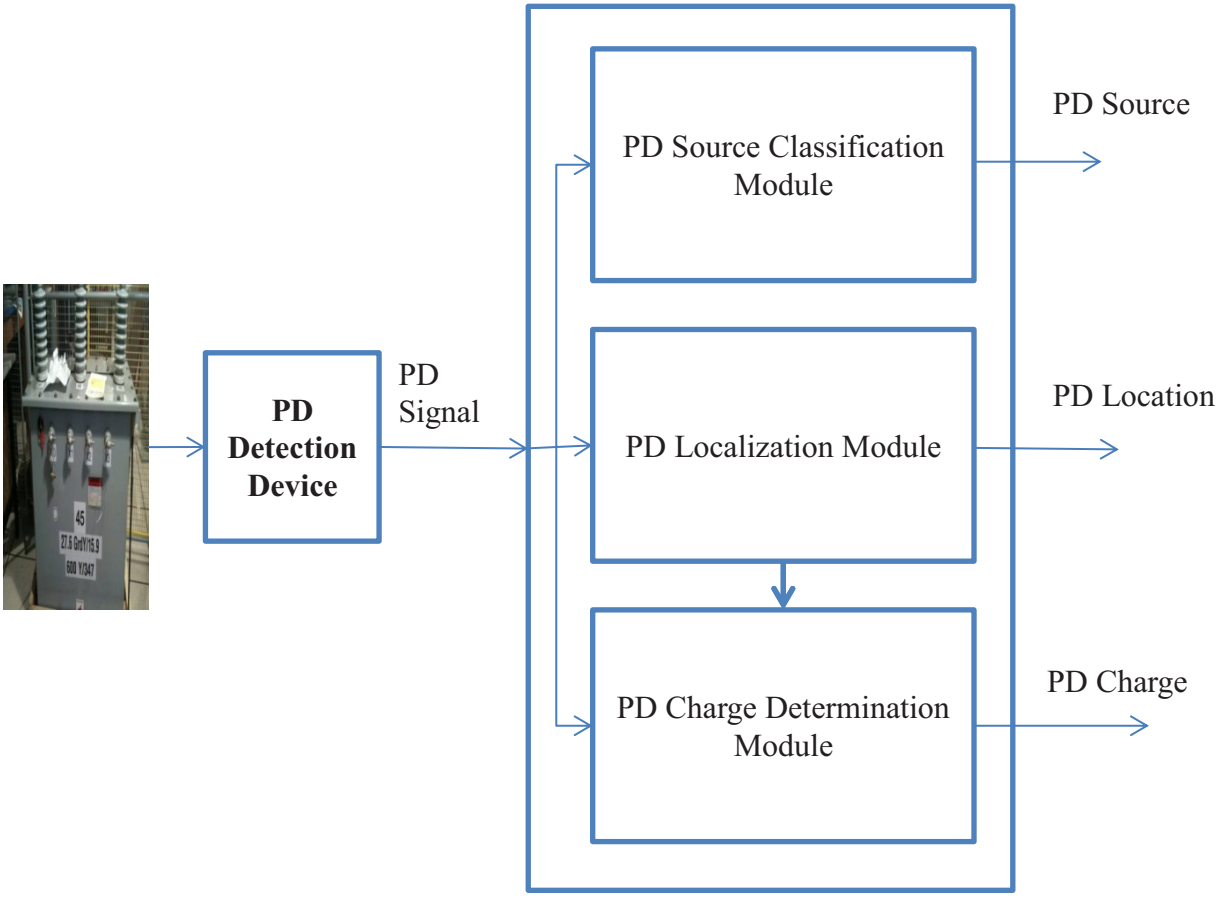

Figure 3.1: The developed PD detection module

3.2.1 PD Source Classification and Localization Modules in Power Transformer Winding

Power transformer winding insulation systems are highly complex and different PD sources may exist anywhere within the structure. Partial discharge source identification and localization in the transformer winding insulation is a cost-effective method that provides a transformer with needed maintenance to prevent catastrophic failures. However, it is a complicated task, as there is no access to the transformer winding insulation. Therefore, most PD pattern recognition techniques are based on PD signals measured at the transformer's outer parts, tank, or neutral terminals. These measured signals are attenuated and distorted by the PD propagation path through transformer materials and

background noise. The terminal-measured PD signals still carry crucial information and features. Partial discharge pattern recognition is an excellent tool to determine the location and the source of these PD signals in the transformer winding. PD pattern recognition depends mainly on the assumption that PDs of the same origin are subjected to the same attenuation and distortion, and hence can be recognized [56]. PD pattern recognition involves two steps: PD detection and PD signal processing, both discussed in detail below.

i. PD Detection

Conventional and non-conventional methods are used to detect the PD in power transformers. However, not all these methods can be used for the detection of PD occurring in transformer winding insulation. For instance, ultra-high frequency antennas and acoustic techniques are immune to background noise and hence very effective in PD pattern recognition for PD occurring in the transformer tank. These methods use an array of sensors fixed on a transformer tank. Depending on the time PD signals arrive at each sensor of the array, the shortest passage from the PD origin to the sensor can be calculated, along with the PD location. Transformer insulation systems are very complex; therefore, the high frequency and acoustic PD signals are greatly attenuated and scattered through their propagation path from the winding to the sensors mounted on the transformer tank, causing errors in signal arrival time. Therefore, they are not suitable for PD pattern recognition when the PD exists in the transformer winding insulation [56].

In contrast, electrical PD detection methods have proven to be very effective in PD pattern recognition for PD sources inside transformer winding. These methods depend mainly on detecting PD current pulse signals at transformer neutral or bushing terminals. The detected PD current waveform contains useful information that enables the classification of PD sources coming from the same origin, source, or location [56]. For these reasons, the electrical method is used in this research for detecting the PD in transformer winding insulation.

ii. PD Signal Processing

In general, PD signals detected from transformers are processed in four steps (Figure 3.2):

- signal de-noising,
- multiple-source pattern separation,
- feature extraction, and
- pattern recognition.

The detection of PD signals in a transformer environment is complicated by the existence of interference from noise disturbances, harmonics, or pulses. PD signal de-noising is performed either online in hardware or by signal processing techniques using digital filtering, based on the Fourier transform [57].

The detection of PD signals in a transformer environment is complicated by the existence of interference from noise disturbances, harmonics, or pulses. PD signal de-noising is performed either online in hardware or by signal processing techniques using digital filtering, based on the Fourier transform [57].

Multiple PD defects may exist simultaneously in transformer insulation systems, and therefore the detected PD waveform is composed of multiple PD signals coming from these defects. Various techniques are employed to separate the PD signals, including phase-resolved PD techniques and artificial neural networks.

For PD pattern recognition, the remarkable features are then extracted from PD signals, as each PD class, source, or location produces a signal with distinct features (e.g., wave shape, repetition rate, rise time, and apparent charge) [58]. Using a feature extraction process reduces the complexity and the time of the computation process. Three types of features can be extracted from PD signals: basic quantities, deduced quantities, and statistical operators. The basic quantities include the PD apparent charge, the inception voltage, and the location of the PD in the voltage cycle. The deduced features are the integrated quantities of the basic quantities observed over a much longer time span. The statistical features are related to the waveform's shape and include factors such as variance, skewness, and kurtosis [59]. Skewness and kurtosis have proven to be very effective in the PD pattern recognition process, as they are not affected by attenuation caused to the PD signals by the propagation path through the winding [60].

When the extracted features corresponding to different patterns are completely separable, they can be used as a pattern classification method. However, for the most part, interference exists between the features of the different classes. Therefore, to enhance recognition-process efficiency, these features are used as input features for pattern recognition classifiers, such as fuzzy logic, expert system, and PD fingerprint. Although these classifiers have succeeded in PD pattern recognition for various cases, they depend mainly on human expertise [61].

Recently, artificial neural networks have been proved to be particularly useful for multiple PD pattern recognition applications [62]. Neural networks are similar to the human brain, in that they are composed of a number of parallel processing elements called neurons. These neurons are connected together with weighted connections similar to brain synapses. The neurons are arranged in input, hidden, and output layers which are connected through synaptic weights (Figure 3.3). Each neuron is a small processor that takes the summation of its weighted inputs and maps them using an activation function. The activation function can be a sigmoid, signum, step, or linear function [63]. In this parallel computing process, neural networks are trained with system input-output data to adjust their weights and represent this system. After training the neural networks, they can identify the system output for new inputs [60]. For their convenience in PD pattern recognition, feedforward neural network classifiers are used in this research, both for PD source identification and for PD localization inside power transformer winding insulation [64].

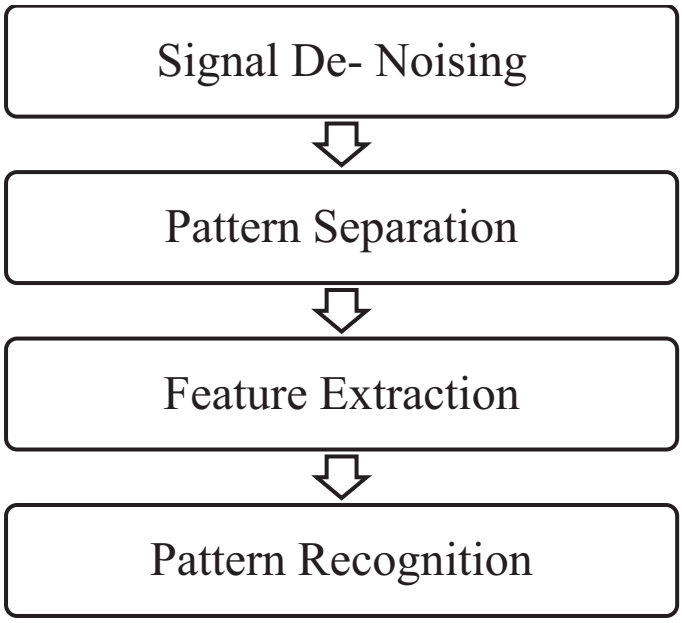

Figure 3.2 : PD signal processing steps

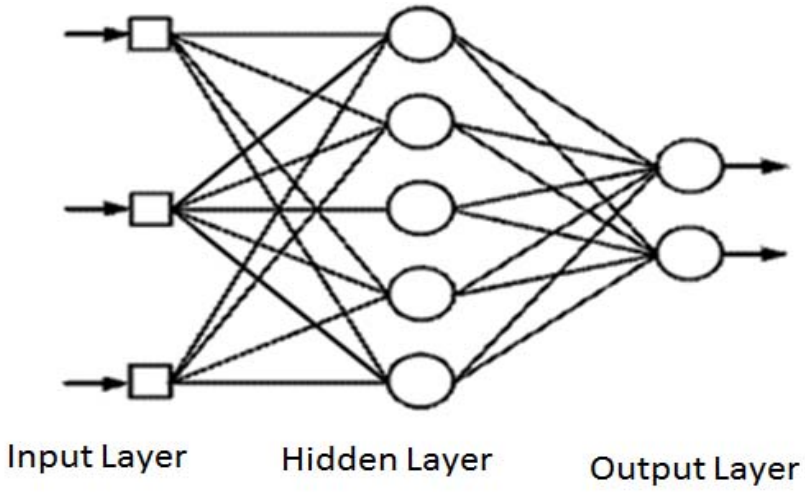

Figure 3.3: Feedforward neural networks

iii. PD Source Identification and Localization Modules

PD pattern recognition modules for same-structure transformers require the construction of a knowledge base of different classes of PD input-output signals. To develop this knowledge base, various PD sources are simulated and injected into multiple locations along transformer windings. Based on the above discussion, electrical PD detection is highly suitable for PD occurring in transformer winding insulation. Hence, the leakage current at the transformer neutral is measured and used in the PD pattern recognition module developed in this thesis. In this module (Figure 3.4), statistical features, including variance, skewness, and kurtosis, are extracted from the leakage current signals measured at the transformer neutral. They are then used for training and testing feedforward neural networks with different topologies. Various combinations of features are used as input vectors to the different topologies' neural networks – first individually, then in twos, and finally all three. To determine the best neural network, a recognition rate is computed in each case. The recognition rate is the ratio of correctly recognized PD signals to the total number of PD tested signals [3].

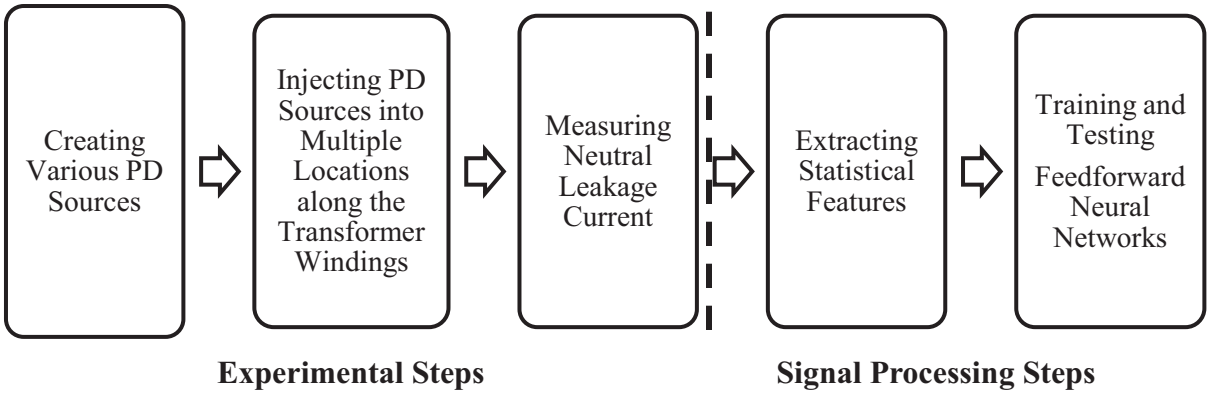

Figure 3.4: Steps for developing the PD source classification and localization modules

3.2.2 PD Charge Calculation Determination Module

To avoid underestimating the damage caused to transformer insulation, I develop a module for calculating the PD charge corresponding to the PD current injected into the transformer winding during a PD event and not the PD terminal measured leakage current (Figure 3.5). The injected PD current is calculated by reflecting the leakage current measured at the transformer neutral terminal back to the PD injection point using a winding model. Different approaches can be used to model transformer windings (Figure 3.6), such as circuit, mathematical, or hybrid modeling. The first approach is modeling the transformer winding as [64]:

i. a pure capacitive model,

ii. a lumped circuit model,

iii. a continuous parameter model, or

iv. a multi-conductor transmission line model.

The capacitive network model covers a narrow frequency range, which is difficult to determine for some winding types [64].

The lumped circuit model is acceptable over a frequency range of several kHz to 1MHz, which does not cover the frequency range for all propagated PD signals through the transformer winding [64].

The maximum frequency for a continuous parameter model is limited to several kHz, restricting its applicability to PD detection [64].

The multi-conductor transmission line model (MTLM) is acceptable over a larger frequency spectrum, which is adequate for PD detection. However, for large transformers, the computations become very complex, limiting the application of this approach in the industry [64].

The second approach is modeling the transformer winding mathematically with differential equations (DE), a frequency response (FR), or a transfer function [65]. Modeling the transformer winding with a frequency response is a well-known non-destructive transformer condition assessment technique used especially in evaluating the mechanical integrity of a transformer after faults [66]. The winding frequency response depends mainly on the winding circuit elements, i.e., resistance, inductance, conductance and capacitance, which depend on the winding structure. Therefore, any deformation in transformer windings can be identified by comparing the transformer winding current frequency response with the original one [67]. The hybrid techniques use the frequency response to build a winding circuit model that is used to estimate the transfer function [68]. Due to the frequency limitations and calculation difficulties inherent in the circuit modeling of transformer windings, this research focuses on a mathematical approach to transformer modeling.

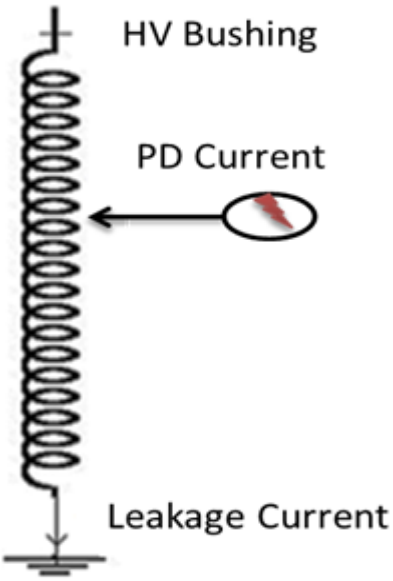

Figure 3.5: PD current injected into transformer winding and the corresponding leakage current at transformer neutral

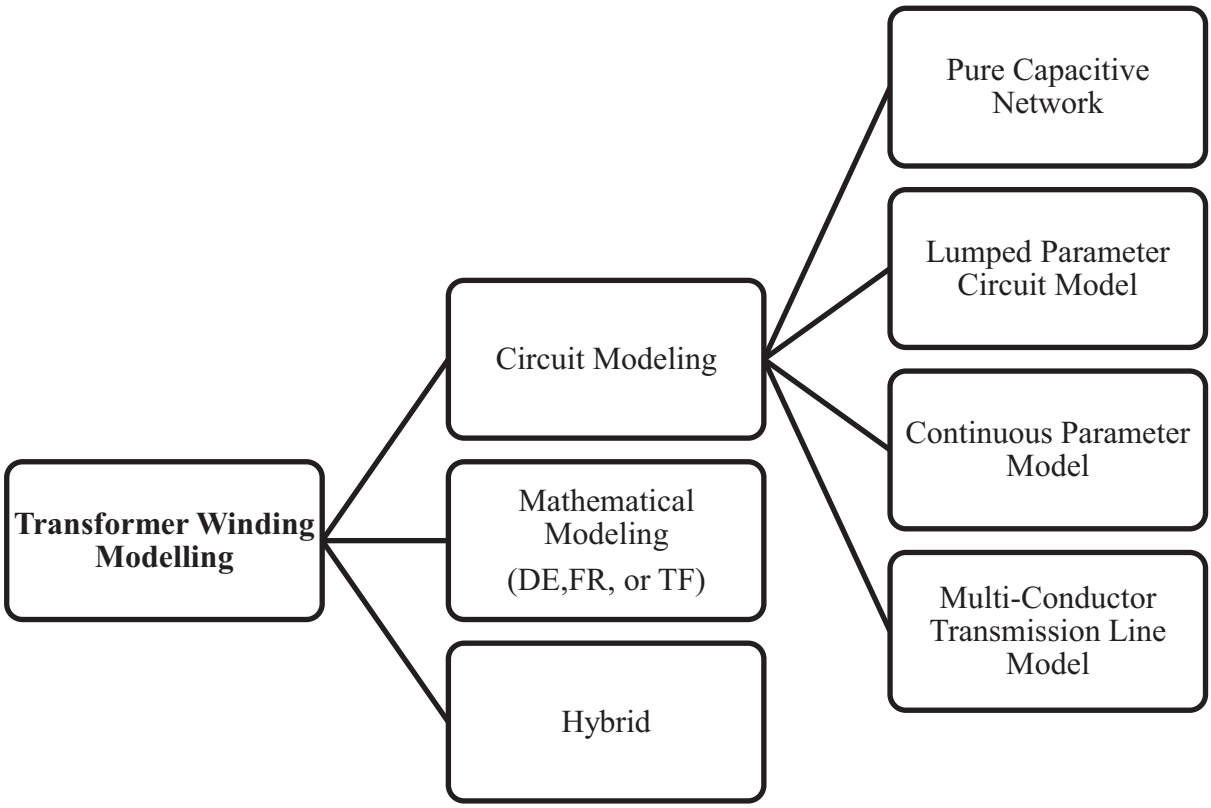

Figure 3.6: Transformer winding different modeling approaches

3.2.2.1 Mathematical Modeling of Transformer Winding

A physical system is a group of hardware parts that convert a group of input signals into a group of output signals. The system can be analog or discrete, depending on the type of input and output signals, and it can be linear or nonlinear, depending on the relationship of the system input and output. A linear system satisfies the superposition principle which states that if two input signals are linearly injected into the system, the resulting output is the linear combination of their expected individual outputs. Systems can either be time-variant or time-invariant. If a delayed input signal is injected into a time-invariant system, the output would be the expected one, delayed with the same time shift as the input with no other changes.

To investigate system behavior, a physical system can be modeled in the time or frequency domains. In the time domain, a linear time-invariant (LTI) system can be entirely modeled by one function called the impulse response, which has a very short duration. Delta functions are commonly used for analog systems, and Kronecker delta functions are used for discrete systems. The system

impulse response is the system output corresponding to an impulse signal input. Due to linearity and time-invariant properties, if the system impulse response is identified, the system output resulting from any other input can be calculated. Since any input entered into the system can be decomposed into the summation of scaled and time-shifted impulse signals (Equation 3.1), the output would then be the summation of all scaled time shifts of the system impulse response, as shown in Equations 3.2 and 3.3 for discrete and analog systems. For transformer windings, if their impulse response is known, the output of any input (or vice versa) – including the PD signal – can be identified.

$$x[n] = \sum_{k=0}^{\infty} x[k]\delta[n-k] \qquad 3.1$$

$$y[n] = \sum_{k=0}^{\infty} x[k]h[n-k] \qquad 3.2$$

$$y(t) = \int_{-\infty}^{\infty} x(t)h(t-\tau) \qquad 3.3$$

where, $h[n]$ is the system's impulse response.

The above equations demonstrate the convolution theory, which stipulates that for any input signal to an LTI system, the system's output is equal to the corresponding input signal convoluted by the system's impulse response. The convolution of the two signals expresses the amount of overlap between a function and a time-inverted version of another function as a function of the time delay between them. The convolution theorem also states that a convolution of two signals in one domain (time) is a product in another domain (frequency or Laplace), and vice versa. While numerical convolution is possible, it is sometimes complex and time-consuming, since the computation process has multiple steps. The Fourier transform can be used to transfer the system's differential equations into algebraic equations in the frequency domain, at which point the convolutions become algebraic multiplications (Figure 3.7). In this research, the transformer winding is modeled using the frequency response and transfer function techniques.

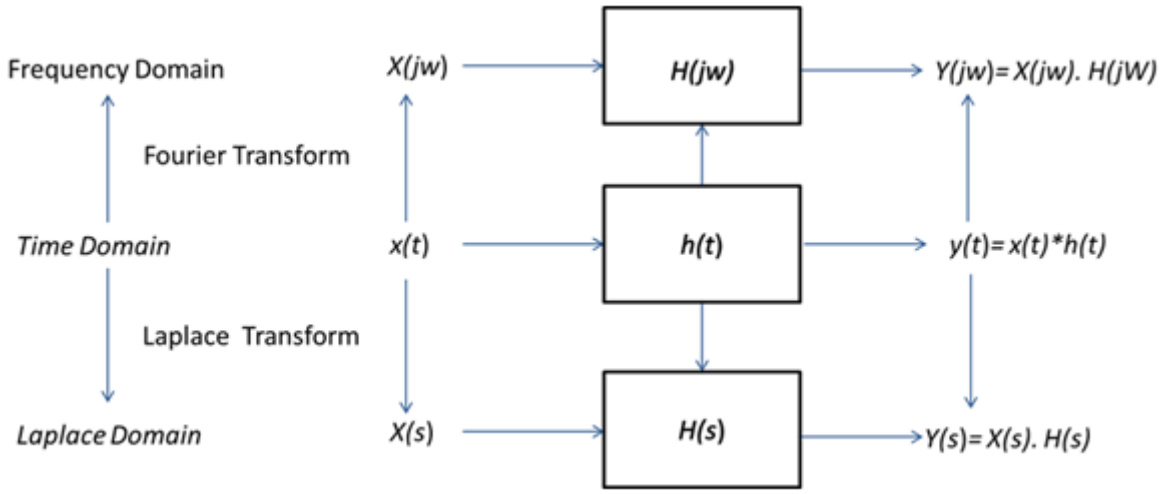

Figure 3.7: Convolution in the time, frequency, or Laplace domains

i. Transformer Winding Frequency Response

The impulse response of the LTI system in the frequency domain is called the system frequency response. This response is usually plotted as a Bode plot in a logarithmic scale. A Bode plot is a graph of the magnitude (in dB) or phase of the frequency response versus frequency. Utilizing the logarithmic scale is helpful for showing the signal transferable intensity over a broad range of frequencies.

Transformer windings are considered as LTI systems. The transformer winding frequency response has general sub-band regions dominated by different transformer components that are frequency-dependent. At very low frequencies, the winding frequency response is dominated by the core, whereas at higher frequency bands, the winding frequency response is dominated by the winding inductance. Then, with higher frequency values, the winding capacitive inductance dominates the frequency response, and at very high frequencies, the transformer equivalent circuit consists mainly of the shunt and series capacitance, which reaches very low values and can be neglected. Thus, the test configuration and connection cable determine the behavior of the circuit [69, 70, 71].

According to the power supply nature, the winding frequency response can be measured by two methods: impulse response or sweep frequency. In the impulse frequency response measuring method, an impulse function is injected into the transformer winding input terminal, and the impulse response is detected from the output terminal. The frequency response can then be obtained using Fourier transform.

In the sweep frequency response method, a sinusoidal signal with a voltage magnitude (in Volts) from one to twenty RMS and a sweep frequency from a few Hz to a few MHz is used to excite the transformer input. The corresponding output is measured from the transformer output terminals. The frequency response magnitude is calculated as the ratio of the output signal magnitude to the input signal magnitude, and the angle is calculated as the difference between their angles. The recommended frequency range differs according to the standard used, with the lower frequency ranging from 10 Hz up to 1 kHz and the upper frequency ranging from 1 up to 10 MHz [72]. The upper frequency is limited by the test setup and connection cables [73].

The impulse response method and sweep frequency method are compared in [74], which concluded that the impulse response method is fast and that multiple transfer functions can be measured simultaneously. However, the frequency resolution is the same over the entire frequency range, making this method not only imprecise at lower frequencies but rendering the detection of faults related to lower frequencies difficult. This method also requires multiple devices, and filtering out the noise from the measured signals is complicated.

Sweep frequency analysis is slower than the impulse response method, as only one measurement at a time is made at each frequency. However, compared to the impulse response method, the sweep method has a much better signal-to-noise ratio, a broader frequency response range, and controllable frequency resolution; it also has an easier reproduction of results and requires fewer pieces of equipment [74, 75]. Thus, based on its merits, the sweep frequency method is used in this research.

Various standards exist for sweep frequency response testing of power transformer windings, such as the Chinese Standard DL 911/2004, CIGRE WG A2.26 Brochure, IEC 60076-18, and IEEE C57.149. Each of these standards recommends the test configuration and problem interpretation approach using frequency response. Some of the recommended test configurations are (Figure 3.8):

- End-to-end open circuit test

The input signal is injected into one terminal of the winding under test, and the response is measured from the other terminal of the winding, while all other terminals are left open [76, 77].

- End-to-end short circuit test configuration

This test configuration is similar to the previous circuit test, but the secondary terminals are connected to each other and are short-circuited. The secondary short-circuiting removes the influence

of the core's magnetizing inductance from the response so that the only characterizing impedance in the low frequency range is the leakage inductance of the winding [76, 78].

- Capacitive inter-winding test

The input is injected into a winding terminal and the output is measured at the secondary, while all the other terminals are left open. Because the capacitance between the winding affects the response, this test is not recommended for certain transformers [76].

- Inductive inter-winding test

This test configuration is similar to the capacitive one, except that non-measuring secondary terminals are grounded. Various methods of fault interpretation are recommended under these standards. One of the most widely accepted methods is the one recommended by the CIGRE WG A2.26 brochure, which suggests that the latest frequency response of the winding be compared to a reference frequency response. This reference frequency response can be a previous healthy frequency response of the same winding, a frequency response of another phase of the same transformer, or a frequency response of an identical transformer (e.g., a sister unit) [76].

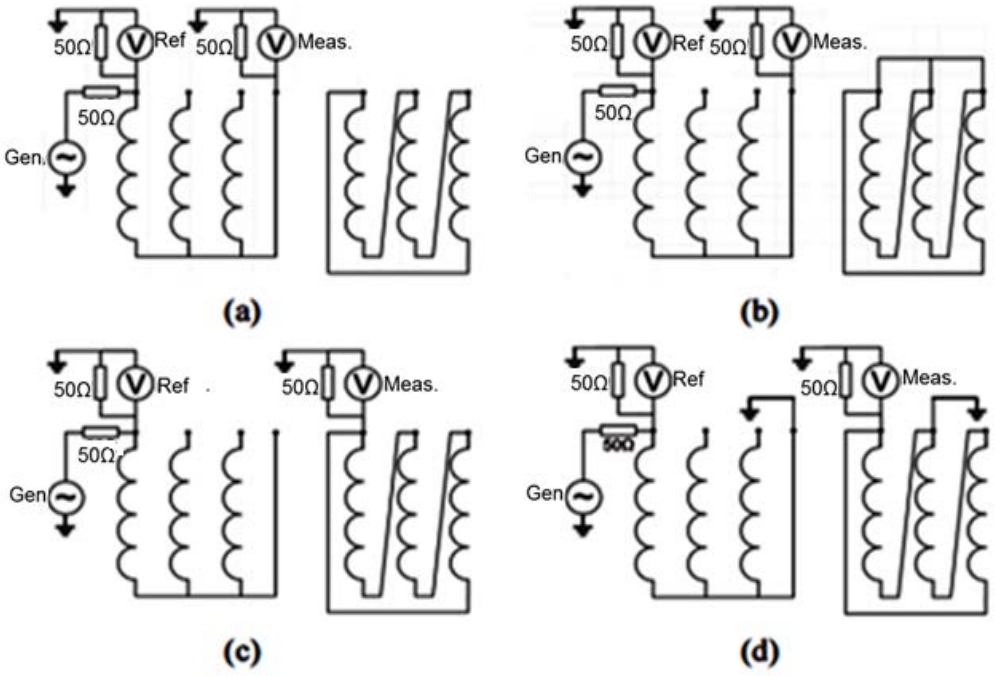

Figure 3.8: Frequency response test configurations: (a) End-to-end open circuit, (b) end-to-end short circuit, (c) inter-winding (capacitive), and (d) inter-winding (inductive) [76]

ii. Transformer Winding Transfer Function

Although various standards exist for measuring the frequency response of transformers; interpreting transformer problems from the frequency response is usually done by "human expertise", limiting the application of the frequency response technique to only the assessment of the mechanical deformation of winding. Therefore, researchers have been developing numerical techniques for interpreting transformer problems from frequency response. These numerical techniques can be classified into two categories: statistical and transfer function. Statistical indicators are used to correlate before-and-after-fault transformer frequency responses [79], while the transfer function method is based on replacing the frequency response with a rational function so that if any change occurs to the transformer, the parameters of the function will be changed.

The transfer function of a linear system is the ratio of the Laplace transform of the system output to the Laplace transform of the system input, assuming zero initial conditions. Equation 3.4 shows the general form of the transfer function, and Equation 3.5 shows the factorization of the transfer function numerator and denominator into the zero-pole-gain form. The poles and zeros of a system are also called the resonance and anti-resonance frequencies. The system has an infinite gain at the pole positions, making it resonate with zero damping. At the zero positions, the system output is zero, and these frequencies are completely cut out of the output signals. Therefore, studying system poles and zeros is important for investigating system stability. The transfer function is given by:

$$H(s) = \frac{b_0 s^n + b_1 s^{n-1} + \cdots + b_{n-1} s + b_n}{s^n + a_1 s^{n-1} + \cdots + a_{n-1} s + a_n} \qquad 3.4$$

$$H(s) = k\frac{\prod_{i=1}^{m}(s-Zi)}{\prod_{i=1}^{n}(s-pi)} \qquad 3.5$$

The frequency response and transfer function represent the impulse response of a system in different domains. They can be calculated from each other using multiple methods, including visual inspection and vector fitting. Visual inspection is based on the concept that, at the frequencies related to the pole or zero, the slope of an asymptotic diagram changes. At frequencies lower than pole or zero frequencies, the asymptote slope is flat. At the pole or zero frequencies (break points), the asymptote slope starts to change. At frequencies higher than the break points, the asymptote slope becomes 20 or -20 dB/decade for a single zero or a single pole, respectively. For double zeros or poles, the asymptote slope becomes 40 or -40 dB/decade at the high frequencies. In the case of two complex

poles (underdamped response), the asymptote slope is flat in the lower frequency range; the system resonates at the natural frequency of the system; the asymptote slope is -40 dB/decade in the high frequency region [76]. This method is difficult to use with complex systems such as transformer winding. However, it can be used for an initial evaluation of the poles and the zeros of the transformer winding. The complete analysis of the winding transfer function will be done using the vector fitting techniques after completing the initial evaluation stage.

The vector fitting technique fits the vector frequency response vector with a rational function approximation by converting complex frequency responses into a polar-residue rational transfer function, which then uses the least square method to optimize process errors [80]. This method is robust and convenient for fitting high-order system responses such as transformer windings [80]. It has been used in multiple studies for PD detection in transformer winding insulation. In [81], the effect of the PD propagation path through the winding of a transformer is investigated and removed by measuring the winding frequency response from 0 to 10 MHz, and calculating the transfer function using vector curve fitting techniques. In [82], this method is used for PD localization in a dry-type transformer. The convenience of this method in estimating the transformer winding transfer function (TF) makes it highly suitable for use in this research.

The winding transfer function is considered a powerful diagnostic technique for evaluating power transformer winding condition, as well as for testing insulation coordination, detecting inter-turn short circuits, identifying insulation defects, detecting mechanical deformations, investigating surge overvoltages, and determining the PD location and charge along the winding [83]. Since the PD signal path from a source to a detection point has unique characteristics, the transfer function concept is applied to detect and localize PD in winding insulation systems. In [84], a multi-step module is introduced for PD localization inside a transformer winding, specially prepared with multiple access locations. The sectional winding transfer functions (SWTFs) are measured using a network analyzer and then calculated using impulse response measurement for verification. Other classification and localization techniques, such as neural networks and distance functions, are used invalidating the results. In [85], the lumped circuit parameters model is used for estimating SWTFs, which are used for PD localization inside a disk-type transformer winding. In this model, the transformer winding is grouped into sections of disks, with each disk being represented by an R-L-C unit. The PD input signal is simulated by a current source, and the output signal is detected from the bushing and the neutral via detection impedances. Two transfer functions are calculated at different locations along the winding, from the PD injection point to the bushing and to the neutral. These calculated transfer

function can be used to determine the PD current and PD location. In [64], a similar technique is used, but the ratio of the transfer function from the PD source to the bushing to the transfer function to the neutral is calculated. This ratio is used to train and test one hidden layer neural network for location recognition.

3.2.2.2 PD Charge Determination Module

Based on the above discussion, the input /output of the transformer winding can be calculated from the corresponding output/input and winding transfer function. Specifically, the PD current (and charge) injected (input) into the transformer winding during a PD event can be calculated using the corresponding leakage current and the winding transfer function from the PD location to the transformer neutral terminal. Therefore, constructing the PD charge determination module requires the developing of two components (Figure 3.9): a PD localization module for selecting a certain transfer function corresponding to the PD location, and a bank of transfer functions from all accessible points along the transformer winding. These transfer functions can be calculated from the corresponding winding frequency response.

During a PD event, the leakage measured at the transformer neutral terminal undergoes the localization module (introduced earlier in this chapter) to select the transfer function corresponding to the PD location. Using the leakage current and the selected transfer function, the input PD current can be calculated in either the time or frequency domain. The PD charge is calculated by integrating the input current waveform (Figure 3.9).

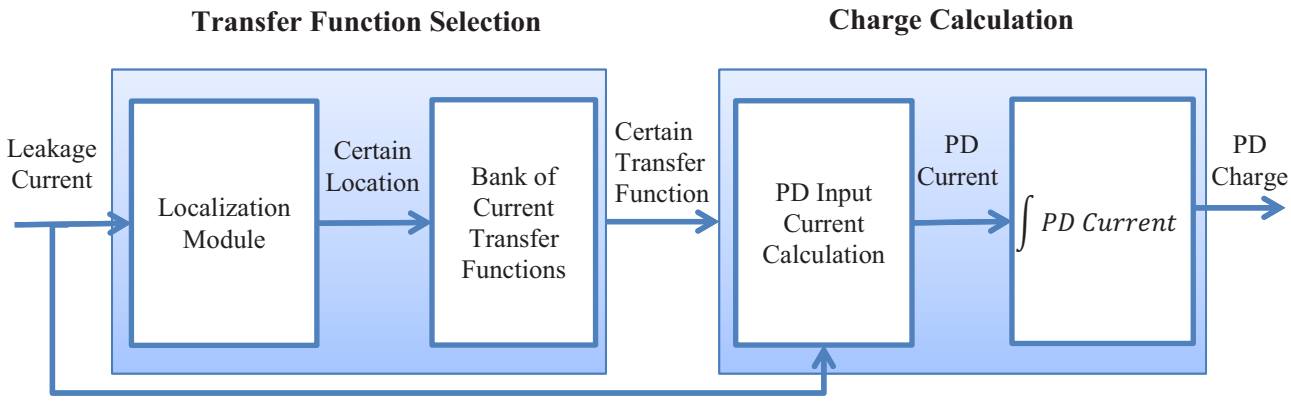

Figure 3.9: PD charge determination module

3.3 Transformer Winding Condition Assessment Based on Partial Discharge Detection

Transformer insulation assessment based on PD activity is usually performed using PD apparent charges measured at transformer terminals, neglecting the effects of the propagation path and other PD characteristics. Moreover, the justifications for using certain PD charge values, such as 500 pC by IEC, as acceptance criteria are not clear in terms of the damage caused to insulation systems. On the other hand, studies that have comprehensively investigated the damage caused to oil-paper insulation do not correlate their conclusions to the insulation systems of real transformers [11, 14].

To overcome these shortcomings, I have developed a new transformer condition assessment technique that uses multiple PD features. In a comprehensive study, the damage caused to an insulation system is correlated to real transformer insulation conditions. The developed assessment technique has two main components: a PD severity assessment module and a condition assessment of power transformers based on the PD severity assessment

i. PD Severity Assessment Module

The uncertainty arising from the PD ranges suggested in various studies is dealt with using fuzzy logic. Fuzzy logic is very similar to the human inference process; in fact, the theory was first presented by Professor L. A. Zadeh as an extension to classic logic theory. Unlike classic logic theory, however, in which space elements' degree of membership to a classic set is either one or zero, fuzzy logic sets are more flexible and allow the elements to have a partial degree of membership. This partial degree of membership can be any value between zero and one, with zero representing no membership and one representing full membership to the set. This flexibility suits many real-life applications and problems that cannot be solved by classical logic. With its highly random nature, PD is certainly one of these applications

Fuzzy inference is a five-step module that involves input variable fuzzification, fuzzy-logic-operator application, implication method application, aggregation method application, and output defuzzification (Figure 3.10). In the fuzzification step, the degree of belonging of each input to each fuzzy set is determined based on the variables' membership function. Membership functions (MFs) express the degree of membership of each element in a space to the fuzzy sets. Different types of waveforms are used for constructing MFs, such as triangular, trapezoidal, bell-shaped, sigmoidal, and S-curve waveforms. Determination of the membership function waveform depends on the nature of each variable. For each rule, there are a number of values that represent the degree of membership of

each element to the fuzzy set in that rule. The fuzzy operators AND and OR are applied to select one of these values for the consequent output function via the implication method. For each rule, the output of the implication method is a fuzzy set. All of the rules' output fuzzy sets are then combined into one set, using an aggregation method. In the defuzzification step, this set is converted back into a crisp value that represents the output of the fuzzy logic. Various methods can be used for the defuzzification process, including the mean of maximum (MOM), the center of gravity (COG), and height methods [63]. Figure 3.10 shows the steps for the fuzzy inference process, where DOMnk is the degree of membership of element (k) to the set in rule (n); DOMn is the degree of membership function selected to represent this rule after applying the fuzzy operators; FCSn is the nth fuzzy consequent set resulting from applying the implication method; and FOS is the fuzzy output set.

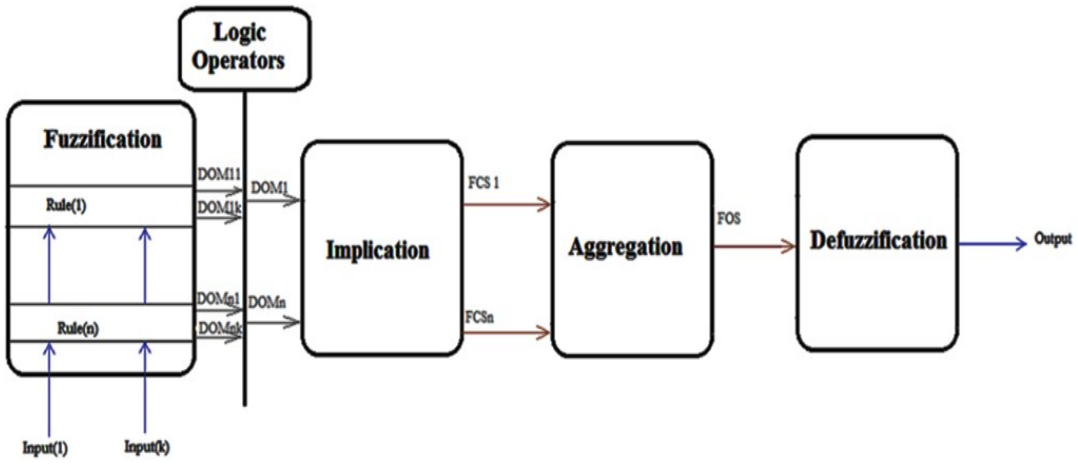

Figure 3.10: The fuzzy inference process

Due to the random nature of PD and the uncertainty of its detection techniques, fuzzy logic is convenient for PD classification and assessment applications. In [86, 87], a fuzzy logic system is used to categorize the PD sources (i.e., air voids, surface discharge, oil-corona, and corona). In [86], the inputs to the fuzzy system are the time of PD occurrence in the voltage cycle, the number of PD pulses, and the PD apparent charges. In [87], besides classifying the PD sources, the authors add two more output categories: invalid data and noise. Fuzzy logic systems are also used to classify the same PD type into different categories, as in [88], where fuzzy logic separates void defect sizes into three categories with regard to five PD waveform shape features (apparent charge, rise time, fall time, width and area).

As the PD charge and source type have a direct relationship with the damage caused to the insulation system, they are used to assess the transformer winding insulation condition based on PD activity. A Mamdani fuzzy logic system is used to develop the PD severity assessment module (Figure 3.11). The inputs to the fuzzy system are the skewness value of the measured leakage current pulse, which is an indication of the PD source type, and the PD charge, whereas the output is the PDI, which reflects the number of damaged papers under certain PD activity as reported in [11]. In this thesis, the fuzzy MFs and rules are determined based on laboratory experiments and the existing literature.

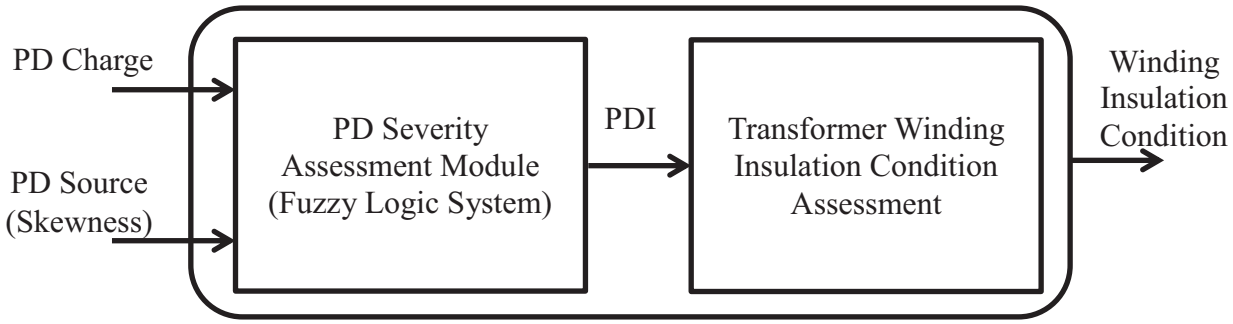

Figure 3.11: Transformer condition assessment

ii. Transformer Winding Insulation Condition Assessment Based on PD Detection

Transformer condition assessment based on PD activity is performed by correlating the insulation damage classification based on the number of damaged papers reported in [11] with the transformer insulation classification reported in [89]. The first assessment is based on control experiments, and the second is based on the terminal PD charge. To correlate the assessments, various PD sources are injected into transformer windings at multiple locations. By measuring the input PD current and output PD current, and then calculating the corresponding PD charges, attenuation factors are formulated, as in Equation 3.6. This attenuation factor is used to verify that the condition classification used in [89] is valid for this study. The input-output data is already available from the knowledge base of the PD source and localization module.

$$\mathrm{AF} = \frac{\text{PD Charge (input)}}{\text{PD Charge (output)}} \qquad 3.6$$

3.4 Thesis Outline

Based on the discussion provided in this chapter, PD detection and PD severity assessment modules are developed for transformer winding insulation (Figure 3.12). The PD detection module is composed of PD source classification, PD localization, and PD charge determination modules. The techniques used for PD source classification and localization modules are presented in Chapter 4. To develop the PD detection modules for a transformer, different PD sources, such as air bubbles, sharp edges, and surface discharge, are simulated and injected into different locations (taps) along the windings of a three-phase transformer. The corresponding leakage current signals are then measured at the transformer neutral terminal. Statistical features such as variance, skewness and kurtosis are extracted from the measured signals and are used to train and test feedforward neural networks with different topologies. Each neural network has one hidden layer, and the number of neurons is changeable. Different combinations of features are used as input vectors to the neural networks – first individually, then in twos, and finally in all three. The average recognition rate is calculated in each case.

In the PD charge determination module developed in this thesis, the leakage current, measured at the transformer neutral, undergoes the localization module to select the transfer function corresponding to the PD location and form a bank of transfer functions. Using the leakage current (output) and the selected transfer function, the PD input current and corresponding charge can be calculated. Therefore, developing this PD charge determination module for a transformer requires developing a localization module and a bank of transfer functions from all possible locations to the transformer neutral. These transfer functions are then calculated from the corresponding measured frequency responses by means of vector fitting.

In calculating a PDI that is suitable for assessing transformer insulation conditions and also to be included in the transformer health index calculations, the PD severity assessment utilizes fuzzy logic to formulate the PD charge and features associated with the PD source. These are calculated using the PD charge determination as well as the PD source classifier. The fuzzy membership function and rules are determined based on the experiments done in this study and the existing literature. Finally, a correlation between the findings of controlled experiments on the transformer winding insulation materials and transformer condition classification is made by calculating the attenuation factors between injected and measured PD charges.

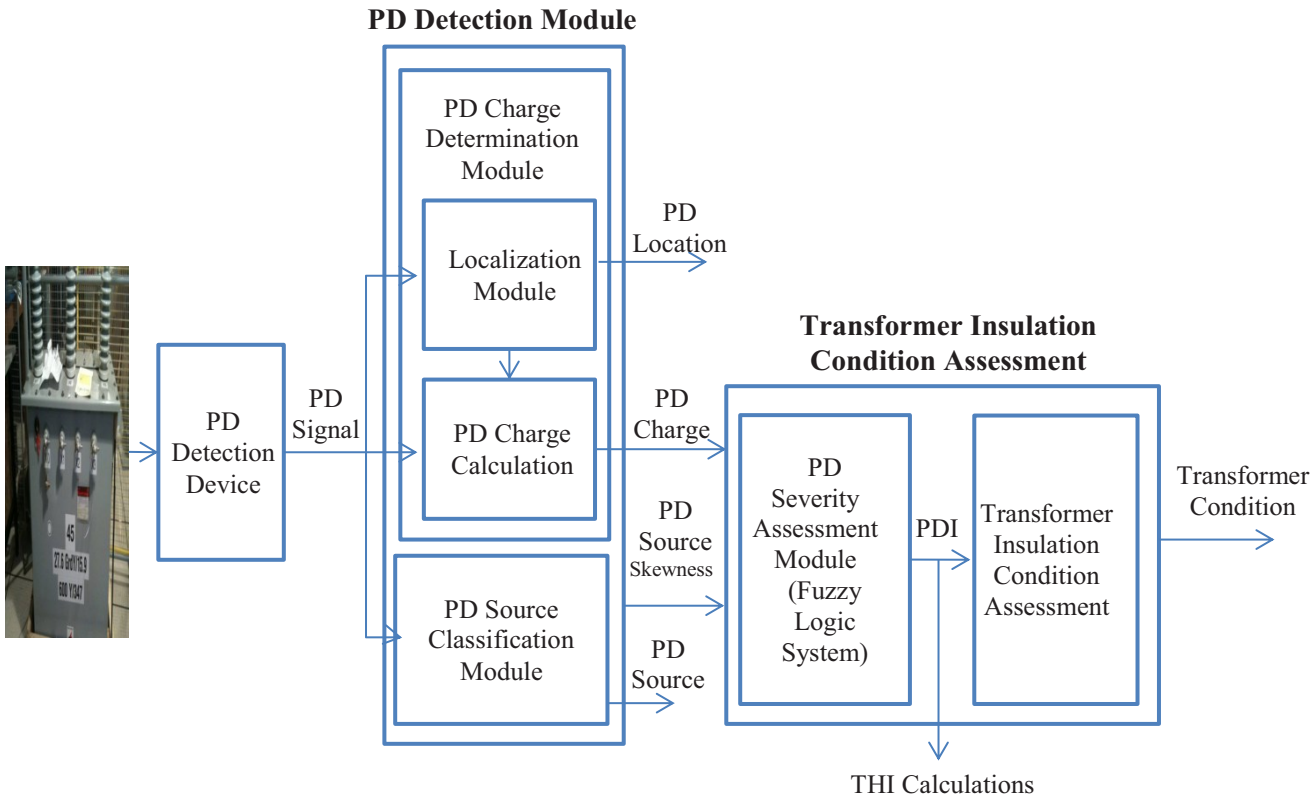

Figure 3.12: The developed PD detection and severity assessment modules

3.5 Summary

In this chapter, I discussed the research gaps that motivated me to develop the PD detection and the PD severity assessment modules for power transformer insulation winding. The reasons for choosing certain techniques to address the PD discharge detection in a transformer were discussed in details, a brief overview of the techniques was provided, and the thesis outline was highlighted

For a transformer under study, the PD detection modules: source, localization and charge determination, are developed in Chapter 4 and 5. The severity assessment module is developed in Chapter 6.

Chapter 4
Partial Discharge Detection and Localization in Power Transformer Winding

4.1 Introduction

Power transformers are the backbone of power systems, so their sudden outage or failure can cause huge losses for electric utilities and their customers. Most power transformer failures occur due to insulation system breakdown. PD is a major cause of transformer insulation deterioration. Early detection of the nature and location of the PD within the transformer insulation can help prevent or mitigate losses associated with transformer failure.

Transformer windings are responsible for approximately 30% of transformer failures [5]. One of the primary causes is insulation failure due to PD, so continuous online monitoring of PD in transformer winding insulation is the main focus of this research. Winding insulation systems of oil-filled power transformers are highly complex structures that can contain various defects that cause PD such as internal discharge, surface discharge, corona, and electrical trees. Because different types of defects have different severity impacts on insulation systems, identifying the source type is essential for evaluating the transformer insulation condition. Moreover, localization of PD defects within the transformer winding is important for applying the correct maintenance action [90]. In this research, PD localization is used in the PD charge determination module. Multiple electrical and non-electrical techniques can be used for PD detection in power transformers, including conventional PD detectors, high frequency antennas, acoustic sensors, high frequency current transformers, and optical sensors. Acoustic sensors and high frequency antennas are suitable for detecting PD occurring in the transformer tank, whereas electrical PD detection is useful for detecting PD occurring in transform winding insulation [56].

PD signals coming from the same origin (a source or location are exposed to the same kinds of distortion and attenuation and hence have unique features that enable them to be distinguished from signals of different origins. Statistical features are not affected by attenuation caused by the PD signal propagation path through the transformer winding [60], so they can be used to recognize PD signals coming from different origins, even though the features might overlap. Therefore, a pattern recognition method would be highly useful for enhancing the classification process. To this end,

feedforward neural networks have been proven to be beneficial in PD pattern recognition applications [58].

This chapter develops PD source identification and localization modules as a part of the detection module shown in Figure 4.1. Three PD sources are created and injected into different locations along the windings of a real transformer under study, and the corresponding leakage currents are measured from the transformer neutral. The statistical features- variance, skewness, and kurtosis- are extracted from the measured signals and are used to design feedforward neural networks for PD pattern recognition purposes.

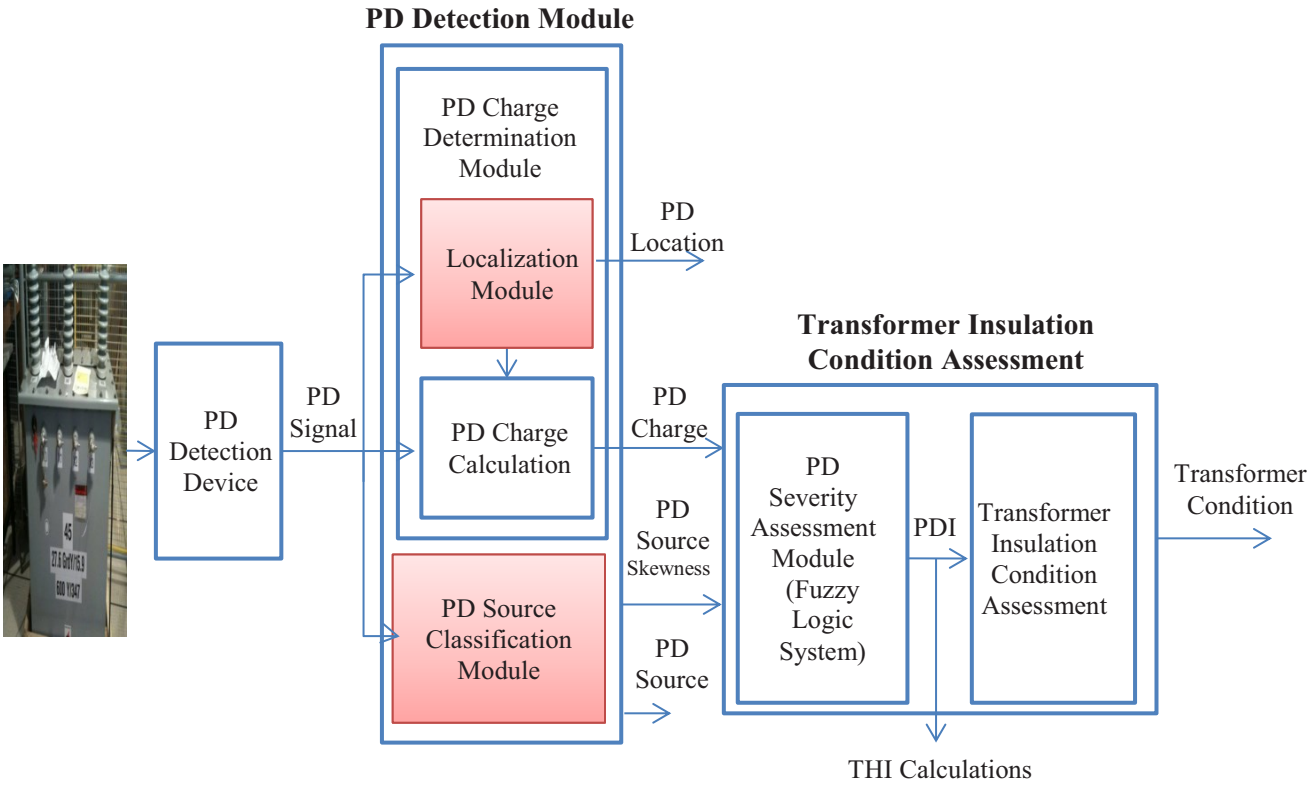

Figure 4.1: PD source classification and localization modules as part of the developed PD detection module

4.2 PD Pattern Recognition in Transformer Windings

The modules for PD source classification and PD localization in transformer windings involve several steps: creating multiple PD sources, injecting the sources into different locations along the transformer winding, measuring the corresponding leakage currents from the transformer neutral,

extracting the statistical features, and training and testing feedforward neural networks (Figure 4.2). This section discusses the details of these steps and their applicability to a 45 kVA transformer.

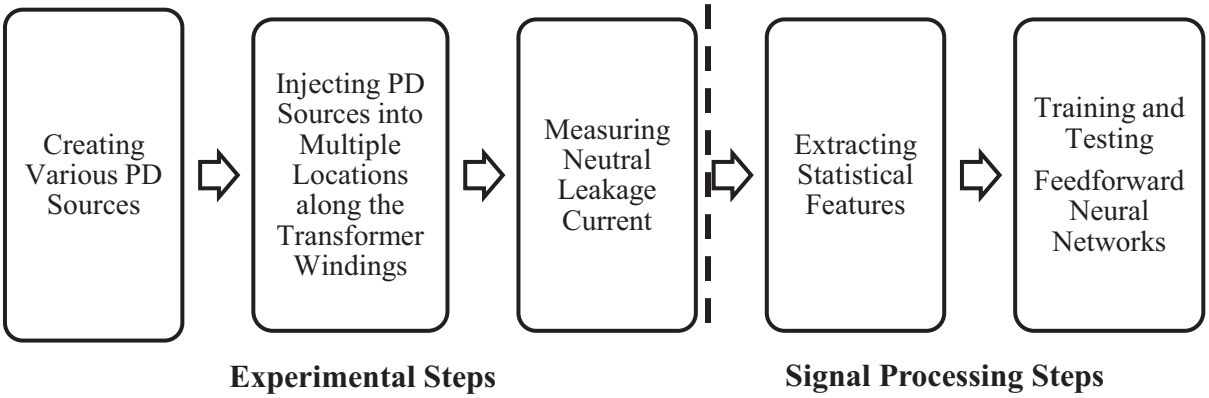

Figure 4.2: Steps for developing the PD source classification and PD localization modules

4.2.1 PD Signal Creating and Injecting into Transformer Winding and Measuring Leakage Current Measurement (setup)

Three types of PD – air bubble, sharp edge, and surface discharge – are created using a needle-plane electrode arrangement in a cell filled with air, oil, and oil and Kraft paper, respectively [84]. A high voltage is applied to the needle electrode using a discharge-free transformer while the plane electrode is connected to the winding of the real transformer under test (Figure 4.3). In real-life applications, it is difficult to physically access a transformer's winding to monitor PD activities, but it is relatively easy to reach the winding tap locations. Therefore, in this research, the laboratory experiments and hence PD pattern recognition modules are based on injecting PD signals into every tap of each winding of the transformer.

The transformer under study is a 45 kVA three phase transformer that has six tap position, T1, T2, T3, T4, S2 and F1(Figure 4.4). The winding's number of turns and the resistance associated with each tap connection are shown in Table 4.1. During this research, tap S2 is connected to tap F1, permitting 5 tap locations for PD injection. Seventy PD signals of each type are injected into each tap.

Figure 4.3 shows the experimental setup used in these experiments. The input and output PD signals are measured as voltage drop signals across two 150 Ω resistors, using a four-channel Tektronix digital storage oscilloscope (TDS5104/1P/16). The input resistance is connected between

the plane electrode and the transformer tap connection under test. The output resistance is connected between the transformer neutral and the ground. As the input resistance is not connected directly to the ground, the voltage across it is measured as the difference between its terminal-to-ground voltages. Typical input and output voltage signals for the PD air bubble are shown in Figure 4.5.

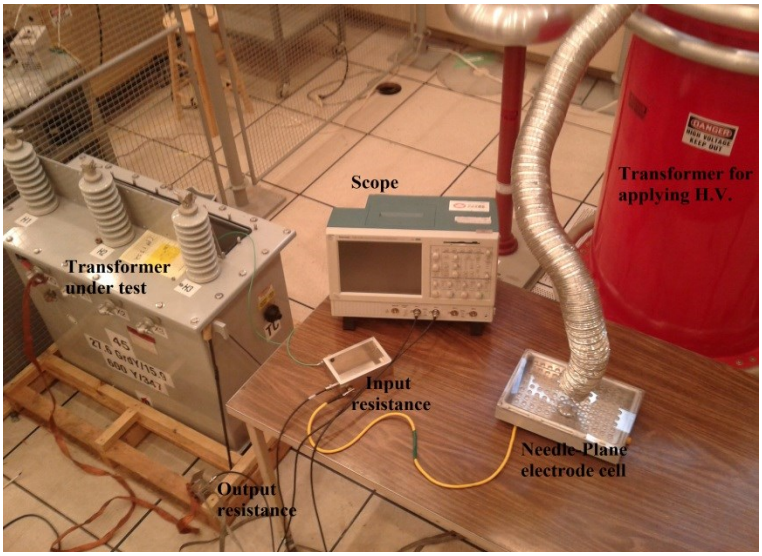

(a)

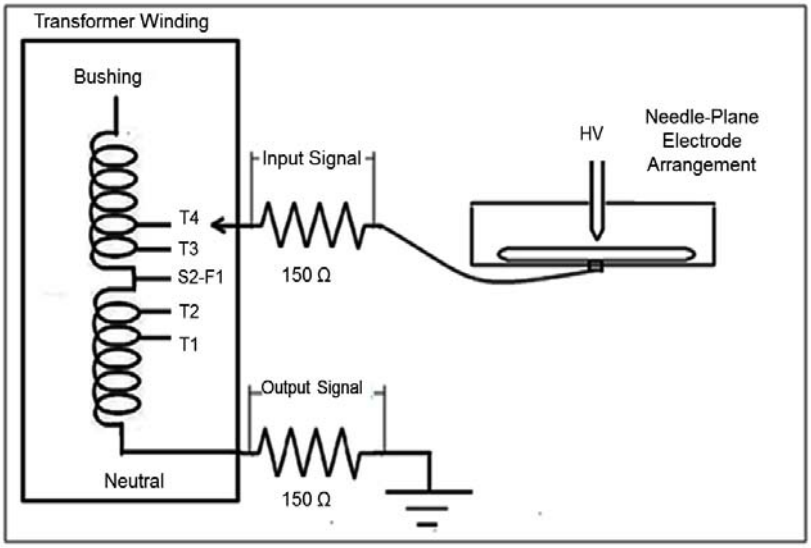

(b)

Figure 4.3: Experimental setup. (a) The laboratory equipment, (b) The schematic diagram

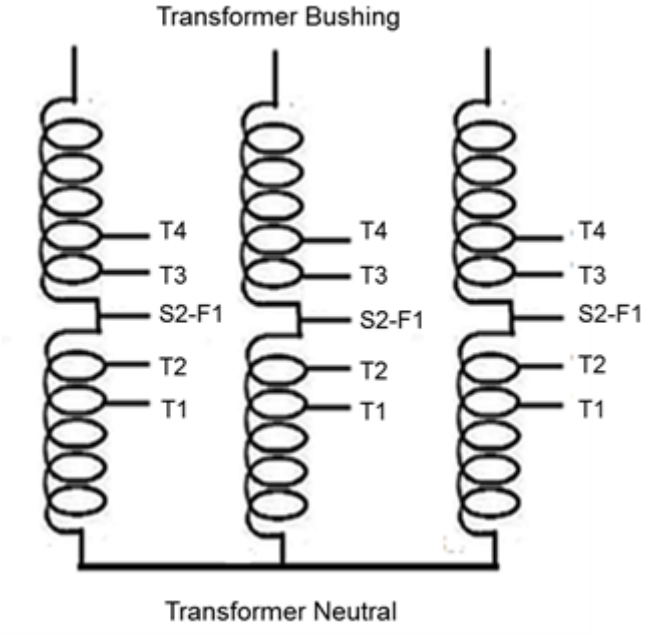

Figure 4.4: Transformer winding under study

Table 4.1: Tap positions and associated number of turns and resistance

Tap Position	**Tap Connection**	**Turns**	**Resistance (Ohms)**
1	S2-F1	3188	126.96
3	T3-F1	3112	123.94
3	T3-T2	3036	120.91
4	T4-T2	2960	117.88
5	T4-T1	2884	114.86

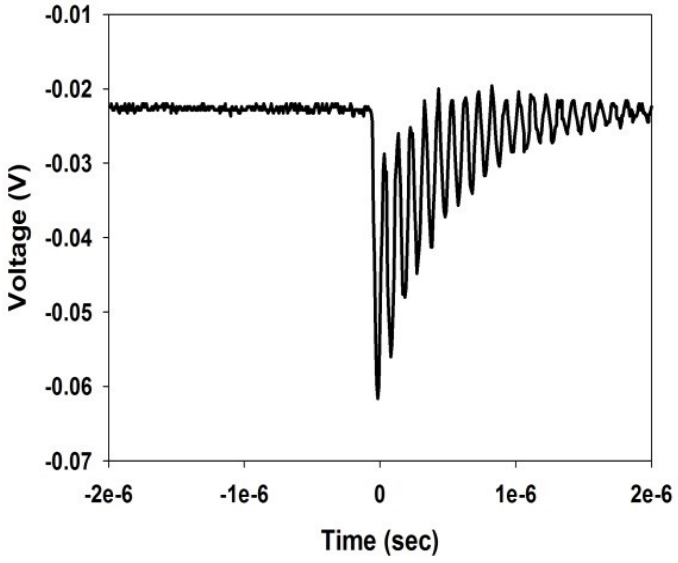

(a)

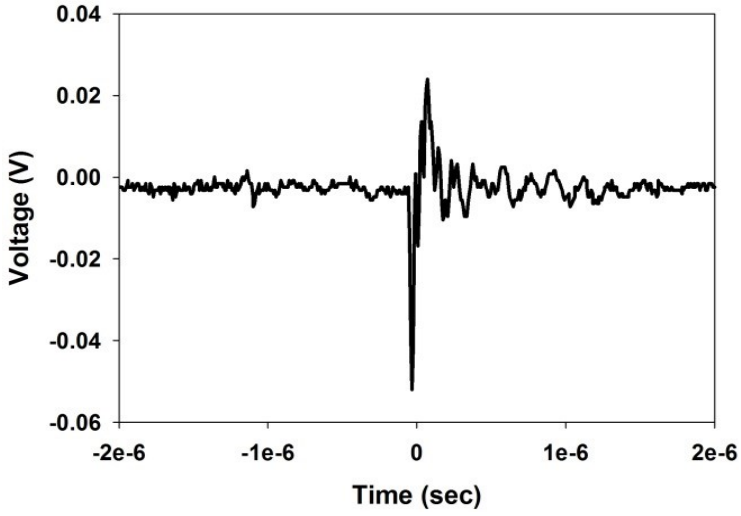

(b)

Figure 4.5: Air bubble PD: (a) Input PD signal, (b) output PD signal

4.2.2 Statistical Feature Extraction

Instead of dealing with complete PD measured waveforms, informative features are extracted and used in the pattern recognition process. In this research, statistical features such as variance,

skewness, and kurtosis are extracted from the normalized PD output signals. The statistical features are defined as [91]:

$$\text{Variance: } \sigma^2 = \frac{\sum_{i=1}^{N}(x_i-\mu)^2 f(x_i)}{\sum_{i=1}^{N} f(x_i)} \quad 4.1$$

$$\text{Skewness: } S_k = \frac{\sum_{i=1}^{N}(x_i-\mu)^3 f(x_i)}{\sigma^3 \sum_{i=1}^{N} f(x_i)} \quad 4.2$$

$$\text{Kurtosis: } k_k = \frac{\sum_{i=1}^{N}(x_i-\mu)^4}{\sigma^4 \sum_{i=1}^{N} f(x_i)} - 3 \quad 4.3$$

Where, N is the number of phase windows in a half cycle, and $\boldsymbol{\mu}$ is the mean value.

4.2.3 Artificial Neural Network Classifiers

The statistical features extracted from the PD output signals are used to train and test one hidden-layer feedforward neural network for PD source classification and localization purposes (Figure 4.6). To determine the best network, the number of neurons is increased from two to twenty, in increments of two. For each neural network, sixty percent of the available data is used for training and forty percent for testing. Five different combinations of the available training and testing data values are used, and the average recognition rate is calculated for this input vector. The recognition rate is calculated as the number of correctly classified signals with respect to the total number of tested signals.

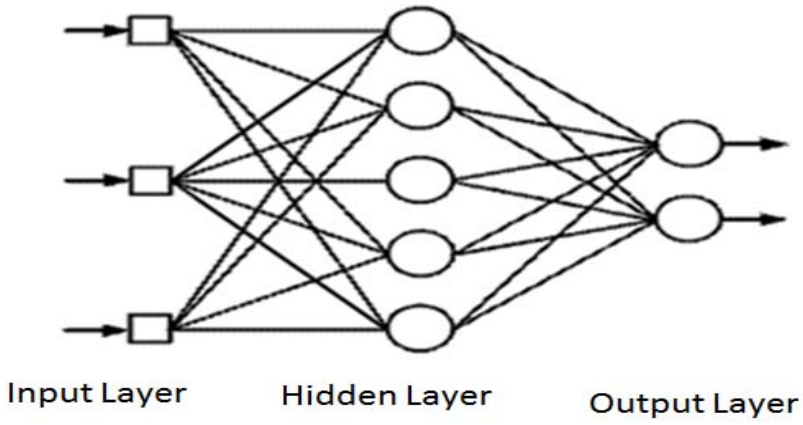

Figure 4.6: Feedforward neural network with one hidden layer

4.2.4 Results and Discussion

4.2.4.1 PD Source Type Classification Module Results

Using MATLAB, the statistical features are extracted from the leakage current signals corresponding to the three types PD defects: air bubbles, sharp edges, and surface discharges. The histograms of variance, skewness, and kurtosis are shown in Figures 4.7 through 4.9. In order to investigate the overlap between the features corresponding to different PD sources, the frequencies of the histograms are normalized by dividing them by the maximum frequency of each feature. The extracted features corresponding to the air bubble PD signals are entirely separable from the features of the other two types, except for a few skewness values. For sharp edge and surface discharge PD defects, there is interference in their features, especially in the variance values. Therefore, feedforward neural networks with different topologies are trained and tested using these features to enhance the networks' recognition capabilities.

The number of neurons in the hidden layer is increased from two to twenty, in increments of two. For each neural network, sixty percent of the available data is used for the training and forty percent for the testing. For every input vector, five different arrangements of the available training and testing data values are used, and the average recognition rate is calculated. The statistical features are used individually, in twos, and finally all of them together to train and test the neural networks. For different input vectors, the neural networks with the best average recognition rate are shown in Table 4.2.

The best recognition rate is obtained when kurtosis and skewness are used together as input feature vectors. Combining these vectors with the variance results in the recognition rate reduction, which is expected as the values for the variance for the sharp edge PD and surface PD are in the same range (Figure 4.7).

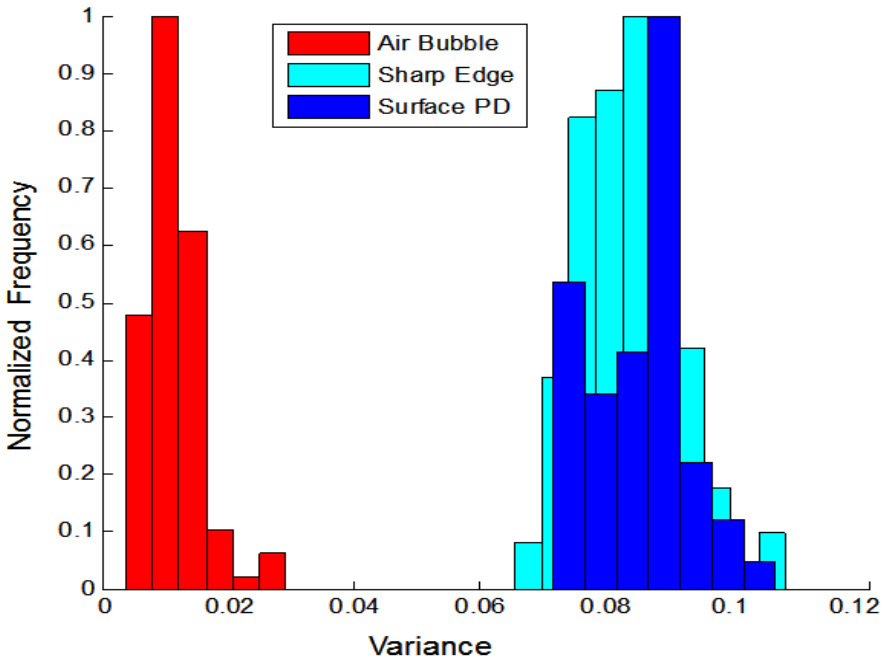

Figure 4.7: Histograms of variance values of the air bubble, sharp edge, and surface PD

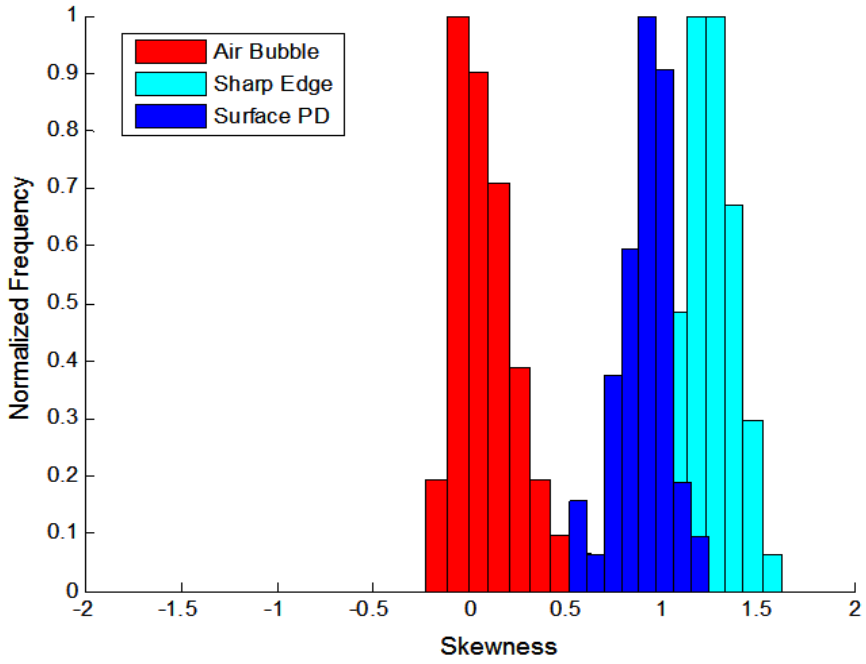

Figure 4.8: Histograms of skewness values of the air bubble, sharp edge, and surface PD

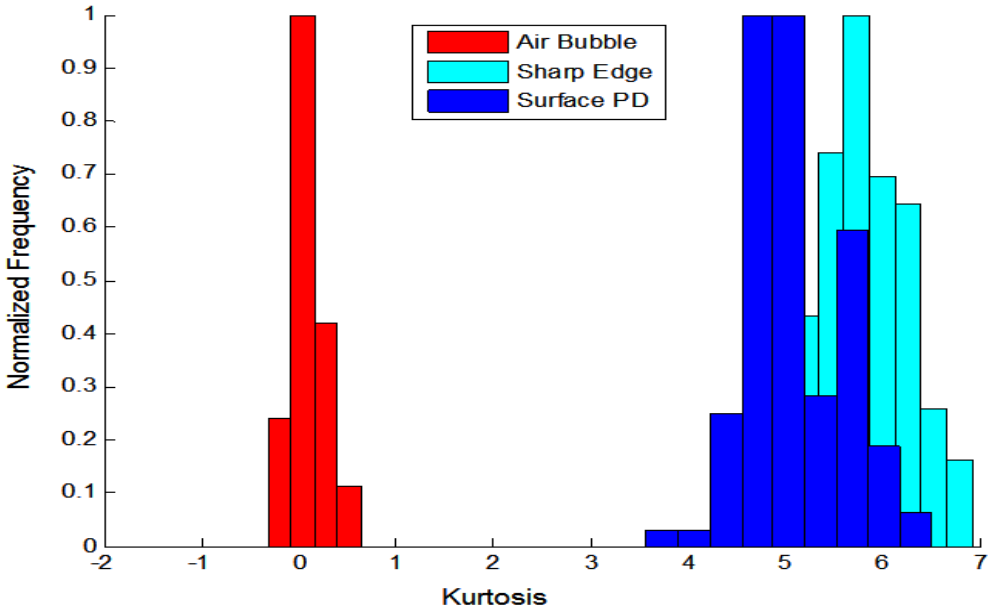

Figure 4.9: Histograms of kurtosis values of the air bubble, sharp edge, and surface PD

Table 4.2: Neural network results for PD source classification

Input Feature/s	**Best Average Recognition Rate**	**Number of Hidden Neurons**
Variance	45%	14
Skewness	79%	10
Kurtosis	76%	18
Variance and Skewness	85%	8
Variance and Kurtosis	83%	16
Skewness and Kurtosis	97%	18
Variance, Skewness, and Kurtosis	94%	20

4.2.4.2 Localization Module Results

Seventy PD signals of each type are injected into the five tap locations in each phase of the transformer winding, and the corresponding leakage currents are measured at the transformer neutral. The statistical features extracted from the measured signals corresponding to each tap location are used to train and test neural network classifiers for PD localization purposes. Because the tap locations in the same phase are close to each other (only 76 turns between them), the effect of the winding propagation path on the injected PD signals may be comparable. Furthermore, as the tap location distribution in all three phases is identical, the signatures of the different windings on the PD signals occurring at the same tap position may be indistinguishable. Therefore, the PD source is localized within the taps of the same phase and within the same taps of different phases.

i. Localization of PD within taps of the same phase

The best average recognition rates for the localization of PD sources within each phase of the transformer are shown in Tables 4.3 through 4.5. Recognition rates of 60% to 70% are achieved when using the variance individually; however, when combined with skewness or kurtosis, the recognition rate rises to 96% in some cases. Combining the three features results in the best recognition rates, unless the variance affects the efficiency of the classification module.

Table 4.3: Neural network results for localizing air bubble PD in three phases

Input Feature/s	**Best Recognition Rate (Phase 1)**	**Best Recognition Rate (Phase 2)**	**Best Recognition Rate (Phase 3)**
Variance	69%	61%	62%
Skewness	80%	76%	78%
Kurtosis	96%	92%	95%
Variance and Skewness	87%	83%	85%
Variance and Kurtosis	94%	92%	94%
Skewness and Kurtosis	96%	94%	96%
Variance, Skewness, and kurtosis	97%	96%	95%

Table 4.4: Neural network results for localizing sharp edge PD in three phases

Input Feature/s	**Best Recognition Rate (Phase 1)**	**Best Recognition Rate (Phase 2)**	**Best Recognition Rate (Phase 3)**
Variance	57%	59%	61%
Skewness	87%	86%	88%
Kurtosis	83%	83%	87%
Variance and Skewness	81%	81%	83%
Variance and Kurtosis	86%	87%	91%
Skewness and Kurtosis	94%	95%	94%
Variance, Skewness, and Kurtosis	96%	98%	99%

Table 4.5: Neural network results for localizing surface PD in three phases

Input Feature/s	**Best Recognition Rate (Phase 1)**	**Best Recognition Rate (Phase 2)**	**Best Recognition Rate (Phase 3)**
Variance	73%	71%	72%
Skewness	84%	83%	85%
Kurtosis	95%	92%	95%
Variance and Skewness	90%	89%	91%
Variance and Kurtosis	96%	94%	97%
Skewness and Kurtosis	94%	92%	94%
Variance, Skewness, and Kurtosis	97%	96%	98%

ii. Localization of PD signals occurring at the same tap in different phases

To ensure that the leakage current signals corresponding to PD sources occurring at the same tap location in the three phases are recognizable, statistical features are extracted from twenty signals corresponding to tap locations T1 and T2 in phases (1) and (2). Figure 4.10 shows a three-dimensional distribution of variance-skewness-kurtosis for these signals. For T1 and T2 in both phases, the variance values for the two locations overlap, although there is less overlap in the kurtosis and skewness values. To enhance the recognition process, these statistical features are used in different combinations to train and test feedforward neural networks. Compared to the results obtained for the recognition of a tap location within the same phase, higher recognition rates are achieved (Table 4.6). Using the variance alone as the input vector in the training and testing process results in 76%- 81% recognition rate, while combining the three features results in 100% recognition rate.

Table 4.6: Neural network results for localizing different PD source for the taps (T1 and T2) in different phases.

Input Feature/s	**Air Bubble PD**	**Sharp Edge**	**Surface Discharge**
Variance	76%	79%	81%
Skewness	86%	88%	91%
Kurtosis	85%	86%	89%
Variance and Skewness	93%	93%	95%
Variance and Kurtosis	92%	93%	94%
Skewness and Kurtosis	96%	98%	99%
Variance, Skewness, and Kurtosis	99%	100%	100%

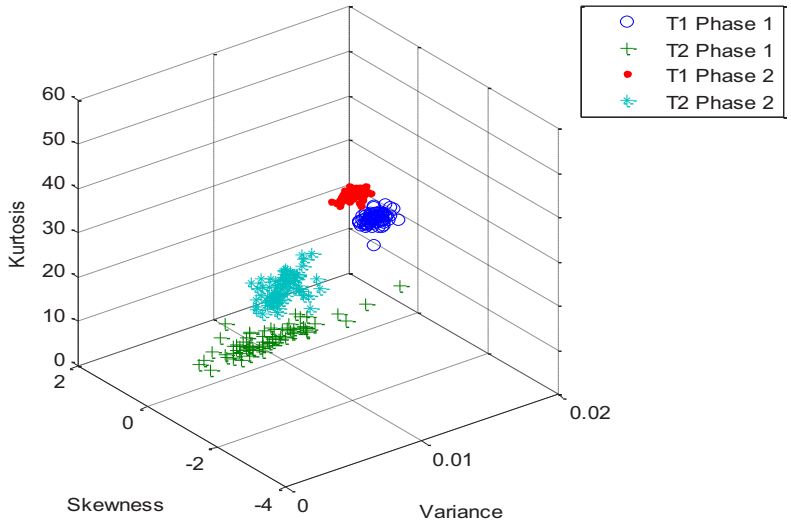

Figure 4.10: Three- dimension distribution of the variance- skewness- kurtosis for measured signals that result from air bubble PD injected in tap1 and 2 in first and second phase

4.3 Summary

In this chapter, leakage currents measured at a transformer neutral terminal have been used to construct the database required for developing the PD source classification and localization modules for a transformer under study. Three PD types were created and injected into each tap of a 45 kVA transformer. The corresponding leakage currents were then measured from the transformer neutral. The statistical features- variance, skewness, and kurtosis- were extracted from the measured signals and used to train and test feedforward neural networks of different topologies. Combining features in the training process resulted in better recognition rates.

Chapter 5

PD Charge Determination in Transformer Winding Insulation

5.1 Introduction

Transformer windings are responsible for approximately one-third of all transformer failures [5], and one of the principal causes of winding insulation failures is partial discharge (PD) [50]. The damage caused by PD to insulation is directly related to the PD charge [11, 14]. Although conventional PD detectors are usually used for measuring PD apparent charge, it is not possible to use them in a transformer environment. However, due to the importance of measuring PD charge, several studies have investigated the relationship between the output of other sensors, such as high frequency antennas and high frequency current transformers (HFCTs), and PD charge. The analysis in these studies is based on the terminal measured signals, which are greatly attenuated by the transformer materials, leading to undervaluation of the damage caused to the insulation system.

In this chapter, I develop a module for PD charge determination in transformer winding insulation as a part of the PD detection module (Figure 5.1). The charge calculated in this module is not the terminal charge but the internal PD charge injected into the transformer winding during a PD event. This charge is calculated using the transformer winding transfer function, and the leakage current measured at the transformer neutral, as shown in Figure 5.2.

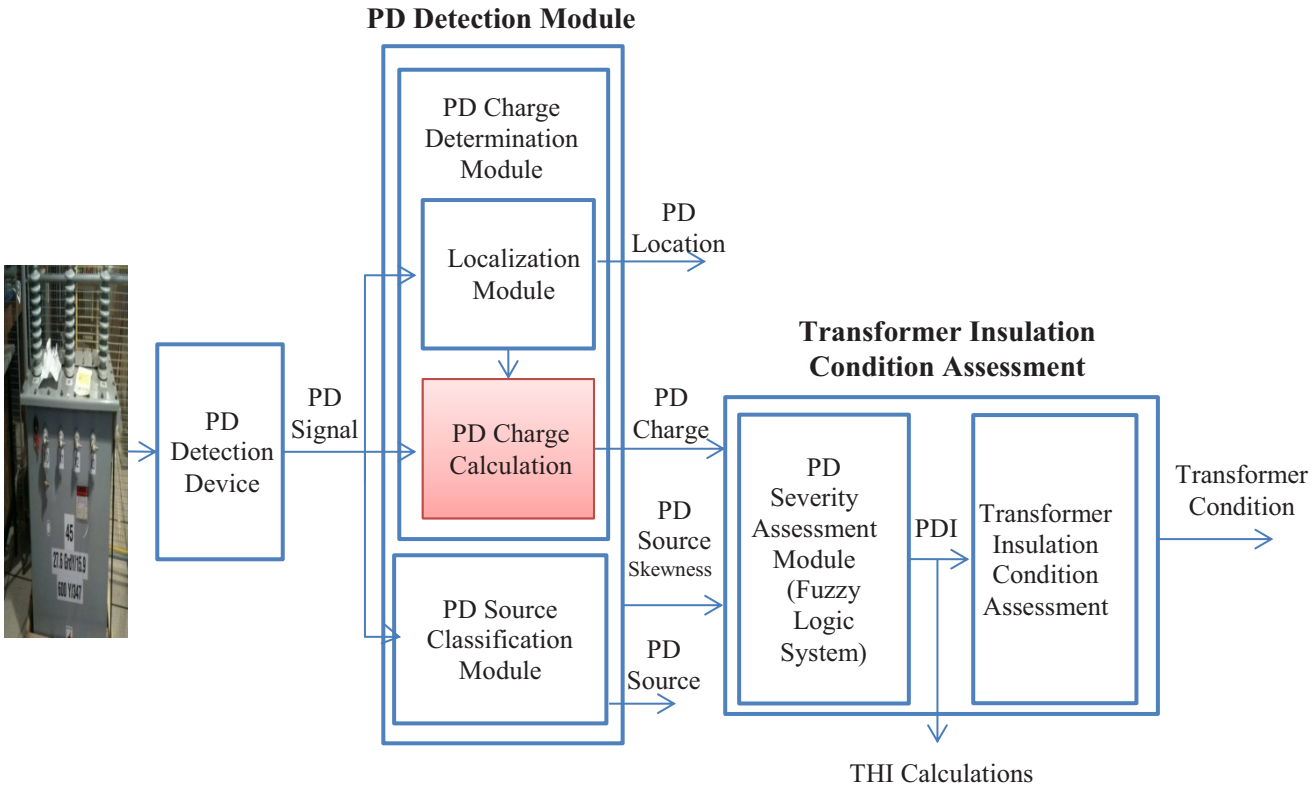

Figure 5.1: PD charge part of the developed PD detection modules

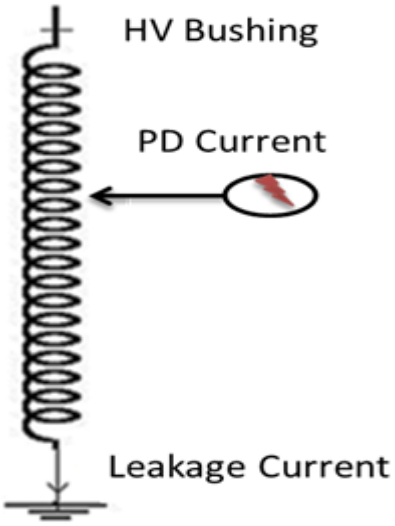

Figure 5.2: PD current injected into the transformer winding and the corresponding leakage current at the transformer neutral

5.2 PD Charge Determination Module

The PD charge determination module developed in this chapter is based on two main steps. The first step is creating a bank of transfer functions of the transformer winding for all possible winding configurations. The second step is the calculation of PD charge using transformer winding transfer function.

The measured leakage current at a transformer neutral undergoes the localization module developed in the previous chapter to determine the PD location along the winding. Hence, the transfer functions of the transformer winding configuration that corresponds to the location of the PD is selected; this is the transfer function selection process shown in Figure 5.3. The PD charge is then calculated using the selected transfer function; this is the PD charge calculation process shown in Figure 5.3.

The transfer functions are calculated by the vector fitting of the corresponding current frequency responses. The sweep frequency response method is used to measure the frequency response of the transformer winding by applying the end-to-end short circuit test (Figure 5.4), whereas the PD charge calculation module uses the selected transfer and the measured leakage current to calculate the PD current injected to the windings. The PD charge is calculated by integrating this injected current.

It is important to note that this method is applied only to PD signals with frequency content of up to 10 MHz. In higher frequency ranges, the winding frequency response is strongly affected by the setup configuration and connection cables, not the transformer structure. The frequency of PD occurring in transformer winding can range from tens to hundreds of kHz for surface discharges, and from hundreds of MHz to a few GHz for some bubble voids. However, the latter type has minimal capabilities to damage an insulation system [92]. Therefore, the frequency range of the developed method is suitable for calculating the PD charge of dangerous PD types.

Because the only accessible points along the winding of real transformers are tap locations, this study is limited to PD events occurring at these locations. However, if a similar transformer unit is specially manufactured with multiple access points along the transformer windings, more locations could be investigated. Another suggestion to overcome this limitation is to use the circuit model approach for calculating transfer functions. This approach depends mainly on R-L-C parameter calculations that require the availability of transformer-type materials and dimensions. For older

transformers that are still in service, this information would not be available. In such cases, the winding frequency response could be used to build the circuit model of the transformer winding.

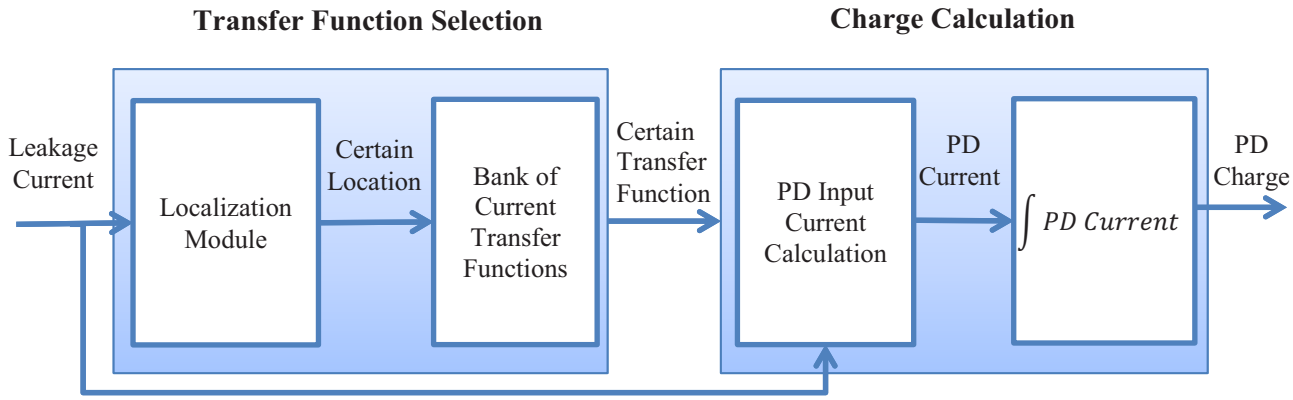

Figure 5.3: PD charge determination module

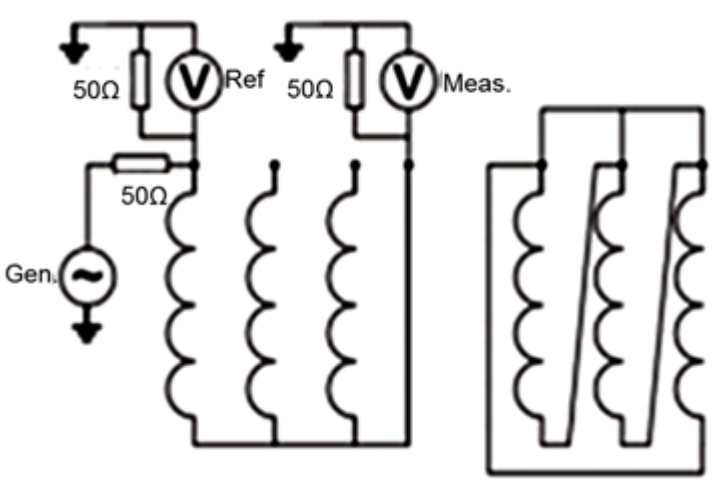

Figure 5.4 : End-to-End short circuit test [76]

5.3 Developing PD Charge Module for a Three-Phase Transformer

Developing the PD charge calculation module for a transformer involves creating a localization module, a bank of transfer functions, and a charge calculation module. The PD localization module for the real transformer under test has been developed in Chapter 4 using neural network classifiers. The only accessible points along the windings are the tap locations, five per phase (Figure 5.5). A

transfer function bank that contains the corresponding fifteen current transfer functions is constructed in this section, followed by the charge calculation module.

(a)

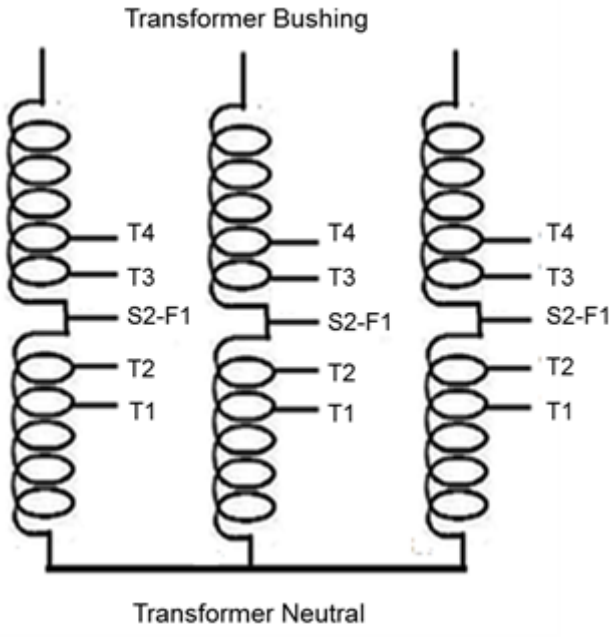

(b)

Figure 5.5: (a) Transformer under test, (b) schematic diagram of the winding

5.3.1 Constructing a Transfer Function Bank

The bank of current transfer functions contains all current transfer functions from the taps of each phase of the transformer to the neutral. The transfer functions are calculated from the current frequency response corresponding to each of the taps, and the sweep frequency response method is used to measure the frequency response. In order to measure the current frequency response associated with a certain tap location, the input to the tap and the corresponding output at the neutral are measured with an oscilloscope as voltage signals across resistances. The resistance used to measure the output current is connected between the transformer neutral and the ground, while the resistance used to measure the input signal is connected between the voltage supply and the tap location (Figure 5.6). The voltage across the resistance corresponding to the input current cannot be directly measured by an oscilloscope, as it is not directly connected to the ground. Therefore, an indirect method is employed to measure the voltage corresponding to the input current.

The current frequency response can be calculated as follows:

$$I_{Input} = \frac{V_1 - V_2}{R} \quad 5.1$$

$$I_{leakage} = \frac{V_3}{R} \quad 5.2$$

$$\frac{I_{leakage}}{I_{Input}} = \frac{1}{\frac{V_1}{V_3} - \frac{V_2}{V_3}} \quad 5.3$$

Where, V_1 is the supply voltage, V_2 is the voltage at the transformer taps, and V_3 is the output voltage.

To calculate the taps' current frequency response, I have measured $\frac{V_1}{V_3}$ and $\frac{V_2}{V_3}$ for each tap. The equations for the corresponding transfer functions are then calculated by means of vector fitting techniques.

5.3.2 Frequency Response Measurement Set-up

The sweep frequency response method, using end-to-end short circuit configuration, is used to measure the two frequency response signals $\frac{V_1}{V_3}$ and $\frac{V_2}{V_3}$ for each tap. The desired $\frac{I_{leakage}}{I_{input}}$ is then calculated using Equation 5.3. Figure 5.6 shows the arrangement used for $\frac{V_1}{V_3}$ and $\frac{V_2}{V_3}$ measurement.

Two equal resistors (50 Ohms) are used for measuring the voltage signals corresponding to the input and output current. A computer program called LV Bode controls a function generator and oscilloscope that respectively inject variable-frequency sinusoidal waves and measure V_1, V_2, and V_3 at each frequency value. These signals are then used to calculate the frequency vectors $\frac{V_1}{V_3}$ and $\frac{V_2}{V_3}$. The user interface for LV Bode, shown in Figure 5.7, illustrates how the user determines the frequency range and the number of measuring points. In this research, the frequency range is determined to be from 10 Hz to 10 MHz; and the number of measuring points is 1000. The function generator used in this study is an Agilent 33220A function/arbitrary, which can generate ten waveform shapes with a frequency of up to 20 MHz (Figure 5.8). The oscilloscope is a 2-channel Agilent 2000 series digital storage oscilloscope with 100 MHz bandwidth (Figure 5.9).

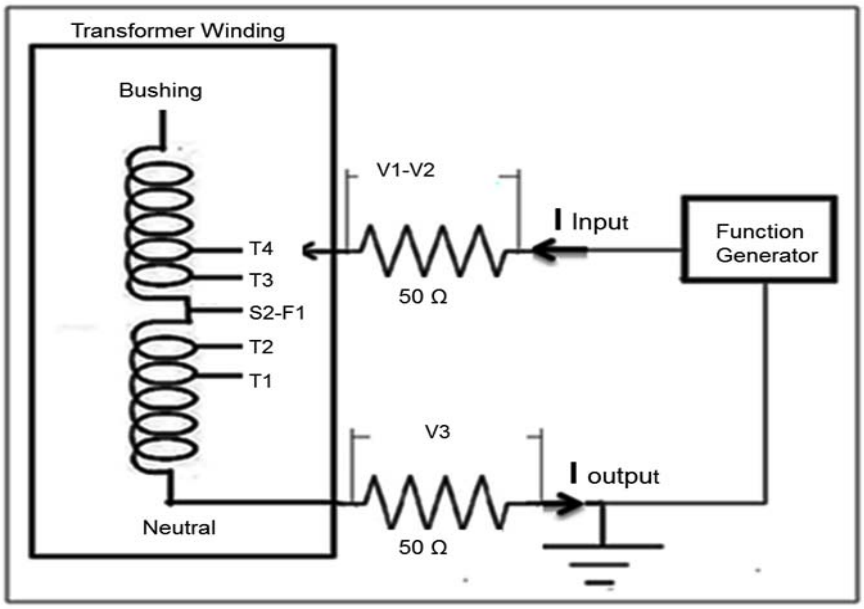

Figure 5.6: Schematic diagram of transformer winding frequency response measurement and calculation

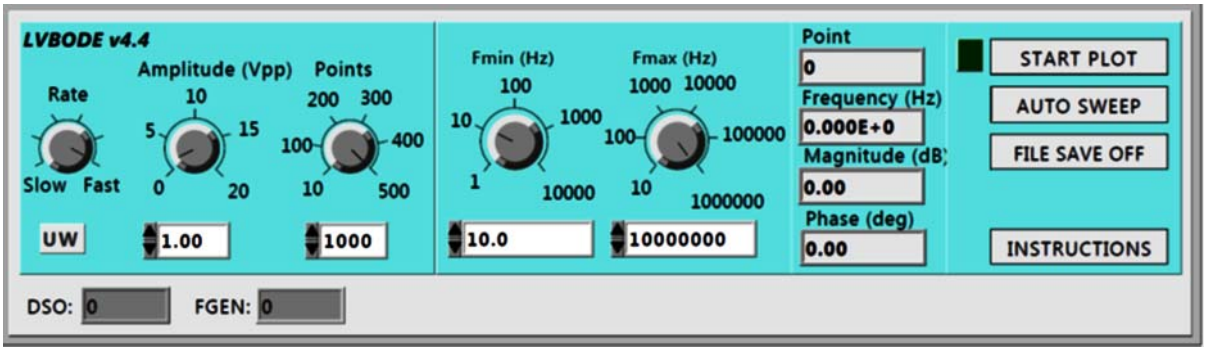

Figure 5.7: LV BODE user interface

Figure 5.8: The generator used in this study

Figure 5.9: The digital storage oscilloscope used in this study

The measured current frequency response magnitudes from each tap of each phase to the transformer neutral are shown in Figures 5.10 to 5.12. In the middle-frequency range, the fundamental resonance of the frequency responses occurs almost at the same frequency for all the taps, except that some taps have with higher magnitudes. The anti-resonance in the higher frequency band is not exactly the same. The current frequency response shows that only partial discharge signals of frequency content from 10 kHz to 1 MHz are detected from the transformer neutral; any other frequency content will be attenuated by the propagation path. The signals with frequency content ranging from 15 kHz to 3 kHz are the least attenuated.

One of the fault interpretation techniques from the winding frequency response is to compare a faulty phase response with that of a healthy phase from the same transformer. The measured input impedance frequency responses from the same tap location (T4) in the three phases (Figure 5.13) prove the applicability of this interpretation method to the transformer under study. The input impedance frequency responses of the three taps are extremely close to each other. Any structural changes occurring in the winding of the three phases would alter the winding impedance frequency response and can be recognized by comparing the phase after-fault frequency response with another healthy phase frequency response.

At very low frequency regions (e.g., from 10 Hz up to 500 Hz), the input impedance is mainly resistive. However, at low frequency bands, from 500 Hz to 2 kHz, the inductive reactance of the winding is greater than the capacitive reactance, hence, the Bode diagram shows a rising trend. In this frequency band, the impedance curve for T4 is higher than that of T1. This indicates a higher inductance value, as the number of turns included from T4 to the neutral is greater than those included in the winding from T1 to the neutral (Figure 5.14). Then, as the impedance frequency response approaches its fundamental resonance at the middle frequency range, the capacitive reactance of the winding becomes comparable to the inductive reactance, and the frequency response is affected by their interaction. Finally, at very high frequencies, the transformer equivalent circuit consists mainly of the shunt and series capacitance, which reach extremely low values and can thus be neglected; therefore, the test configuration and connection cable determine the behavior of the circuit [69, 70, 71].

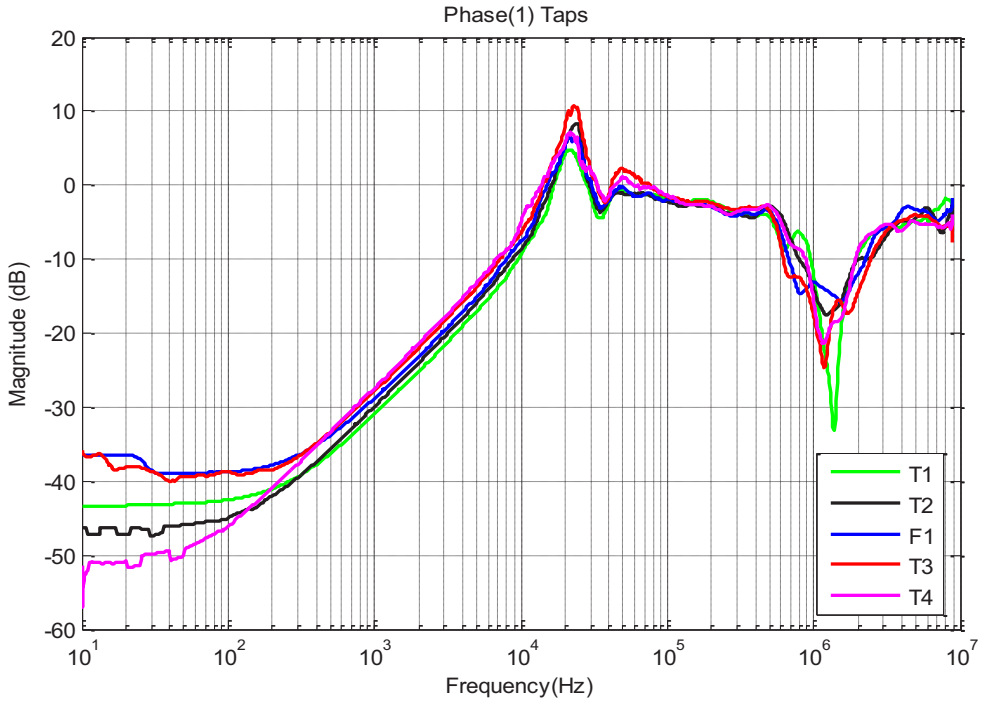

Figure 5.10: Measured current frequency response for the taps in phase 1

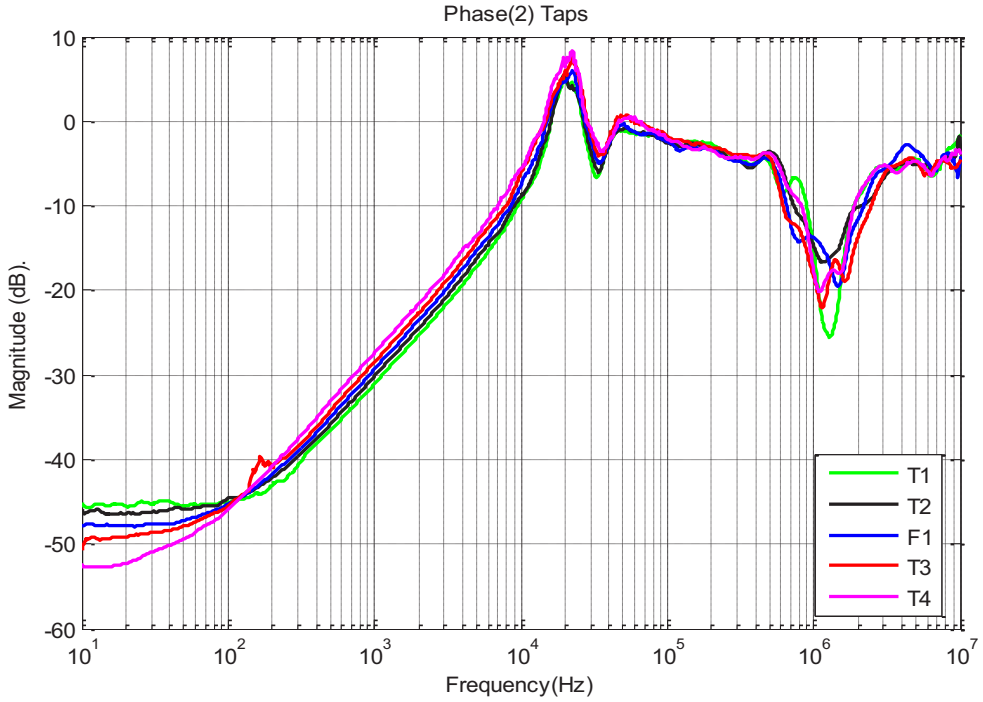

Figure 5.11: Measured current frequency response for the taps in phase 2

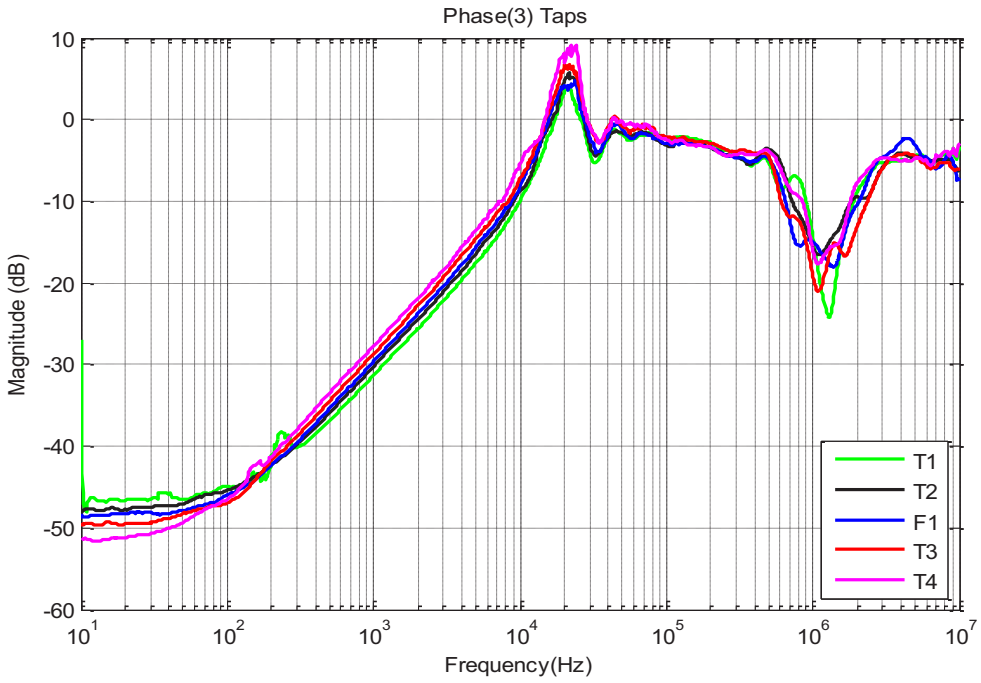

Figure 5.12: Measured current frequency response for the taps in phase 3

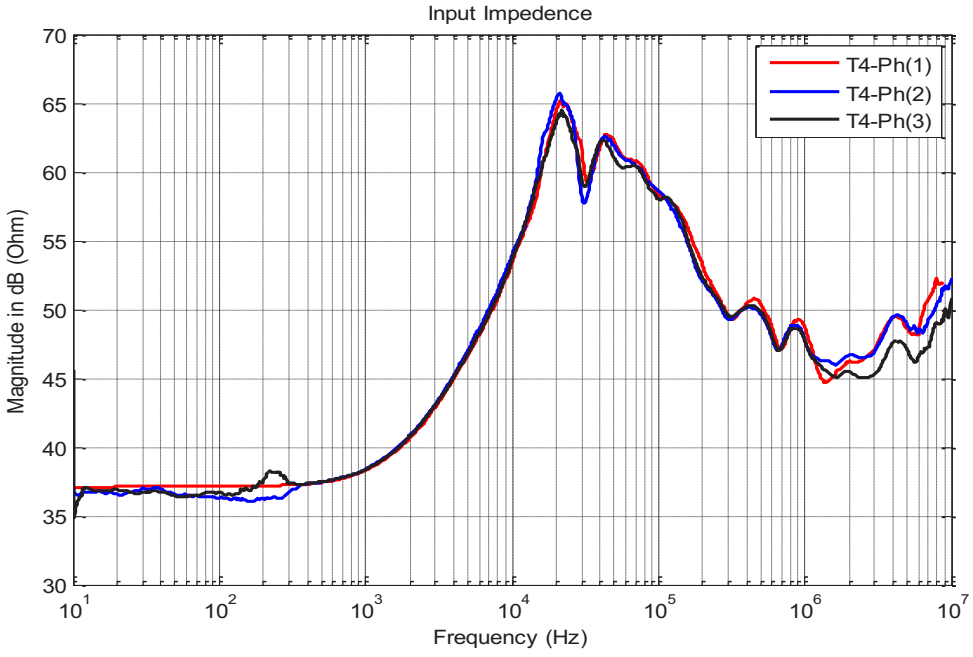

Figure 5.13: Measured input impedance frequency response for the T4 in the three phases

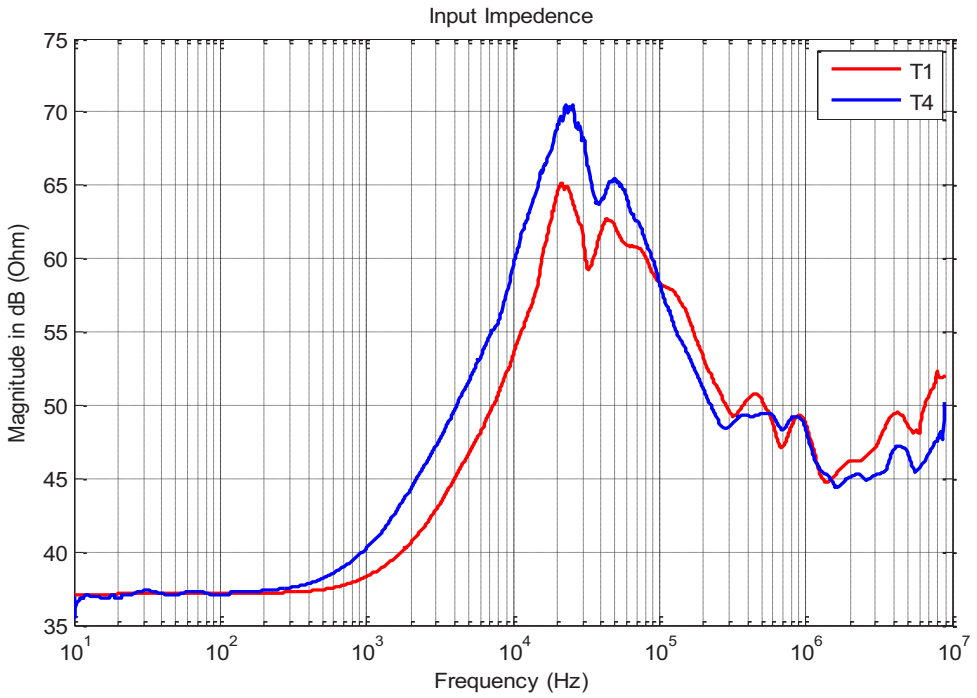

Figure 5.14: Measured input impedance frequency response of T1 and T4 in phase 1

5.3.3 Transfer Function Estimation by Vector Fitting

The numerical representation of the frequency response is valuable in fault interpretation. In this thesis, the transfer function approximation of the measured frequency response is calculated and used in the PD calculation module. As the vector fitting method has proven to be highly suitable for fitting the measured frequency response of transformer winding, the MATLAB toolbox function "rationalfit" is used in this research.

The "rationalfit" function fits the frequency response vector and corresponding frequency values in a pole-residue rational function shown in [93]. The accuracy of the estimated function is controlled by changing either one or both of two values: "error tolerance" and "number of iterations". The error in this function is the root mean square error between two successive iterations. Moreover, because the number of poles and zeros in a system is dependent only on the system structure, the system order should not be affected by changing the error. However, because the transfer function method is a mathematical approximation of the system frequency response, the orders of the transfer functions are affected by changing the minimum required error. The smaller the error, the higher the transfer

function order and computation complexity are. The default error value used in the matlab function "rationalfit' is -40 dB.

For estimating the winding taps transfer functions corresponding to the measured frequency response, using this value (-40 dB.) results in a transfer function with very high orders that would complicate any further calculations. Therefore, the error used in this research in "rationalfit' has to be properly evaluated. To estimate these errors, for each frequency response, first, an estimate of the function orders is done by visual inspection of the break points and asymptote slopes as described in Section 3.2.2.1 (i). Second, in "rationalfit", the error set is changed over a wide range and the corresponding transfer function is calculated. At each error value, the transfer function order is compared with the estimated order; the frequency response is calculated from the calculated transfer function and compared to the measured frequency response; the calculated transfer function and leakage current are used to calculate the input PD charges for test PD signals, and hence the charge, and then compared to measured PD charge values. The error values used in calculating the transfer function of each tap are shown in Table 5.1. Moreover, the number of iterations is changed as well and, for all taps, after a certain number of iterations (20), the transfer function order does not change.

Table 5.1: Errors used in estimating the transfer functions from the corresponding frequency response of each tap in the three phases

	Error(dB)		
	Phase (1)	**Phase(2)**	**Phase(3)**
T1	-20	-18	-18
T2	-14	-17	-18
F1	-16	-18	-16
T3	-14	-18	-14
T4	-20	-18	-18

The approximated transfer functions from each tap of the transformer winding to the neutral terminal are shown in Tables 5.2 to 5.4. The approximated transfer functions are in ordinary rational form as shown in Equation 5.4. For each tap, the frequency response is calculated from the chosen transfer function and compared to the measured frequency response (Figures 5.15 to 5.25). In these figures, the curve in red is the measured current frequency response (at 1000 points over the frequency spectrum 10 Hz to 10 MHz) , and the blue curve is the frequency response calculated from the approximated corresponding transfer functions. The measured and calculated frequency responses are found to fit each other quite closely.

The magnitude of the calculated frequency response that corresponds to the winding section from tap T1, in phase (1), to the neutral terminal closely fits the corresponding measured frequency response, except at the very low frequency region and the anti-resonance region (Figure 5.15). However, the frequencies corresponding to the resonance and anti-resonance are almost the same in the calculated and measured ones. The calculated frequency response that corresponds to T1, in phase (2), has a better fit than the calculated frequency response of T1 in phase (1) in the low frequency region (Figure 5.20). The calculated frequency response of T1 in the third phase has a much better fit, in low and high frequency regions, than the calculated frequency responses of tap T1 in the other two phases (Figure 5.25).The calculated frequency responses for tap T2 in the transformer's three phases closely fit the measured ones except at 5*105 Hz. Around this frequency, the measured frequency response has slight oscillations, which are neglected in the fitted one (Figures 5.16, 5.21, and 5.26). The calculated frequency response of tap F1 in phase (1) is very close to the measured one except at the anti-resonance region. At the anti-resonance region, the measured frequency response has two peaks; however, in the calculated frequency response, there is only one peak with a lower magnitude (Figure 5.17). For tap F1 in the second and third phases, the calculated frequency responses have a better fit to the measured frequency responses than the calculated frequency response that corresponds to F1 in phase(1) (Figures 5.22 and 5.27). The calculated frequency responses for taps T3 in the three phases strongly fit the measured frequency responses, except in the low frequency region (Figures 5.18, 5.23, and 5.28). For T4 in the three phases, the calculated frequency response precisely fit the corresponding measured ones (Figures 5.19, 5.24, and 5.29). In general, the deviations occur either in the very low or very high frequency regions, which are not of interest to this study. The harmful PD types usually exist in the middle region, so these approximations are suitable for PD applications.

$$TF = H(s) = \frac{b_0 s^n + b_1 s^{n-1} + \cdots + b_{n-1} s + b_n}{s^n + a_1 s^{n-1} + \cdots + a_{n-1} s + a_n} \quad 5.4$$

where,

$B = [b_0, b_1, \ldots, b_{n-1}, b_n]$, $A = [1, a_1, \ldots, a_{n-1}, a_n]$.

Table 5.2: Calculated transfer functions for winding taps in phase (1)

Tap	Transfer Function
T1	$B = [7.367 * 10^6, -2.566 * 10^{12}, 1.205 * 10^{19}, -1.859 * 10^{23}, -6.458 * 10^{27}, -7.773 * 10^{32}, 2.964 * 10^{35}]$ $A = [1, 1.188 * 10^7, 2.649 * 10^{13}, 1.92 * 10^{19}, 1.307 * 10^{24}, 7.682 * 10^{28}, 1.056 * 10^{33}, 2.772 * 10^{37}]$
T2	$B = [6.194 * 10^6, -2.568 * 10^{12}, 1.015 * 10^{19}, -3.323 * 10^{23}, 1.993 * 10^{27}, -5.752 * 10^{32}, 6.617 * 10^{34}]$ $A = [1, 1.095 * 10^7, 2.139 * 10^{13}, 1.555 * 10^{19}, 8.358 * 10^{23}, 4.43 * 10^{28}, 5.449 * 10^{32}, 1.637 * 10^{37}]$
F1	$B = [4.41 * 10^6, -1.545 * 10^{12}, 1.01 * 10^{19}, -2.567 * 10^{23}, -2.178 * 10^{27}, -7.179 * 10^{32}, 2.444 * 10^{35}]$ $A = [1, 6.301 * 10^6, 2.232 * 10^{13}, 1.639 * 10^{19}, 9.458 * 10^{23}, 5.56 * 10^{28}, 6.97 * 10^{32}, 1.964 * 10^{37}]$
T3	$B = [5.315 * 10^6, -9.771 * 10^{11}, 9.409 * 10^{18}, -2.808 * 10^{23}, -2.814 * 10^{26}, -5.999 * 10^{32}, -1.33 * 10^{35}]$ $A = [1, 8.725 * 10^6, 2.375 * 10^{13}, 1.296 * 10^{19}, 7.099 * 10^{23}, 3.715 * 10^{28}, 4.549 * 10^{32}, 1.285 * 10^{37}]$
T4	$B = [6.127 * 10^7, 1.777 * 10^{12}, 6.914 * 10^{18}, 5.697 * 10^{24}, -2.001 * 10^{29}, -2.378 * 10^{33}, -4.409 * 10^{38}, 10^{40}]$ $A = [1, 1.111 * 10^7, 3.236 * 10^{13}, 2.281 * 10^{19}, 1.07 * 10^{25}, 5.19 * 10^{29}, 3.101 * 10^{34}, 3.84 * 10^{38}, 1.004 * 10^{34}]$

Table 5.3: Calculated transfer functions for winding taps in phase (2)

Tap	Transfer Function
T1	$B = [6.251 * 10^{6}\ ,\ 2.257 * 10^{13}\ , 1.584 * 10^{18}\ 3.588 * 10^{25}\ , -1.92 * 10^{29}\ , -2.282 * 10^{34}\ , -1.165 * 10^{39}, -6.703 * 10^{43}\ , 1.478 * 10^{40}]$ $A = [1, 1.442 * 10^{7}, 6.353 * 10^{13}\ , 1.082 * 10^{20}\ , 5.708 * 10^{25},\ 5.227 * 10^{30}\ , 2.141 * 10^{35},\ 8.753\ * 10^{39}\ ,\ 1.071\ 10^{44}\ , 2.475 * 10^{48}]$
T2	$B = [7.581 * 10^{6}\ , -3.116 * 10^{12}\ , 1.13 * 10^{19}\ , -3.52 * 10^{23}\ , 4.68 * 10^{26}\ , -6.594 * 10^{32}\ , 1.406 * 10^{35}]$ $A = [1, 1.348 * 10^{7}\ ,\ 2.585 * 10^{13}, 1.867 * 10^{19}\ , 1.023 * 10^{24}, 5.97 * 10^{28}\ ,\ 7.064 * 10^{32}\ , 1.997 * 10^{37}]$
F1	$B = [4.947 * 10^{6}\ , -1.796 * 10^{12}\ , 1 * 10^{19}\ , -3.2 * 10^{23}\ , 1.876 * 10^{27}\ , -5.935 * 10^{32}\ , 1.296 * 10^{35}]$ $A = [1\ , 7.423 * 10^{6}\ , 2.393 * 10^{13}\ , 1.688 * 10^{19}\ ,\ 8.391 * 10^{23}, 4.907 * 10^{28}\ , 5.815 * 10^{32}, 1.627 * 10^{37}]$
T3	$B = [6.016 * 10^{6}\ , -9.043 * 10^{11}\ , 9.2054 * 10^{18},$ $-7.13 * 10^{22}\ , -7.351 * 10^{27}\ , -3.856 * 10^{32}\ , -2.378 * 10^{37}\ ,\ 5.379 *\ 10^{38}]$ $A = [1\ , 1.047 * 10^{7}\ ,\ 2.817 * 10^{13}\ , 1.405 * 10^{19}\ , 1.248 * 10^{24}\ \ , 5.281 * 10^{28},$ $2.217 * 10^{33}\ , 2.818 * 10^{37}\ , 6.118 * 10^{41}]$
T4	$B = [6.141 * 10^{6}\ \ 1.574 * 10^{12}\ \ 6.499 * 10^{18}\ \ 5.027 * 10^{24}\ \ - 1.929 * 10^{29}\ \ 5.805 * 10^{32}\ \ - 3.721 * 10^{38}\ \ 3.998 *\ 10^{40}]$ $A = [1\ , 1.087 * 10^{7}\ ,\ 3.057 * 10^{13}\ , 2.261 * 10^{19}\ , 9.625 * 10^{24},\ \ 4.157 * 10^{29}\ ,\ 2.527 * 10^{34}\ ,\ 2.877 * 10^{38}\ , 8.026 * 10^{42}]$

Table 5.4: Calculated transfer functions for winding taps in phase (3)

Tap	Transfer Function
T1	$B = [5.783 * 10^{6}, -2.01 * 10^{12}, 8.515 * 10^{18}, -1.347 * 10^{23}, -4.071 * 10^{27}, -4.093 * 10^{32}, 9.253 * 10^{34}]$ $A = [1, 9.44 * 10^{6}, 2.178 * 10^{13}, 1.37 * 10^{19}, 9.79 * 10^{23}, 4.983 * 10^{28}, 6.513 * 10^{32}, 1.604 * 10^{37}]$
T2	$B = [7.841 * 10^{6}, -3.343 * 10^{12}, 1.059 * 10^{19}, -2.715 * 10^{23}, -1.596 * 10^{27}, -6.288 * 10^{32,} 1.014 * 10^{35}]$ $A = [1, 1.393 * 10^{7}, 2.464 * 10^{13}, 1.757 * 10^{19}, 1.079 * 10^{24}, 5.776 * 10^{28}, 7.44 * 10^{32}, 1.959 * 10^{37}]$
F1	$B = [4.471 * 10^{6}, -1.736 * 10^{12}, 8.277 * 10^{18}, -2.03 * 10^{23}, -2.252 * 10^{26}, -4.162 * 10^{32}, 1.117 * 10^{35}]$ $A = [1, 6.507 * 10^{6}, 2.073 * 10^{13}, 1.396 * 10^{19}, 7.726 * 10^{23}, 4.039 * 10^{28}, 5.015 * 10^{32}, 1.315 * 10^{37}]$
T3	$B = [5.938 * 10^{6}, -1.539 * 10^{12}, 8.696 * 10^{18}, -2.322 * 10^{23}, -9.233 * 10^{26}, -4.327 * 10^{32}, -7.367 * 10^{34}]$ $A = [1, 1.025 * 10^{7}, 2.44 * 10^{13}, 1.313 * 10^{19}, 7.553 * 10^{23}, 3.613 * 10^{28}, 4.45 * 10^{32}, 1.093 * 10^{37}]$
T4	$B = [6.315 * 10^{6}, -3.036 * 10^{12}, 8.759 * 10^{18}, -3.6 * 10^{23}, 1.762 * 10^{27}, -5.917 * 10^{32}, 7.958 * 10^{34}]$ $A = [1, 1.011 * 10^{7}, 2.093 * 10^{13}, 1.423 * 10^{19}, 6.374 * 10^{23}, 3.726 * 10^{28}, 4.261 * 10^{32}, 1.22 * 10^{37}]$

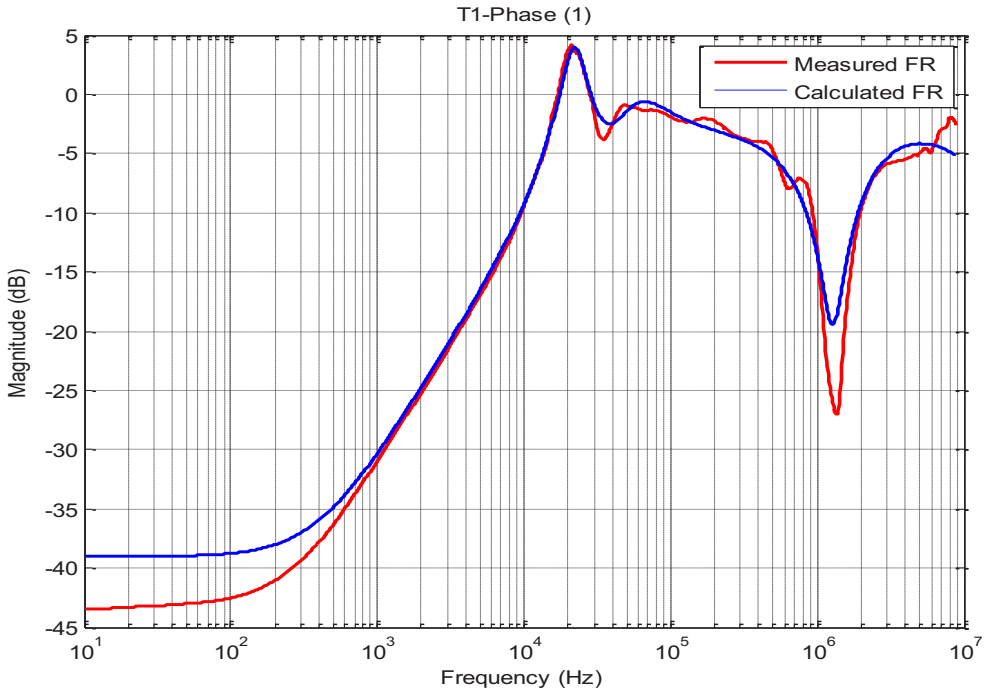

Figure 5.15 : Measured and calculated frequency response for tap T1 in phase 1

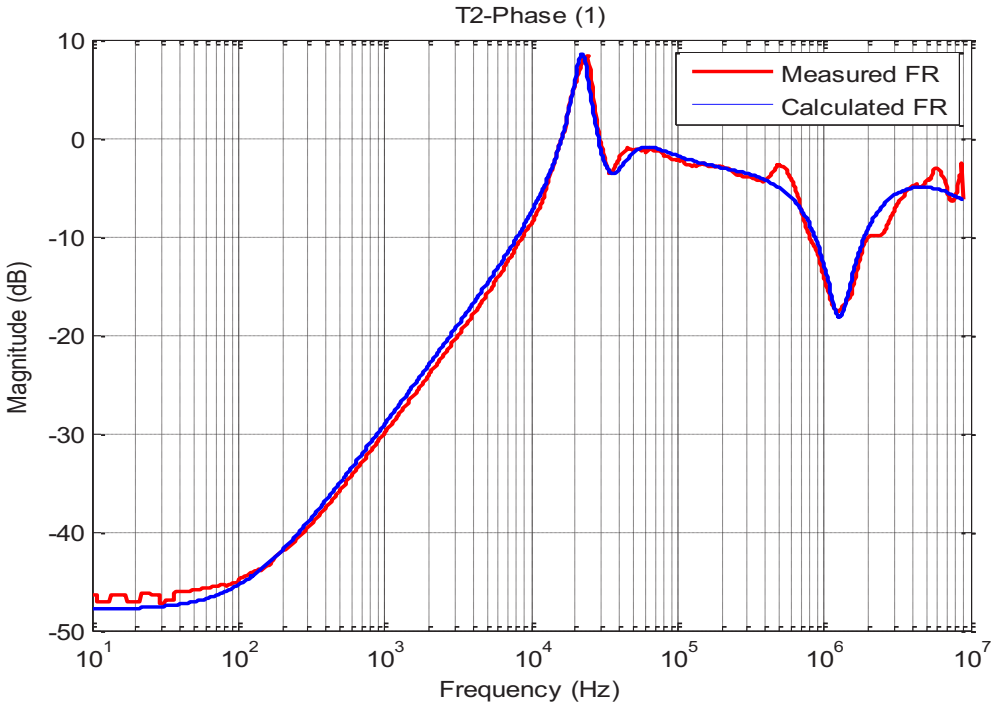

Figure 5.16: Measured and calculated frequency response for tap T2 in phase 1

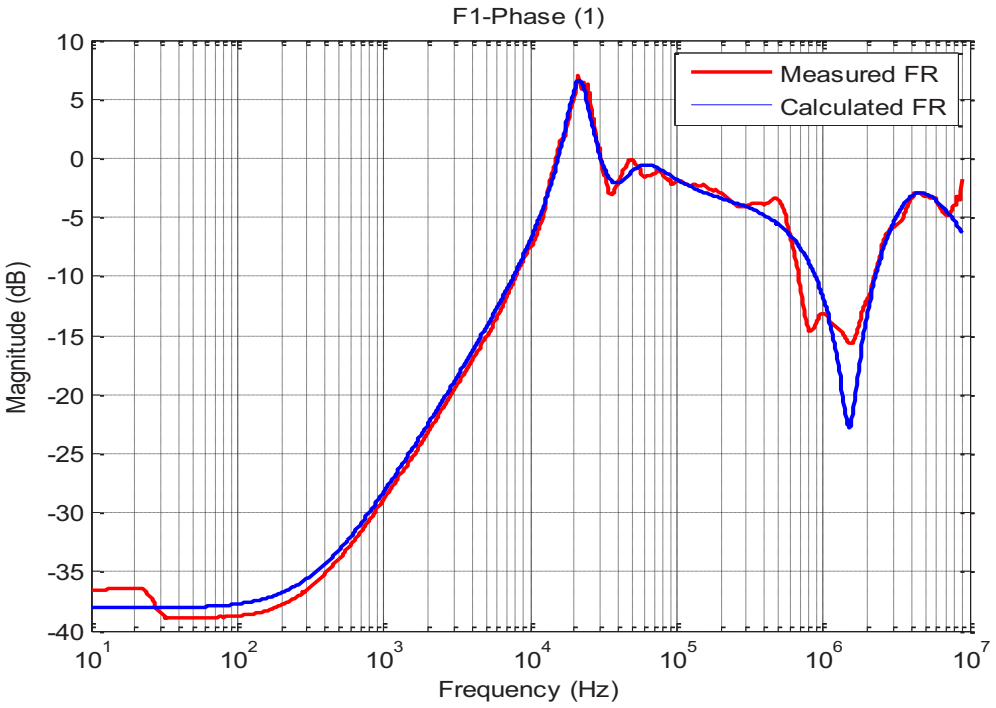

Figure 5.17: Measured and calculated frequency response for tap F1 in phase 1

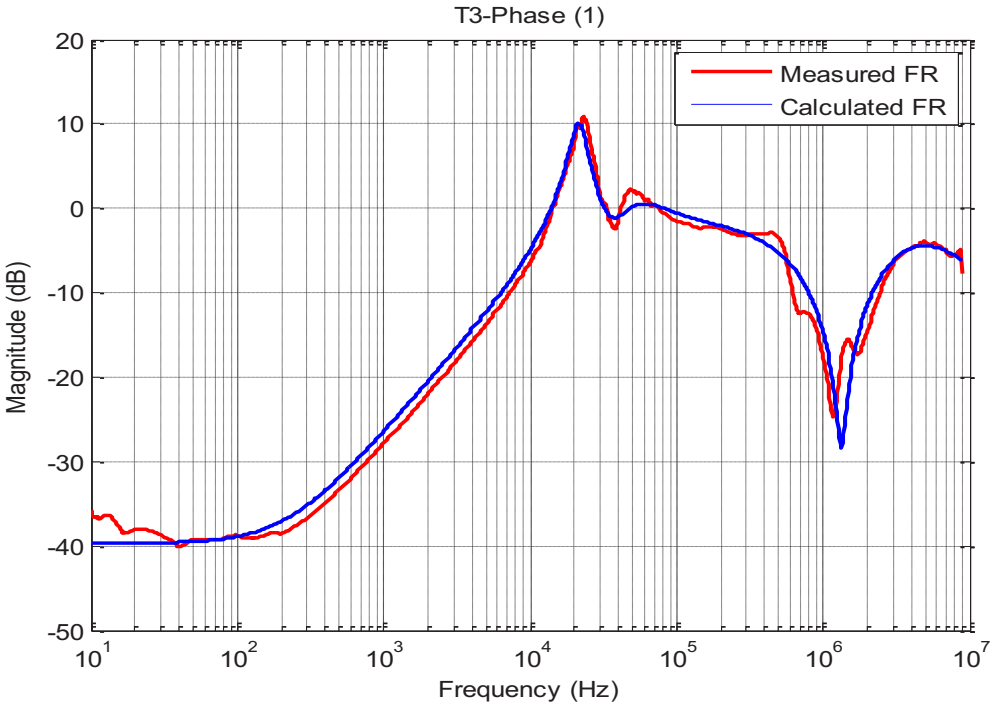

Figure 5.18: Measured and calculated frequency response for tap T3 in phase 1

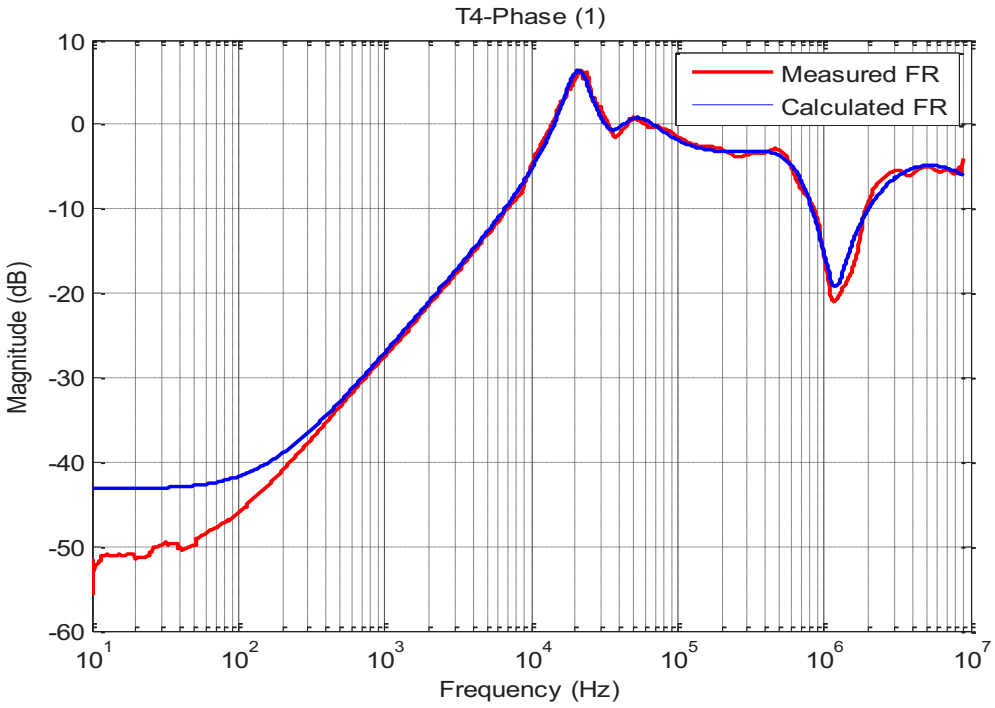

Figure 5.19: Measured and calculated frequency response for tap T4 in phase 1

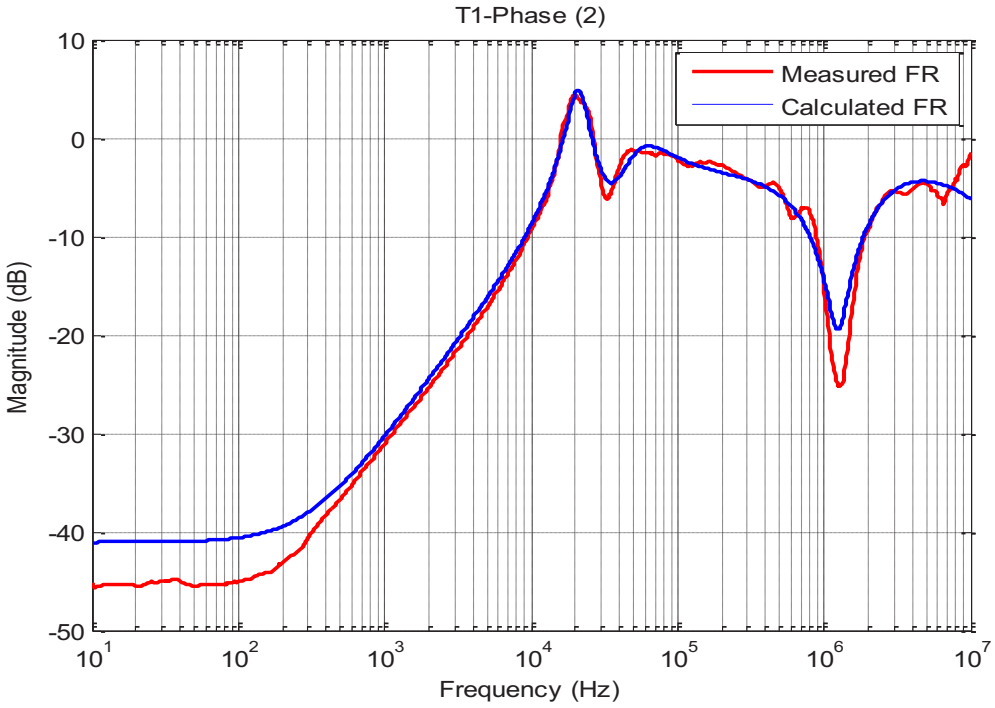

Figure 5.20: Measured and calculated frequency response for tap T1 in phase 2

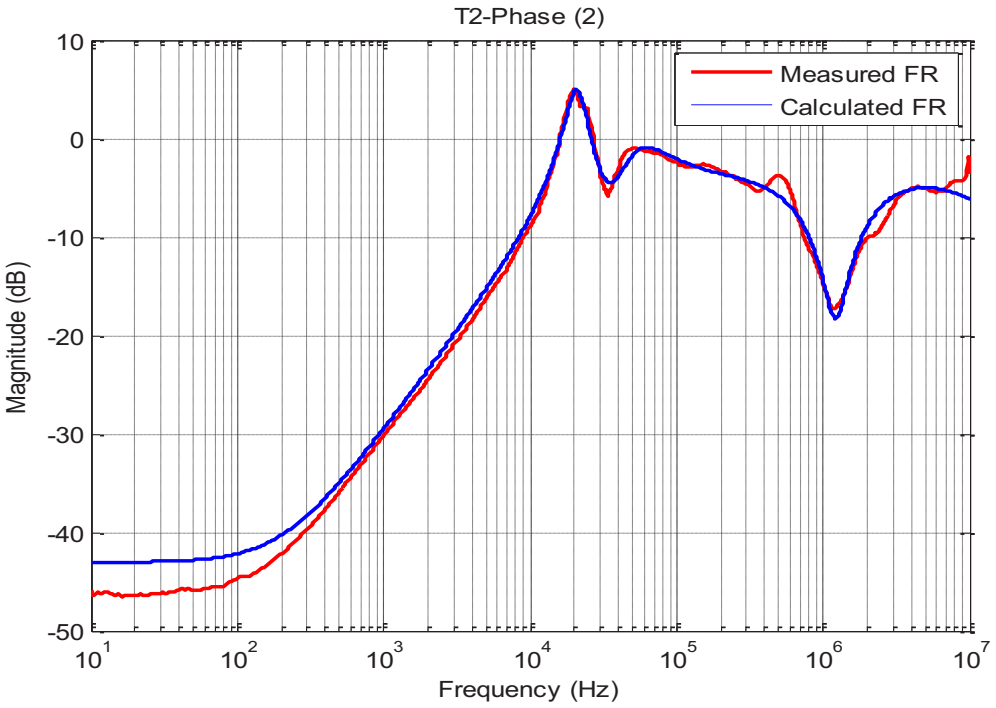

Figure 5.21: Measured and calculated frequency response for tap T2 in phase 2

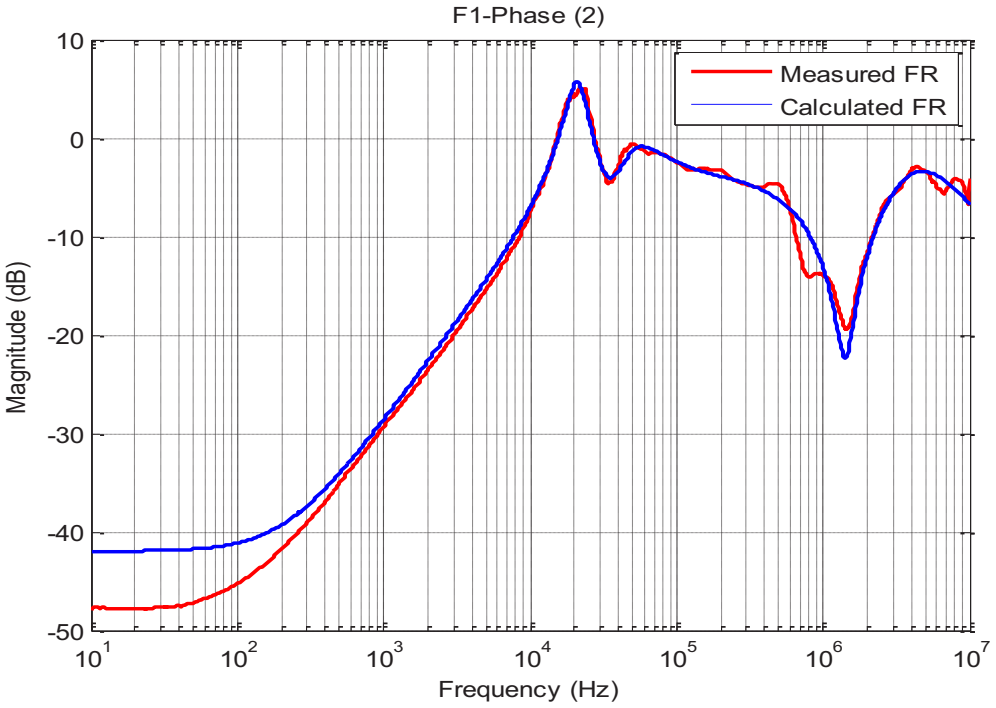

Figure 5.22: Measured and calculated frequency response for tap F1 in phase 2

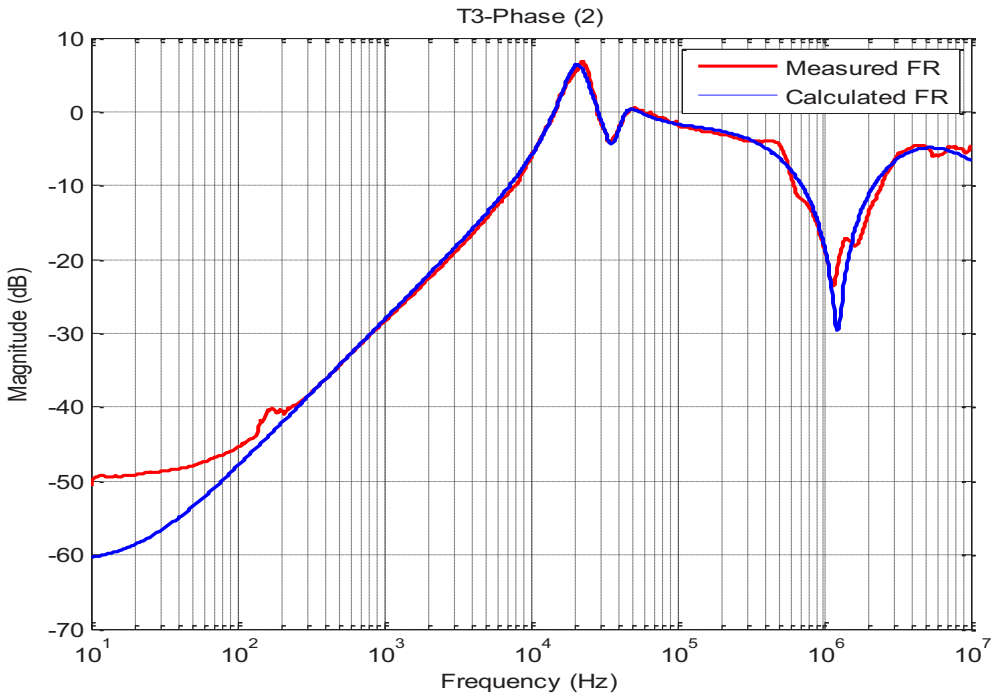

Figure 5.23 : Measured and calculated frequency response for tap T3 in phase 2

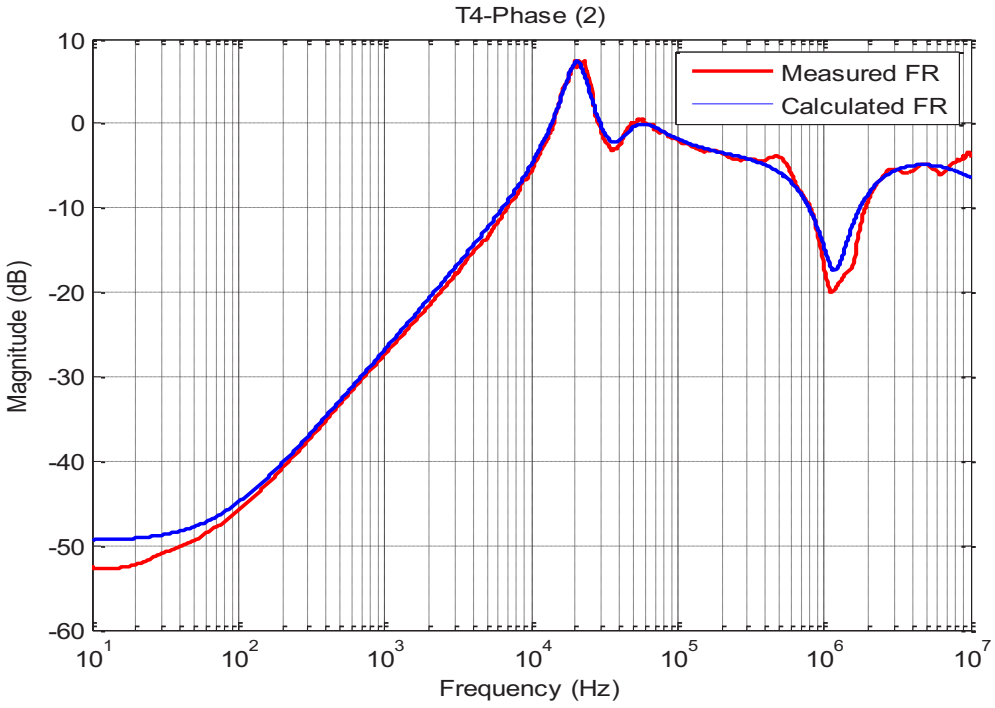

Figure 5.24: Measured and calculated frequency response for tap T4 in phase 2

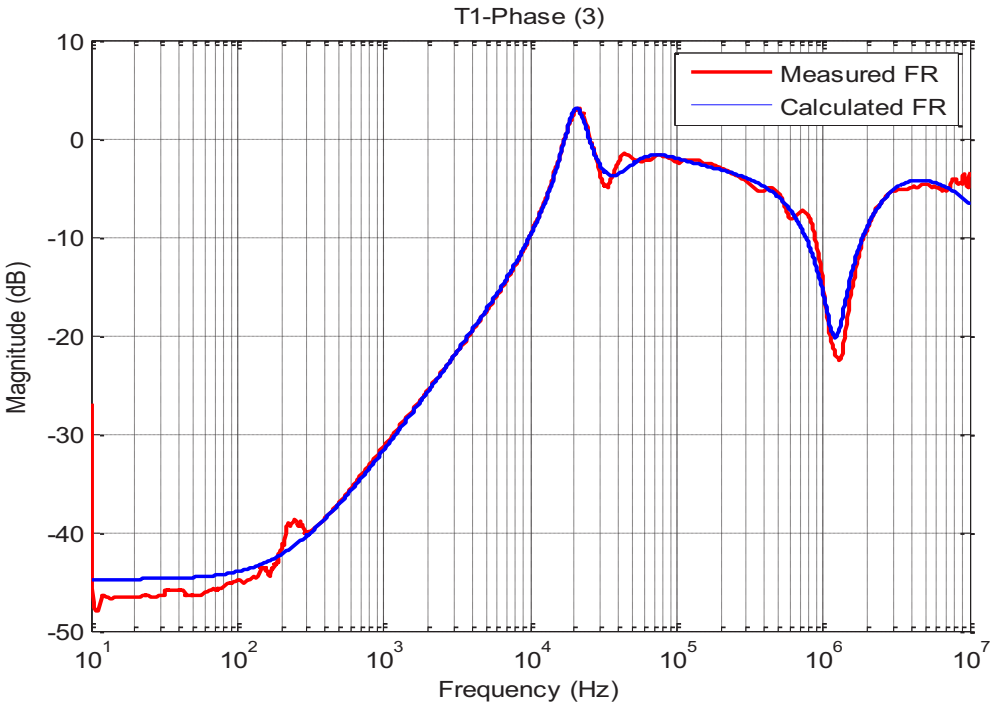

Figure 5.25: Measured and calculated frequency response for tap T1in phase 3

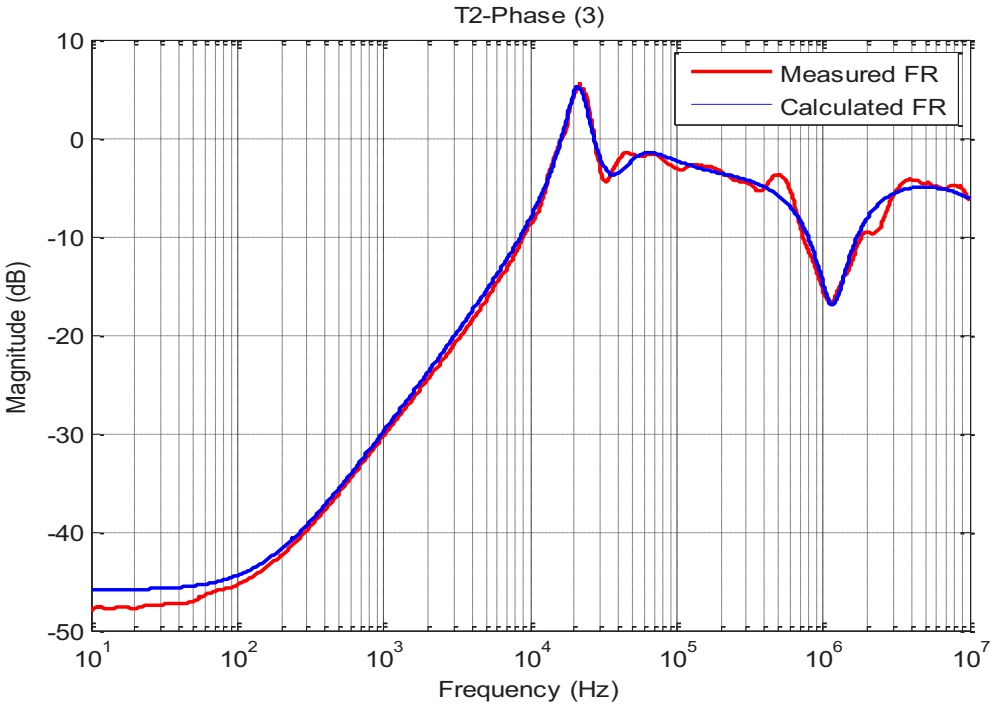

Figure 5.26: Measured and calculated frequency response for tap T2 in phase 3

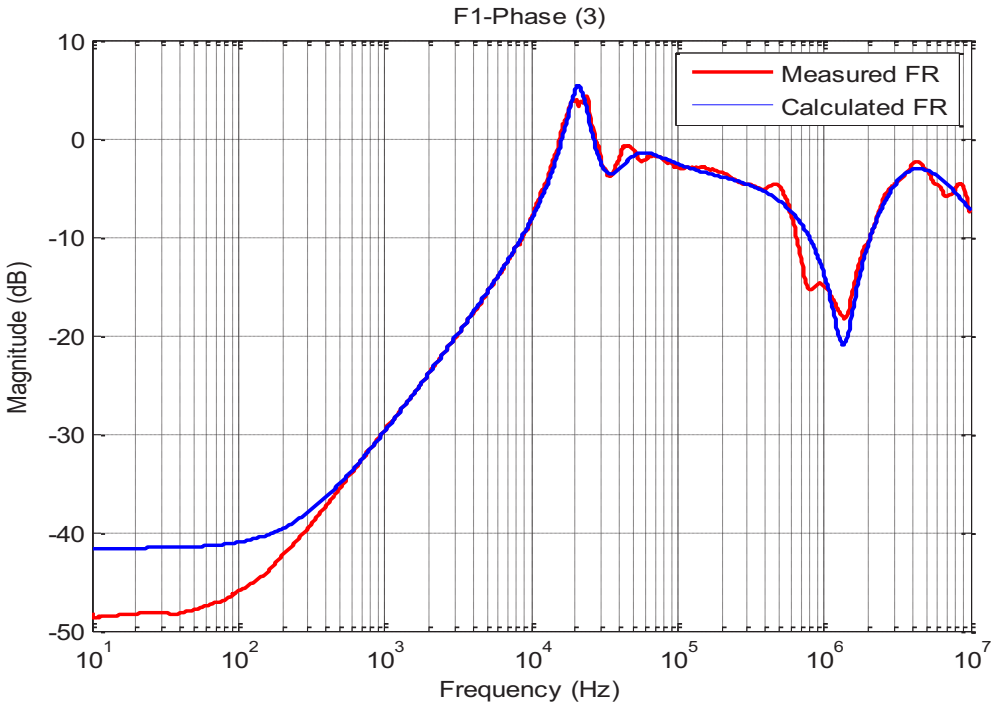

Figure 5.27: Measured and calculated frequency response for tap F1 in phase 3

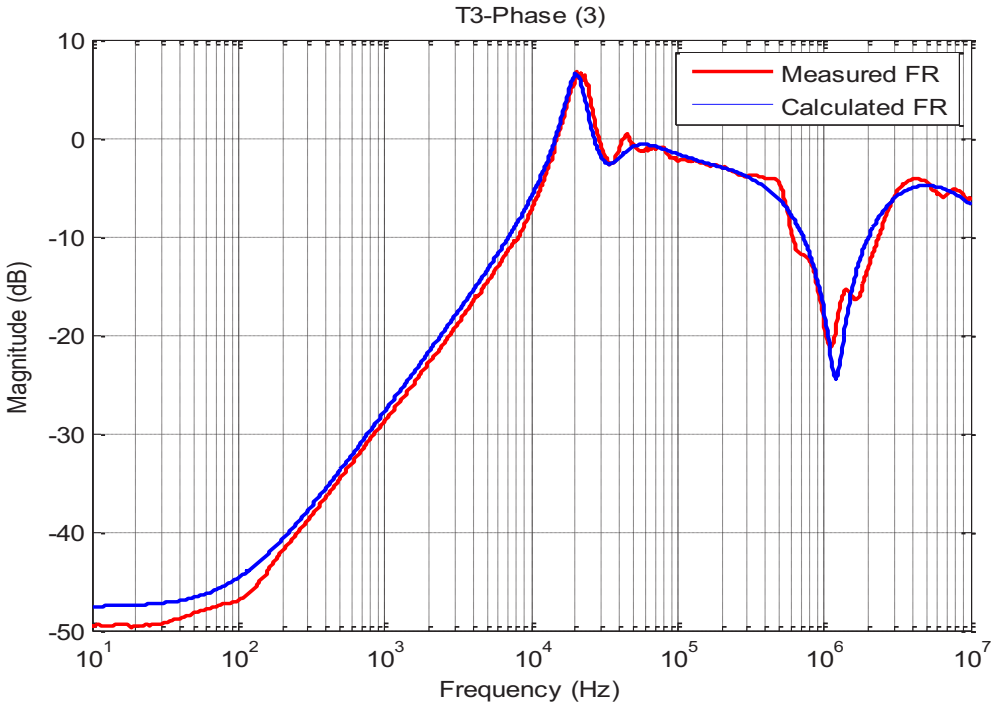

Figure 5.28: Measured and calculated frequency response for tap T3 in phase 3

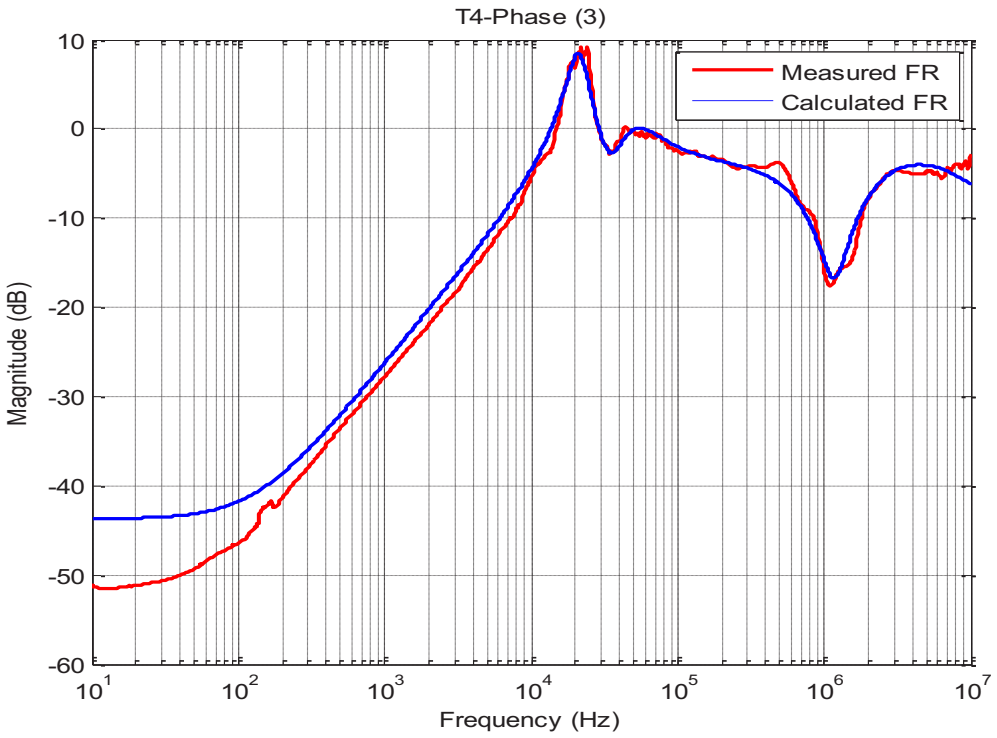

Figure 5.29: Measured and calculated frequency response for tap T4 in phase 3

5.3.4 PD Charge Calculation

The PD charge is the integration of a PD current waveform over time. To avoid the effect of a propagating path on the PD signals through the transformer winding, the PD charge is calculated from the PD input current injected into the transformer winding during a PD event. The PD input current waveform is obtained using a measured leakage current signal and tap winding transfer function. A specific transfer function is selected based on the localization module. The PD input current calculation can be performed either in the time, frequency, or Laplace domains. In the time domain, the transfer function is converted to the time domain, and the input current is calculated using convolution. In the frequency or Laplace domains, the leakage current signal is converted either to the frequency domain or Laplace domain by Fourier transform or Laplace transform, respectively. The input current is then calculated using mathematical operations.

In this study, all the calculations are done in the frequency domain. Fourier transform is used to convert the leakage current into the frequency domain, in which Equation 5.6 is used to calculate the

input PD current. The inverse Fourier transform is then used to convert the calculated PD current from the frequency domain to the time domain. The PD charge injected into the winding during the PD event is the integration of this PD input current waveform.

$$\text{Transfer Function} = \frac{I_{\text{PD leakage}}}{I_{\text{PD input}}} \tag{5.5}$$

$$I_{\text{PD input}} = \frac{I_{\text{PD leakage}}}{\text{Transfer Function}} \tag{5.6}$$

For verification of the charge calculation module, test PD signals are injected into the winding tap locations using the arrangement shown in Figure 4.3, in which the PD input current and the corresponding leakage currents are measured. The measured leakage currents and winding tap transfer functions are used to calculate the PD input currents. The measured and computed PD currents for one of the taps are shown in Figures 5.30 and 5.31, for air void PD and sharp edge PD, respectively.

The measured signals are more damped than the calculated ones because the resistance used in the PD injection circuit is higher than that used in the transfer function calculation circuit. For the air void PD current, the time lag is longer in the measured one due to the use of the high voltage transformer. The frequency content of the sharp edge PD is higher than the air PD signal, and is thus less affected by the change of system, as in the higher frequency region the capacitance of the transformer winding becomes dominant.

The PD charge is calculated from the measured and calculated PD input currents for PD test signals injected into different tap locations. For the air PD current shown in Figure 5.30, the measured charge is 7.4 nC and the calculated charge is 7 nC, with a percentage error of 5.7%. For the sharp edge PD current shown in Figure 5.31, the measured charge is 4.45 pC and the calculated charge is 4.27 pC, with a percentage error of 4%. The percentage error between the measured and calculated charge for the test PD signals is 10% or less. The transformer insulation condition assessment based on the PD charge is usually performed by specifying certain PD ranges corresponding to different transfer conditions, such as the classifications reported in [11, 89]. Usually, error values of a maximum of 10% will not affect the condition evaluation of the transformer insulation unless PD charges are at the edge of a certain range.

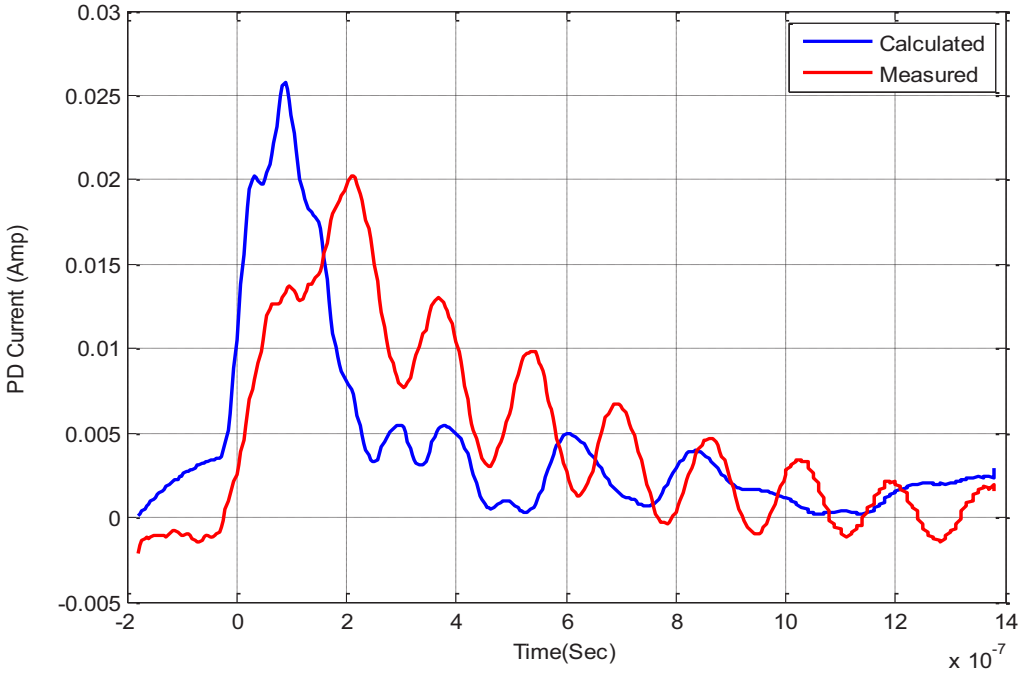

Figure 5.30: Calculated and measured air bubble PD current waveforms

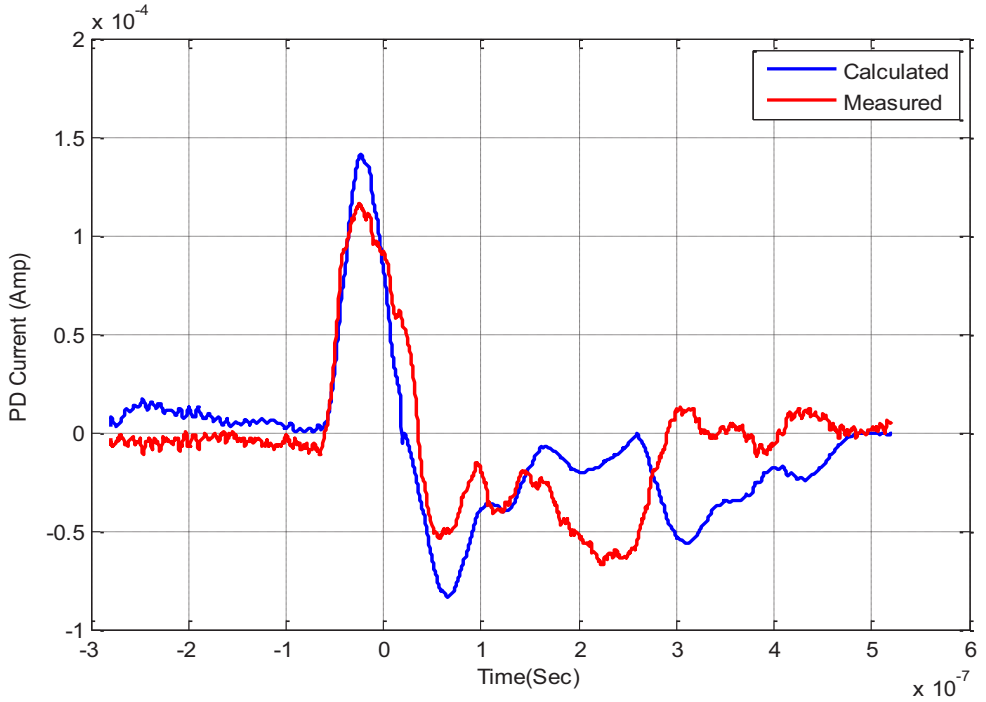

Figure 5.31: Calculated and measured sharp edge PD current waveforms

5.4 Summary

In this chapter, I have developed a PD charge detection method for PD charge determination in the transformer winding insulation using the leakage current measured at the transformer neutral and winding transfer function. In this chapter, detailed explanations were provided for the experiments conducted to measure the winding frequency response for the transformer under test, the calculation of the winding current transfer functions from the measured frequency response, and the calculation of the PD charge using these transfer functions and the leakage current measured at the transformer neutral.

Chapter 6
Transformer Condition Assessment based on Partial Discharge Detection

6.1 Introduction

The integrity of power transformers depends mainly on the correct operation of their insulation systems [94], which constantly experience various types of stresses and defects. Detecting these defects early and providing the transformer with suitable maintenance actions are crucial for preventing sudden transformer failures. One of the most powerful indications of existing defects in a transformer insulation system is partial discharge (PD). PD continuously degrades the system, affecting its correct operation and potentially leading to a complete breakdown [50]. Transformer insulation deterioration rate and intensity due to PD activity depend on multiple PD features, such as the apparent charge, defect type, location, energy, and duration.

Several studies have investigated the relationship between these features and the degree of deterioration in an insulation system. However, most of the investigations are limited to conducting controlled PD experiments on transformer insulation components and not on a real transformer [11, 14], so the correlation between the findings of these experiments and actual transformer insulation behavior is not clear. For instance, some studies suggest that PDs in orders of 104 pC are not harmful, based on the number of Kraft papers damaged in their experiments, whereas the accepted PD level recommended by IEC standards is 500 pC.

The transformer health index (THI) is a technique used to assess transformer condition by combining multiple operational transformer factors and providing a quantitative value that represents the condition. The THI calculation is a multi-step process that includes determining, scoring, and weighting a transformer's operational factors, and then combining them into one quantitative value. These operational factors include multiple test result parameters, such as the DGA, furfural analysis, oil quality, and power factor, plus operational loading and maintenance data. Despite the importance of PD effects on transformer health, PD test results are explicitly considered in only a few studies.

In this chapter , I develop a PD severity assessment in order to assess the transformer winding insulation system based on the PD detected characteristics, source and charge, using the modules developed in Chapters 4 and 5 (Figure 6.1). This module is based on comprehensive experiments

performed in the literature and experiments done in Chapter 4 of this thesis. A fuzzy logic system is used to develop the PD severity assessment, in order to overcome discrepancies in PD levels across various studies. The input variables to this fuzzy system are the PD charge value and the leakage current pulse skewness, which is an indication of the PD source type. The output is the PDI, which ranges from 0 to 100, with 0 representing a very good condition and 100 representing a dangerous condition.

The correlation between the calculated partial discharge index (PDI) and transformer condition is then developed based on the transformer condition classifications suggested in [11, 89]. The validations for adopting these classifications are performed using the input-output PD signals measured in Chapter 4, by calculating attenuation factors. Based on the calculated severity assessment output (PDI) for a transformer, the transformer insulation condition is classified into one of five categories: normal, questionable, harmed, critical, and dangerous. In addition to assessing the transformer winding insulation condition, the PDI can be included in the transformer health index calculation, even though PD test results are explicitly considered in only a few studies [9].

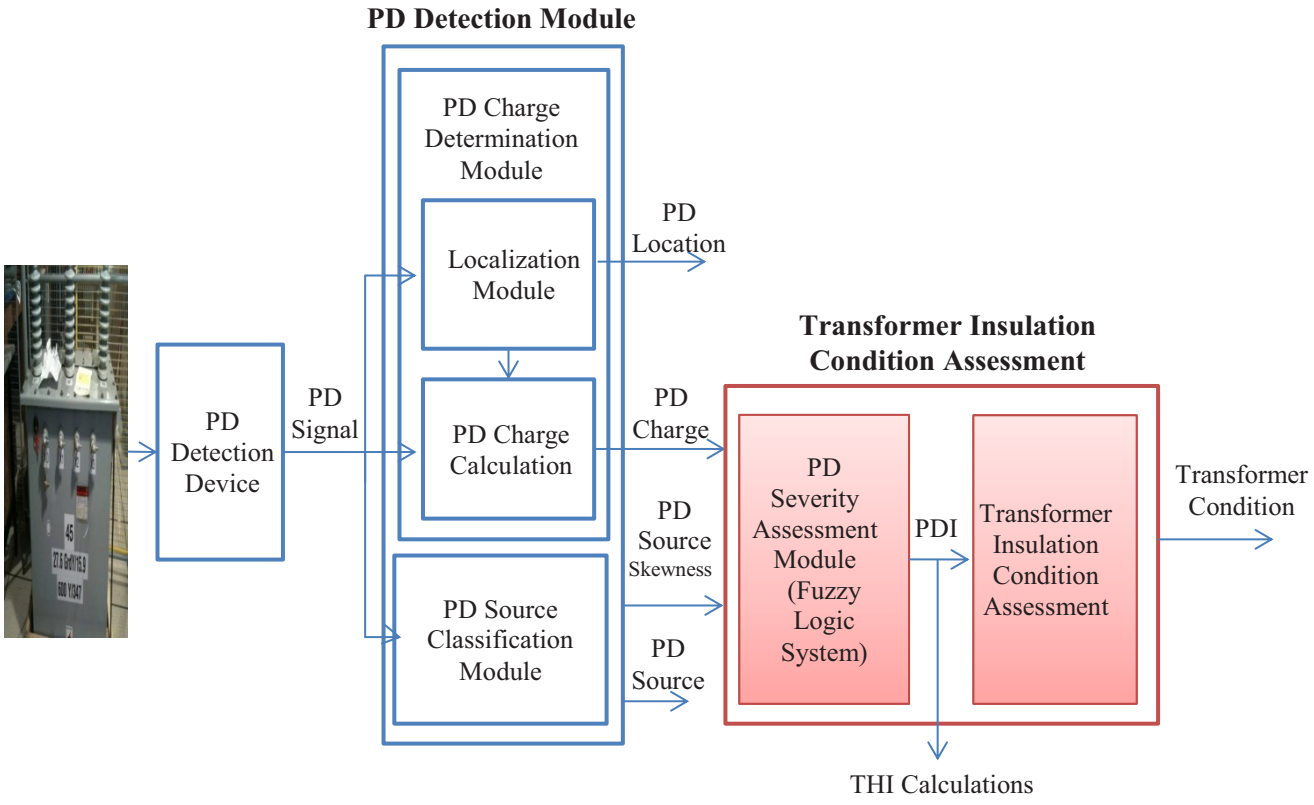

Figure 6.1: PD detection and PD severity assessment modules

6.2 PD Severity Assessment Module

The objective of the PD severity assessment is to provide a quantitative evaluation of the damage caused to an insulation system based on PD characteristics. Due to the random nature of PD and the uncertainty of its detection techniques, fuzzy logic is suitable for PD applications. Therefore, a Mamdani fuzzy logic system is used to construct the PD severity assessment module, using the MATLAB fuzzy logic toolbox. Figure 6.2 shows the steps for the fuzzy inference process, where DOMnk is the degree of membership of element (k) to the set in rule (n); DOMn is the degree of membership function selected to represent this rule after applying the fuzzy operators; FCSn is the nth fuzzy consequent set resulting from applying the implication method; and FOS is the fuzzy output set. The inputs to the PD severity assessment module, the fuzzy system, are the skewness value of the measured leakage current pulse, which is an indication of the PD source type, and the PD charge; whereas, the output is the PDI, which reflects the severity of the PD effects on the winding insulation (Figures 6.3 and 6.4).

This section discusses the steps for constructing a fuzzy logic system for the PD severity assessment module, including variable fuzzification, logic operators, implication method, aggregation, and output defuzzification.

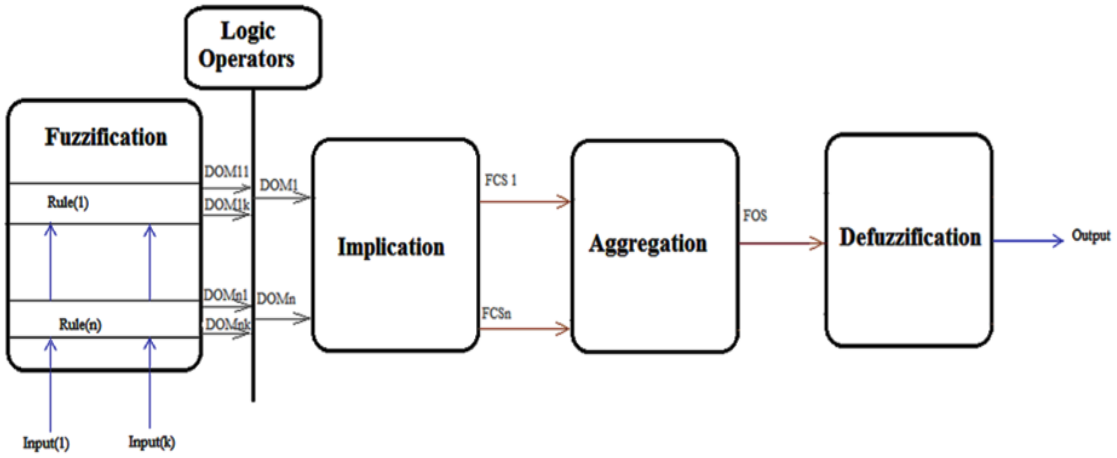

Figure 6.2: The fuzzy inference process

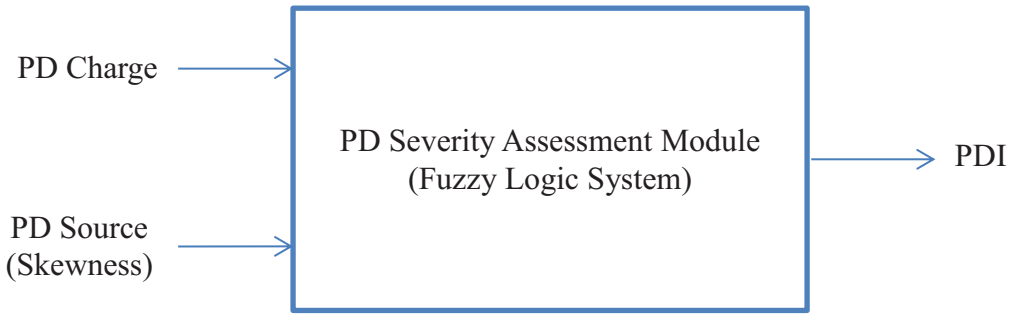

Figure 6.3: PD severity assessment module

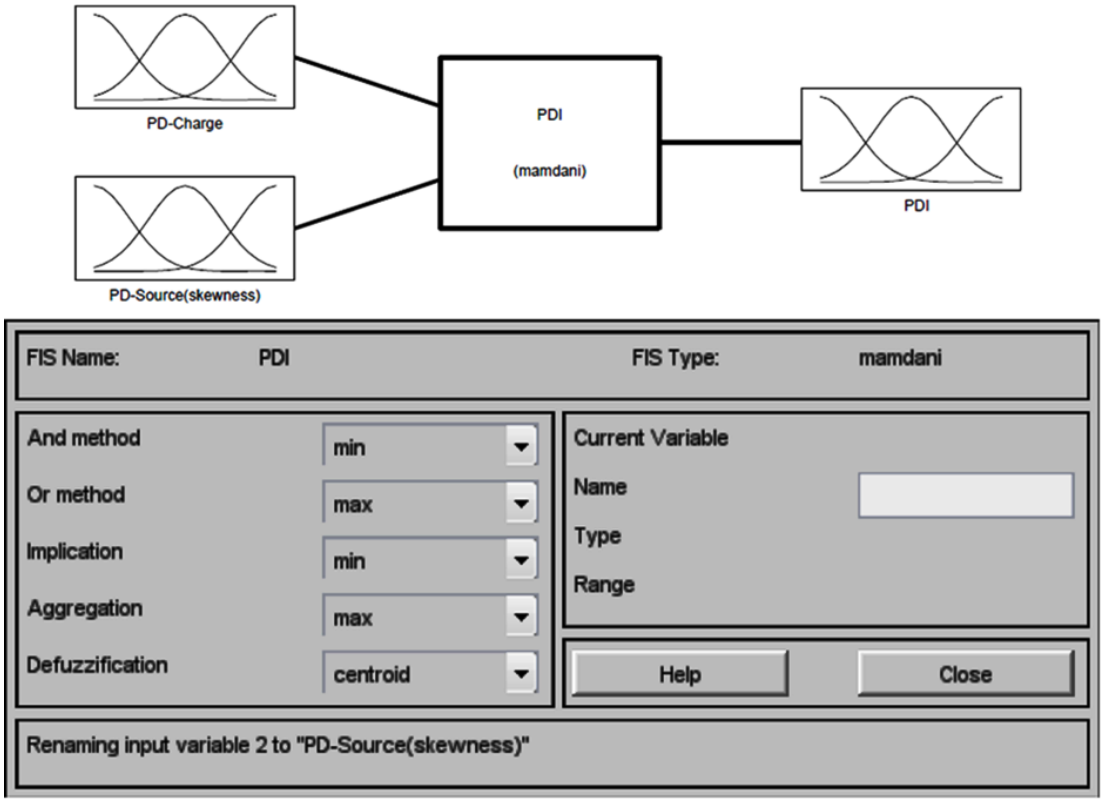

Figure 6.4 : PDI calculation via Mamdani fuzzy logic system

6.2.1 Variable Fuzzification

Variable fuzzification is performed through their membership functions. In this section, the membership function of each variable (input or output) is constructed.

6.2.1.1 Membership Function PD Source

Power transformer insulation systems have a highly complex structure that can contain different PD sources. However, some sources are more dangerous than others, so it is essential to include the source type in the assessment module. In this assessment, two types of PD defects (sharp edge and surface discharge) are considered, since they have very destructive effects on insulation systems [11]. The MFs of the PD source type are constructed using the skewness values obtained based on the laboratory experiments conducted in Chapter 4. The process for constructing these MFs is shown in Figure 6.5.

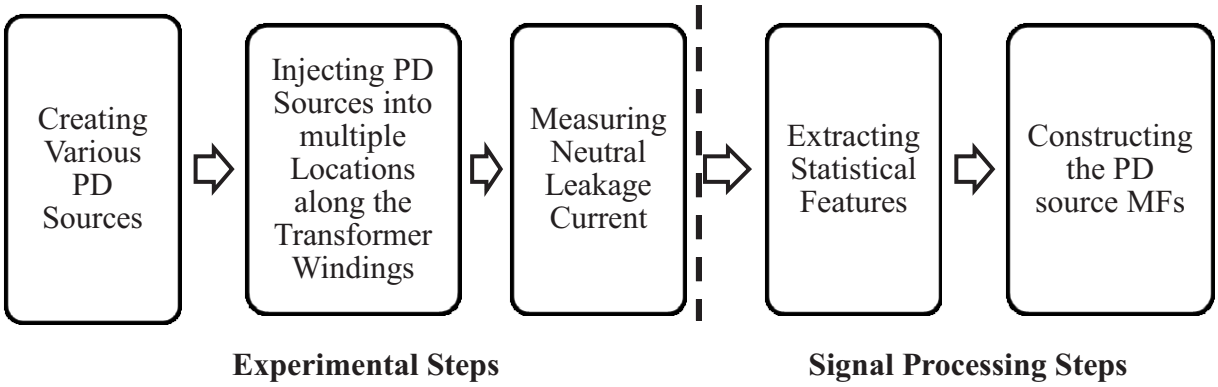

Figure 6.5: Steps for constructing MFs for leakage current skewness

For the transformer under study, the leakage current measurements obtained in the experiments conducted for source type identification module are used in this section (Figure 6.6). In these experiments, seventy PD signals of each source type (i.e., air bubble, sharp edge and surface discharge) are injected into each tap of the transformer. The statistical features (variance, skewness, and kurtosis) are extracted from the normalized corresponding leakage current waveforms measured at the transformer neutral. The histograms of the three statistical features for all the signals are shown in Figures 6.7 to 6.9. The variance values of the sharp edge and surface discharge are completely overlapped, and thus the variance values cannot be used as an indication of source type. The highest-frequent kurtosis regions of the sharp edge source are overlapped with the second-highest region of the surface discharge source. The skewness of the PD waveform is chosen to indicate the PD source type because the highest-frequent values of both types are different.

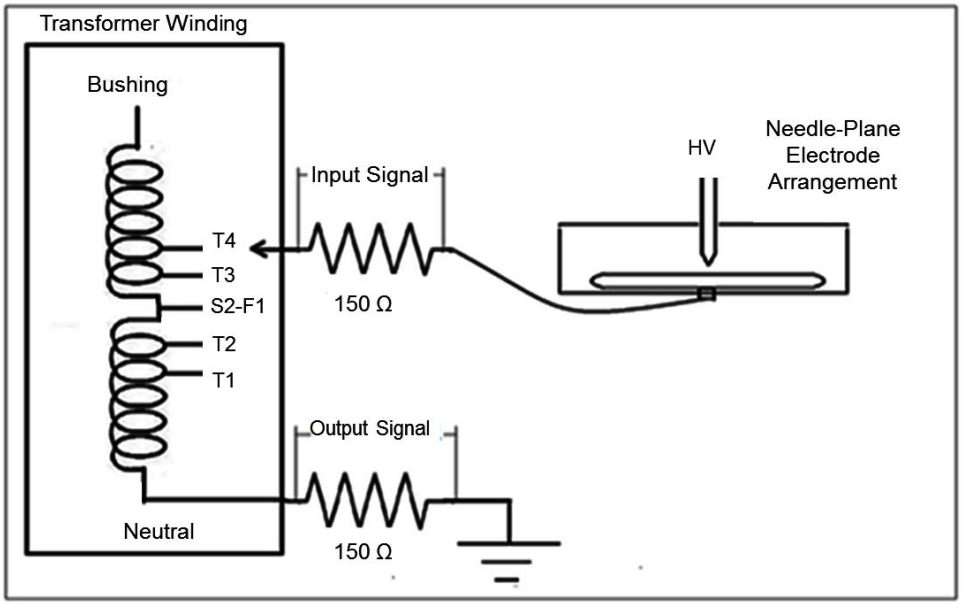

Figure 6.6: Schematic diagram for setup used in PD injection into different transformer taps and leakage current measurements

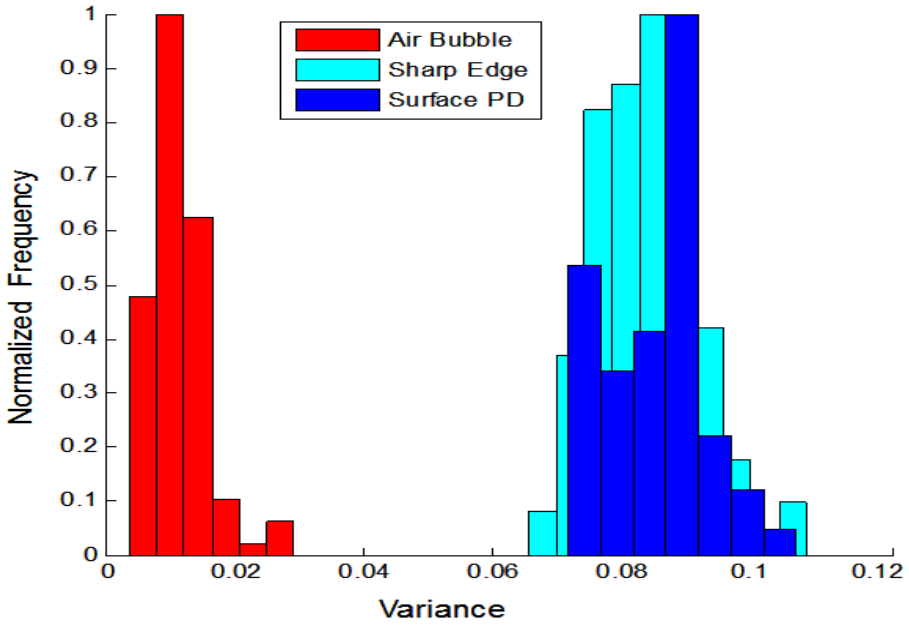

Figure 6.7: Histograms of variance values of air bubble, sharp edge and surface PD

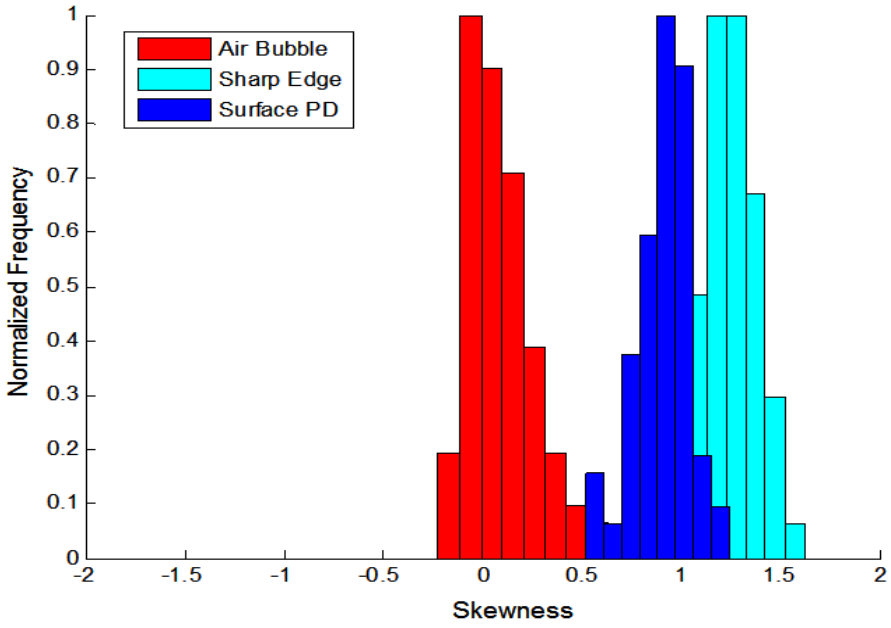

Figure 6.8: Histograms of skewness values of air bubble, sharp edge, and surface PD

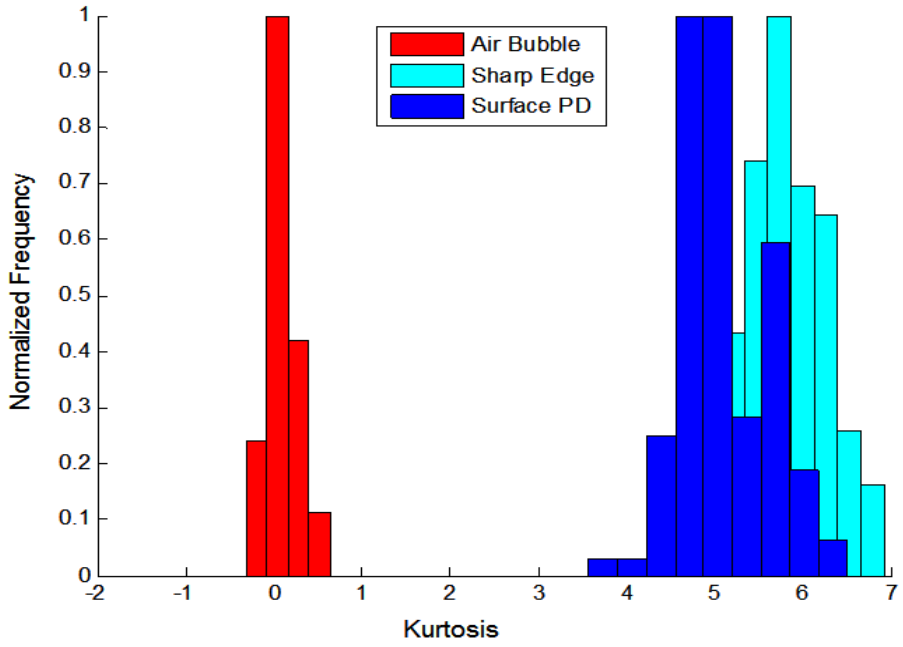

Figure 6.9: Histograms of kurtosis values of air bubble, sharp edge, and surface PD

The membership functions (MFs) of the skewness values related to the two PD types are constructed based on their histograms. The MFs for skewness that relates to the PD type are constructed by converting Figure 6.10 into a continuous curve as shown in Figure 6.11. The skewness MFs are determined to be Gaussian-type waveforms, with means and standard deviations calculated from the mean and standard deviation of the skewness values of the measured leakage current signals. The mean and standard deviation for surface discharge are 0.9419 and 0.1343, respectively, whereas the mean and standard deviation for sharp edge discharge are 1.233 and 0.1655, respectively.

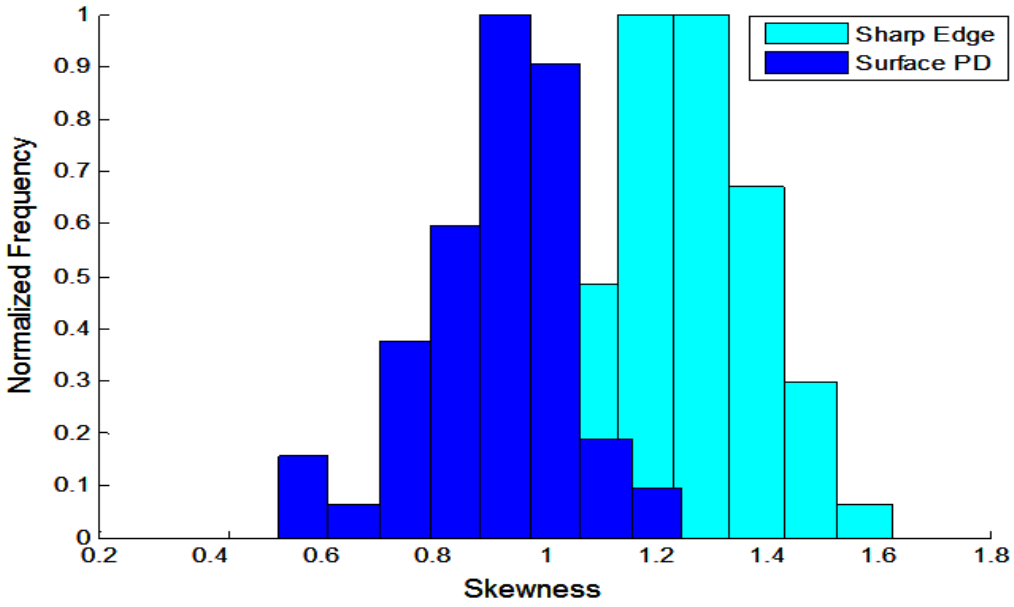

Figure 6.10: Histograms of skewness values for sharp edge and surface PD

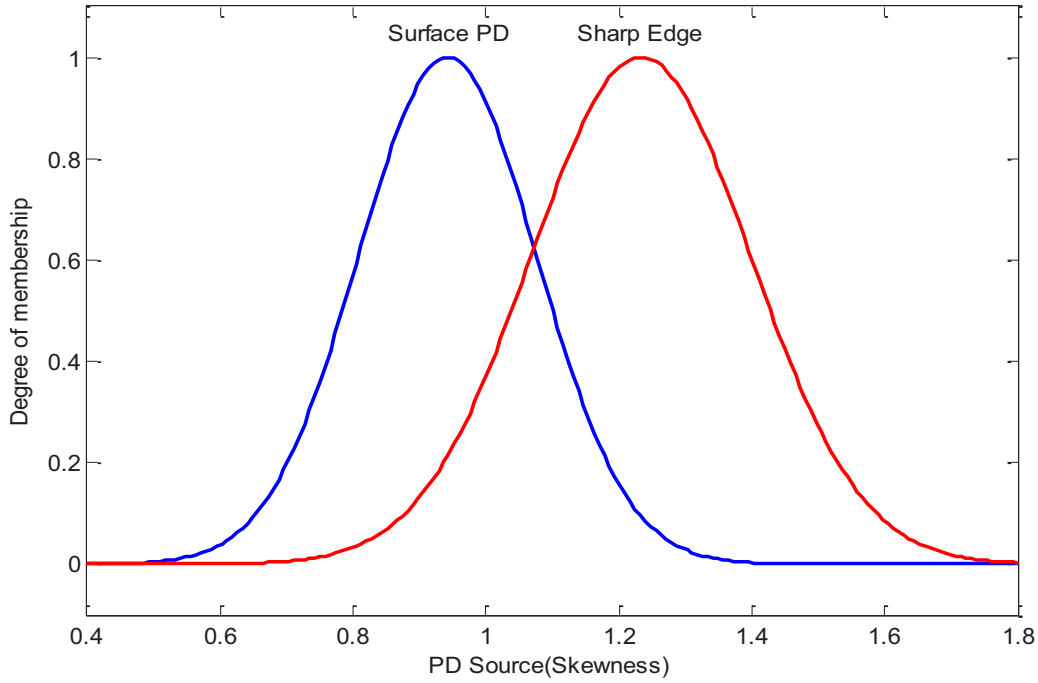

Figure 6.11: Skewness MFs

6.2.1.2 PD Charge MFs

The second input to the fuzzy logic system is the PD charge (Figure 6.1). Based on the damage they cause to oil-impregnated paper insulation, the PD charge values are classified into four categories (MFs): small, moderate, high, and very high. In [11], experiments are conducted to investigate the damage caused by the PD to the oil-impregnated paper in three different models: a simple electrode-plane arrangement, a transformer model, and a real transformer. In these experiments, the one-minute voltage withstand test is followed directly by eight-hour tests at reduced voltages. The maximum value of the charge during each test is recorded, and the number of papers damaged under the same condition is examined.

The relationship between the PD charge and number of damaged papers is shown in Figure 6.12. It is concluded that PD charges in the orders of 10^4 pC are harmful, those in the orders of 10^5 pC cause considerable damage, and those greater than 10^6 pC create extreme damage to the insulation system. Therefore, it is recommended that the PD charge value not exceed 10^4 pC.

The MFs for the PD charge are constructed based on this investigation. The minimum considered charge is 10^3 pC (small), and the maximum charge is 10^6 pC (very high). Figure 6.13 shows four Gaussian MFs: small, moderate, high, and very high. The mean value for the small PD charge MF is 10^3 pC as it is considered not harmful by the study; the mean of moderate MF is $5* 10^4$ pC as no paper is damaged at this value but the paper is about to degrade (Figure 6.12); the mean value of the high MF is $3* 10^5$ pC as charges of this order cause considerable damage to the paper (almost half of the paper number corresponding as the extreme damage case); and the mean value of the very high MF is 10^6 pC, as any charge values greater than this value cause extreme damage to the insulation.

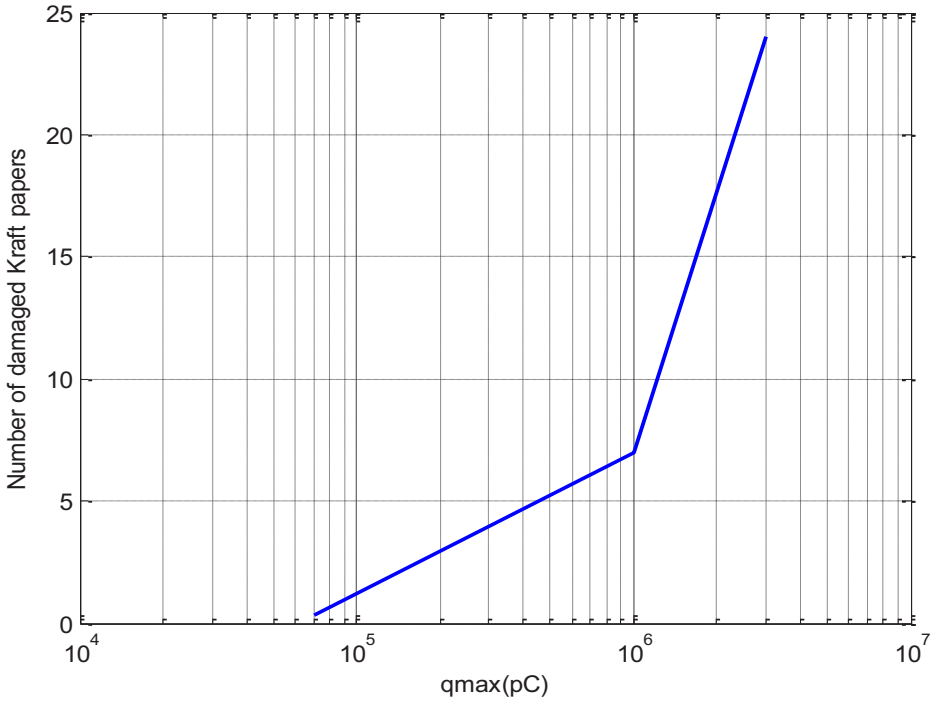

Figure 6.12: Relationship between the number of damaged Kraft papers and maximum apparent charge [11]

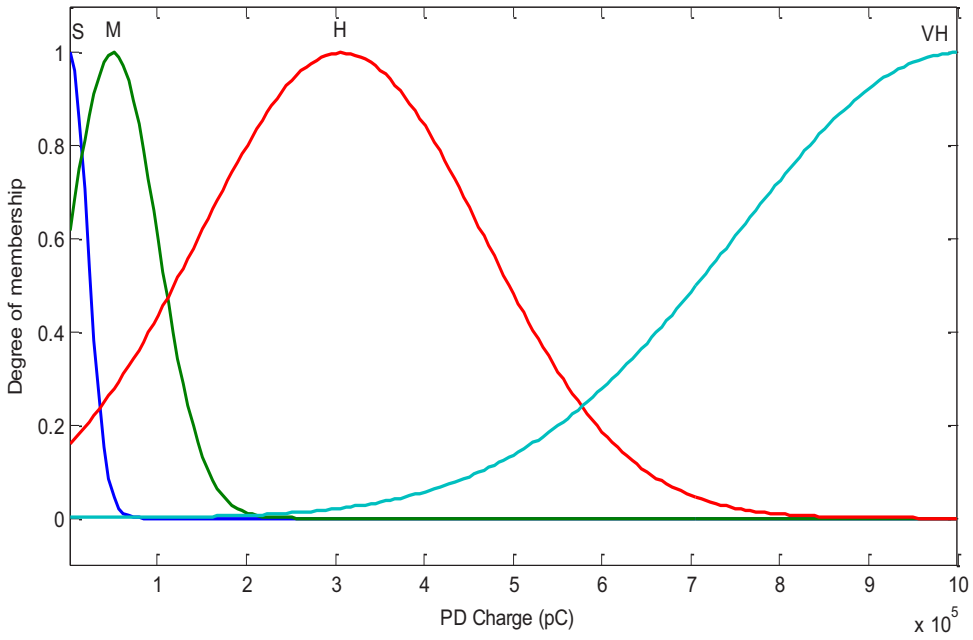

Figure 6.13: PD charge MFs, where S is small, M is moderate, H is high, and VH is very high

6.2.1.3 PDI MFs

PDI is a quantitative value that represents the damage caused to the paper insulation based on certain PD sources with certain PD levels. PDI MFs are constructed based on the number of papers damaged by PD activity (Figure 6.12), as reported in [11]. The PDI ranges from 0% to 100%, with 0% representing no damage to the insulation system (a normal insulation condition) and 100% representing complete damage (a dangerous condition). In Figure 6.12, the damage caused to the insulation system or the number of damaged papers can be divided into the three zones of no damage, critical and dangerous, corresponding to the slope change of the lines. Three Gaussian MFs (low, high, and very high) are used to describe the winding insulation condition based on these three zones (Figure 6.14). The mean values of the three MFs are 0, 56 and 100, whereas the standard deviation values are 10, 18 and 19, respectively. These numbers are calculated based on the number of damaged papers. Specifically, the normal condition is related to a state of no damaged papers, the critical condition is related to 4 damaged papers, and the dangerous condition is related to 7 damaged papers.

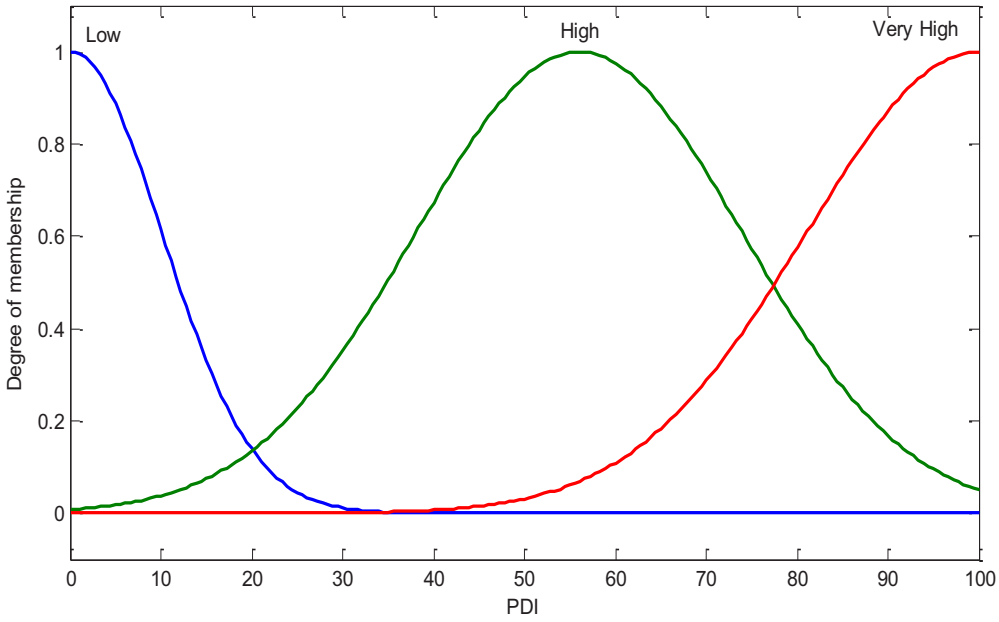

Figure 6.14: PDI MFs

6.2.2 Fuzzy System Operators, Implication, Aggregation and Defuzzification Methods

Different methods are tested, and a min, max, min, max, and centroid are selected for the fuzzy operator, AND and OR, implication, aggregation and defuzzification methods, respectively.

6.2.3 Fuzzy Rules

The rule base has eight rules, the skewness has two linguistic values, the charge has four linguistic values (Table 6.1), and all of the rules have equal weight. The rules are formatted as follows: If the source is (surface, sharp edge) and the charge is (low, moderate, high, or very high), then PDI is (low, high, and very high). The rules are structured based on the cases reported in [11], where, at different voltage levels, the surface PD with charge levels of $3 * 10^5$, 10^6, and $3 * 10^6$ pC damages 2, 7, and 24 papers, respectively. Sharp edge defect-related charge values are less damaging to the insulation system than the same surface PD charge, a sharp edge source with a 10^4 pC charge values causes no serious damage to the insulation system. Figure 6.15 shows the PDI surface generated in adherence with the eight fuzzy rules. It is evident that the PDI values related to charges resulting from surface discharges are higher than those related to charges resulting from sharp edge PD.

Table 6.1: Fuzzy system rules

Rule	**Inputs**		**Output**
	IF PD charge is	And Source (skewness) is	Then PDI is
1	Small	Surface	Low
2	Moderate	Surface	High
3	High	Surface	Very high
4	Very High	Surface	Very high
5	Small	Sharp Edge	Normal
6	Moderate	Sharp Edge	Low
7	High	Sharp Edge	High
8	Very High	Sharp Edge	Very high

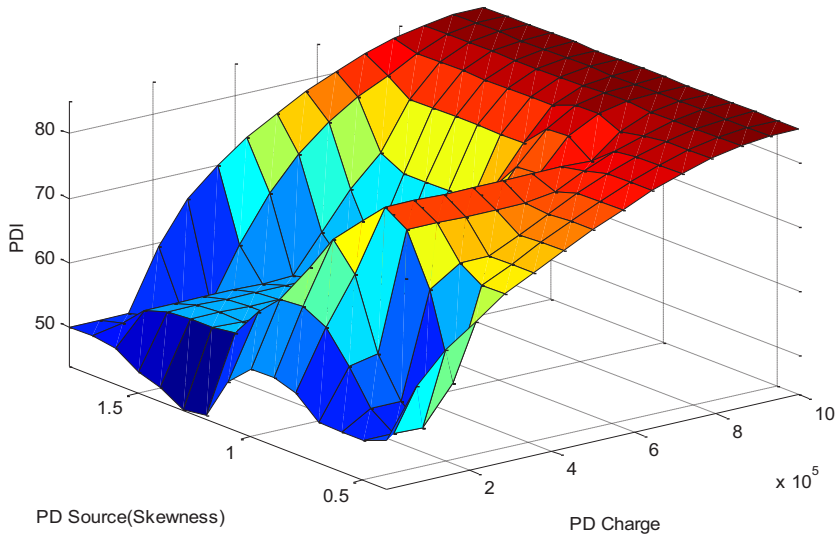

Figure 6.15: Fuzzy system surface

6.3 Classification of Transformer Winding Insulation Condition Based on the PDI

The developed PD severity assessment module is constructed based on controlled experiments. The PD charge values used earlier in this chapter are not the terminal PD charge measured at the transformer neutral but the internal PD charge injected into the transformer winding during a PD event. Most transformer condition classifications in the literature are based on the terminal measured PD charge level, such as in [89]. In this classification, a transformer main insulation condition can be classified as either free of faults, normal, requires clarification, faulty, possibly has irreversible damage, or dangerous. The PD charge levels associated with these condition classes are less than 100 pC, 10^2 to 10^3 pC, 10^3 to $25*10^3$ pC, from $5*10^3$ to $25*10^3$ pC , $25*10^3$ to 10^5 pC, respectively. As the PD charge values for the classes "require clarification" and "faulty" overlap, using fuzzy logic in the severity assessment module developed in this thesis is beneficial.

The PD levels suggested in this classification are much smaller than those used in the developed severity assessment module in [11], as the first levels are the terminal measured PD charges and the second levels can be considered the ones injected from the PD source into the transformer winding. The PD signals measured at the transformer terminals are smaller than the PD signals injected into the windings, due to the attenuation caused by the propagation path. The severity assessment module and the winding condition classification can be correlated if the attenuation effect caused by the propagation path through the transformer winding is known. The attenuation caused by the propagation path can be investigated by injecting various types of PD signals into different locations along the transformer winding and measuring the output from the transformer neutral. By calculating the PD charge of the injected and measured PD signals, the attenuation caused by the propagation path can be estimated, using an attenuation factor (AF). For each PD signal, the attenuation factor is identified as the PD charge input signal divided by the PD charge of the output signal (Equation 6.1).

$$\mathrm{AF} = \frac{\text{PD Charge (input)}}{\text{PD Charge (output)}} \qquad 6.1$$

The propagation path attenuation factors for the windings of the transformer under study (Figure 6.16) are calculated using the experiments described in Chapter 4 (Figure 6.6). In these experiments, three PD types are created, and seventy signals of each type are injected into each tap of

the transformer windings. The input PD current signals and the corresponding leakage current signals are measured. The PD charges that correspond to input and output are calculated by integration and used to calculate the attenuation factors (Table 6.2). The average attenuation factors are calculated for each PD source and each PD tap in phase 1 of the transformer under study (Figure 6.16). As the tap locations are very close to each other, the attenuations caused to the PD signals injected into all of them are very close. However, the attenuations caused to the PD signals injected into the tap location nearer to the ground (T1) are more attenuated than those injected into other locations. These findings completely agree with the findings of [54].

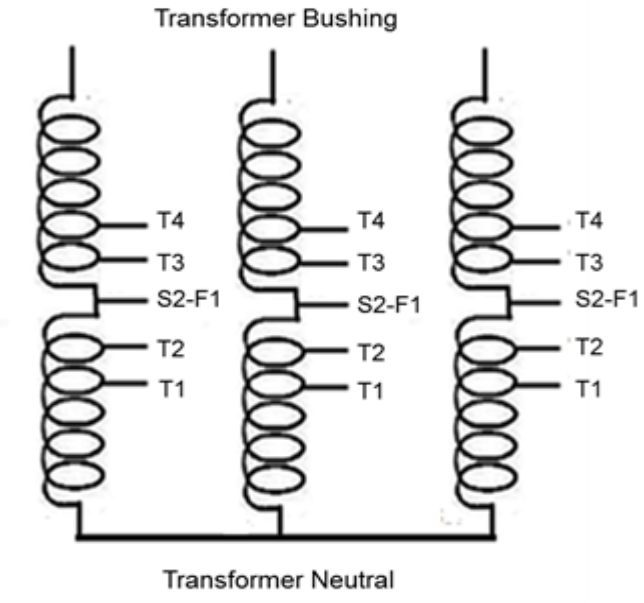

Figure 6.16: Schematic diagram for windings of the transformer under study

Table 6.2: The attenuation factors corresponding to the tap positions in phase 1 of the transformer under study

	Air Bubble	**Sharp Edge**	**Surface Discharge**
T1	4.43	5.33	5.52
T2	4.36	5.30	5.50
S2-F1	4.29	5.29	4.97
T3	4.25	5.26	4.94
T4	4.24	5.23	4.91

In order to correlate the transformer condition classification suggested by [89] and my severity assessment module, the charge levels mentioned in [89] are multiplied by the maximum obtained attenuation factor (5.33), since the PD charge source or location are not mentioned in this study (Table 6.3). The first two columns of Table 6.3 show the transformer condition classes and the corresponding maximum PD charges levels suggested in [89]; the third column maps these maximum terminal PD levels into their corresponding maximum internal PD charge levels by multiplying them by the maximum attenuation factor ; the fourth column provides the classification of the mapped internal PD charge values based on the investigation performed in [11]. To differentiate the two classes of "requires clarification" and "faulty", their charge levels are considered to be from 10^3 pC to 5 *10^3 pC and from 5 *10^3 pC to 25*10^3 pC, respectively. The two classifications in this table totally agree with each other, as a transformer condition is classified as free of faults, normal, requires clarification, faulty, possibly has irreversible damage, or dangerous based on [89], and the corresponding classifications based on [11] are not harmful, not harmful but causing degradation, harmful, causes considerable damage, and causes extreme damage.

The validations behind choosing the PD levels reported in [89] for transformer insulation are not mentioned. Therefore, before using this classification in my study, this transformer condition

classification is validated by comparing it to another transformer classification based on the dissolved gas analysis. In [48], the PD apparent charge and dissolved gas analysis are measured for seven transformers with different deterioration levels (Table 6.4). In (Table 6.4), the condition of each one of these seven transformers is evaluated based on both the detected PD charge and total dissolved gasses according to the classification provided in [89] and [48], respectively. Both classifications agree, except for one transformer (number 4). For this transformer, the condition assessment based on the PD charge is normal while the condition based on the dissolved gases is moderate-bad.

Table 6.3: Transformer condition assessment based on terminal and internal PD charges

Condition Assessment According to [89]	**Maximum Terminal PD Charge (MTPDC)** (pC)	**Corresponding Maximum Internal PD Charge (MTPDC *AF)** (pC)	**Condition Assessment According to** [11]
Free of Fault	10^2	553	Not harmful
Normal	10^3	$5.53*10^3$	Not harmful but close to the harmful level.
Requires clarification	$5*10^3$	$27.65*10^3$	Harmful
Faulty	$25*10^3$	$1.39*10^5$	Cause considerable damage
Critical or Dangerous	10^5	$5.53*10^5$	Cause extreme damage

Table 6.4: Transformer condition assessment based PD charge and DGA

Transformer	DGA (ppm)	PD (pC)	Assessment Based on PD Charge	Assessment Based on DGA
1	5042	1800	Harmful	Bad
2	4105	1250	Harmful	Bad
3	2784	600	Normal	Bad
4	1102	300	Normal	Moderate-bad
5	816	500	Normal	Moderate
6	152	30	No fault	Normal
7	44	20	No fault	Normal

In this research, based on both of the classifications reported in [11, 89], the condition of the transformer winding insulation is classified into five categories: normal, questionable, harmed, critical, and dangerous. Table 6.5 shows the PDI ranges associated with each condition and also compares this transformer insulation winding condition classification and the classifications recommended in [11, 89].

The "normal" condition means that the PD levels are very low and there is no damage caused to the insulation system. According to [11], the normal condition is associated with maximum internal PD charge of 10^3 pC. In [89], the maximum terminal PD charge associated with transformer normal condition is 10^3 pC, which is much larger than the 500 pC suggested by the IEC standard. Furthermore, the attenuation factors are calculated only for the windings tap locations, which are located in the middle of the windings and very close to each other. If a PD occurs in insulation near the bottom of a winding, the 10^3 pC should be multiplied by larger attenuation factors. Therefore, the

normal condition is chosen to be lower than the limit recommended by the IEC standard but higher than the fault-free recommended in [89]. As an example of the normal insulation condition (Figure 6.17), the PDI is calculated for a PD with a charge value of 10^3 pC and a skewness value of 1.22. A charge of 10^3 pC has a full membership to the small membership function and a partial membership to moderate and high membership functions, while the skewness value (1.22) has a full membership to the sharp edge membership function, and a partial membership to the surface discharge source membership function. These conditions would fire all the rules. The Mamdani minimum, as a logic operator and an implication method, is applied to find the area under the corresponding PDI membership functions associated with each rule. The rules' outputs are aggregated using the maximum method, and the centroid method is then used to defuzzify the aggregated membership function. For this specific example, the rules most influencing rules are rules 5 and 6, which state that if the PD charge is small or moderate and the PD skewness is a sharp edge, the PDI would be low or high, respectively. The PDI calculated for this PD is 44%, which indicates normal operation.

The "questionable" condition represents the grey area between normal and deteriorated conditions, meaning that the PD charge is high but more details are required in order to assess the condition of the winding insulation. In Figures 6.18 and 6.19, the PDI is approximately 55% in both cases; however, the PD in the first case is more harmed than the PD in the second one.

The "harmed" condition means that PD activity deteriorates the winding insulation system (Figure 6.20). In Table 6.5, the questionable and harmed transformer conditions have the same internal maximum PD charge ($5*10^4$ pC) limit. The difference between them is the PD source. Neither of the classifications in [11, 89] can differentiate between these two cases. However, by considering the source in this developed assessment, these two classes can be recognized from their associated PDI values.

The "critical" condition means that the insulation system is deteriorating very fast due to PD activity (Figure 6.21). As recommended by [11], PD charges in orders of 10^5 pC cause considerable damage to insulation materials, and $3*10^5$ pC burns almost half (4) the number of papers associated with extreme damage (7). Therefore, the PDI values associated with this PD charge range are correlated to the critical condition.

The "dangerous" condition means that the winding insulation is extensively damaged due PD activity (Figure 6.22). In [11], PD charges in the orders of 10^6 pC cause extreme damage to the

insulation system, so the PDI values corresponding to values from $3*10^5$ to 10^6 pC are considered to represent a dangerous condition.

For all the condition example figures, the PD charge value, the PD skewness value, the fired rules, the most effective rules, the PDI value, and transformer condition are summarized in Table 6.6.

Table 6.5: Insulation condition classification based on the PDI

PDI	**Condition**	**According to** [89]		**According to** [11]	
		Charge (pC)	**Condition**	**Charge (pC)**	**Condition**
0 to 45 %	Normal	~200	Normal	1000	Not harmful
45% to 55%	Questionable	$\sim 10^4$	Faulty	$5*10^4$	Depending on the source
55% to 65%	Harmful	$\sim 10^4$	Faulty	$5*10^4$	Depending on the source
65% to 75%	Critical	$\sim 6*10^4$	Faulty	$3*10^5$	Cause considerable damage
> 75%	Dangerous	$2*10^5$	Critical or Dangerous	10^6	Cause extreme damage

Table 6.6: Various PD characteristics and their associated PDI and condition assessment

Example	PD Charge (pC)	Skewness	Fired Rules	Most Affecting Rules	PDI	Condition
Figure 6.17	10^3	1.22	All	5,6	44	Normal
Figure 6.18	10^4	0.954	All	1,2,4	54.9	Questionable
Figure 6.19	$5*10^4$	1.25	All	6	55.4	Questionable
Figure 6.20	$5*10^4$	0.941	All	2,4	63.9	Harmed
Figure 6.21	$7*10^5$	0.954	All	4	80.8	Critical
Figure 6.22	10^6	0.941	All	4	85.2	Dangerous

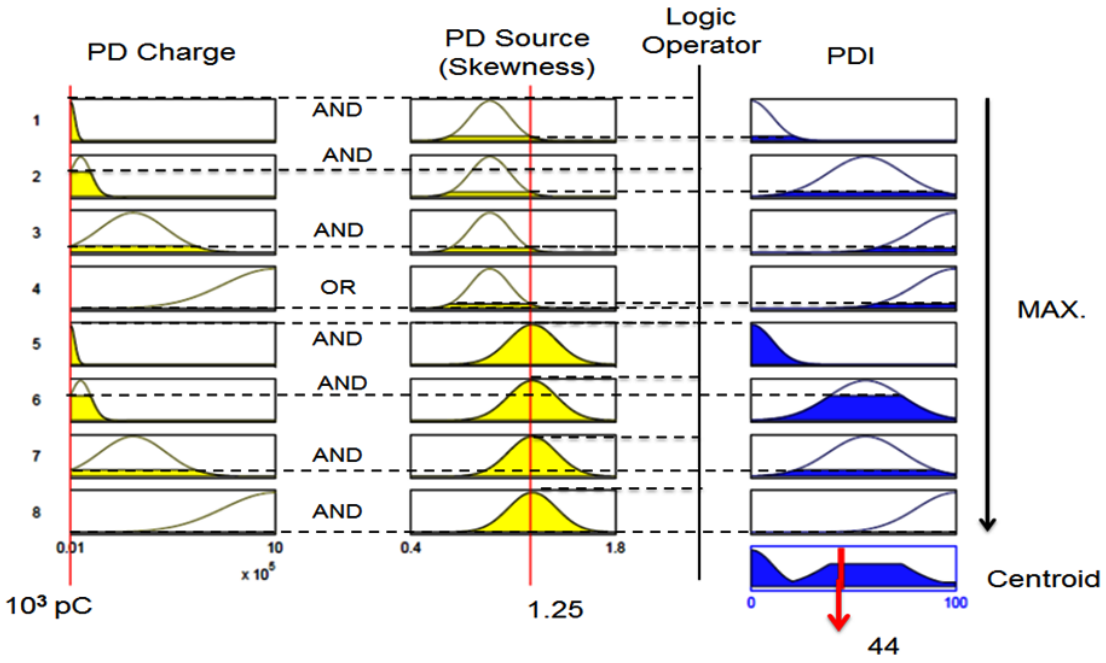

Figure 6.17: PDI value related to a normal condition

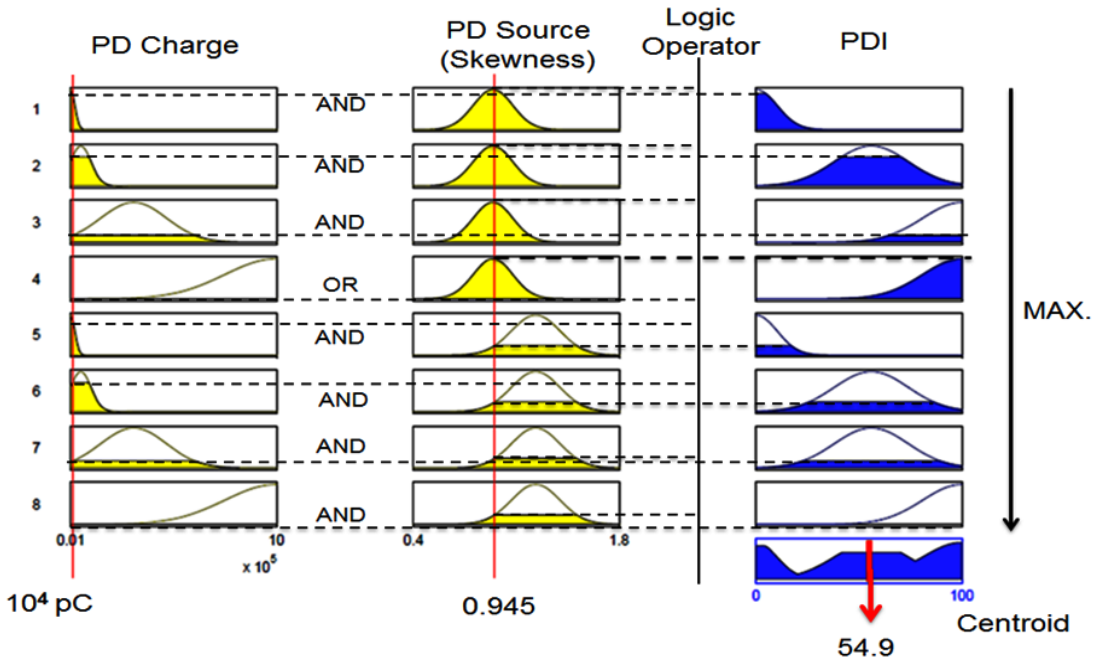

Figure 6.18: PDI value related to a questionable condition

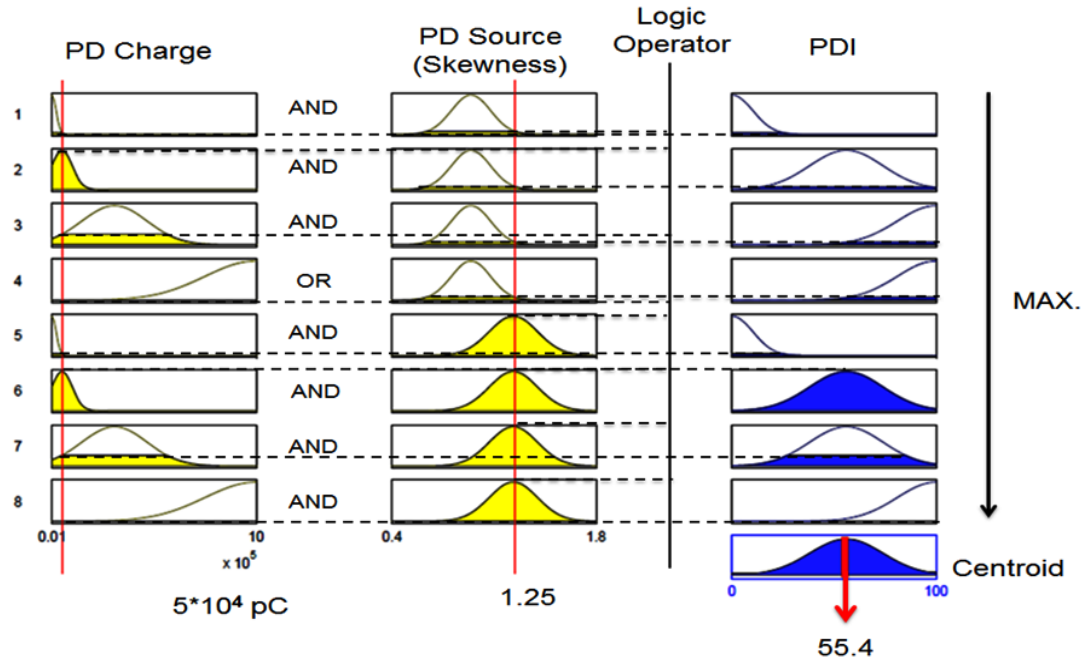

Figure 6.19: PDI value related to a questionable condition

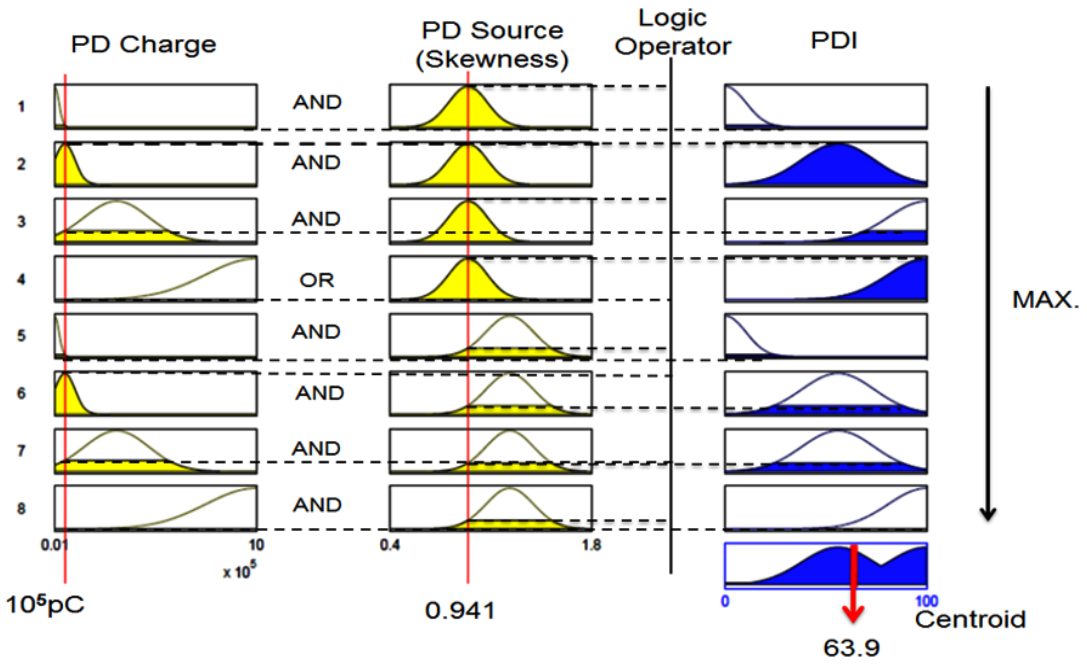

Figure 6.20: PDI value related to a harmed condition

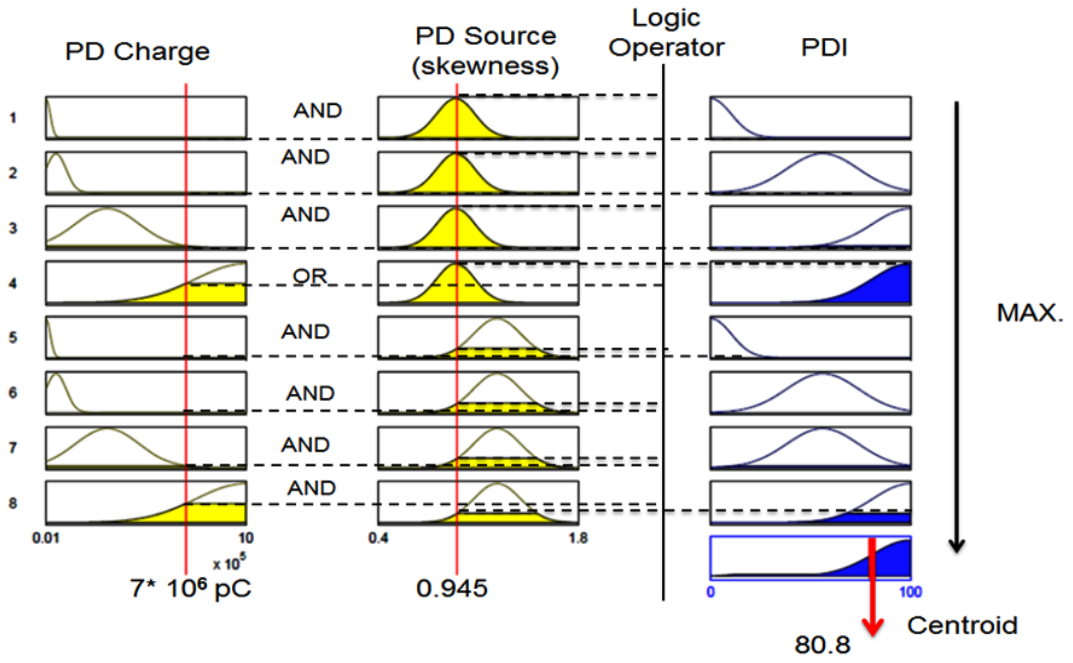

Figure 6.21: PDI value related to a critical condition

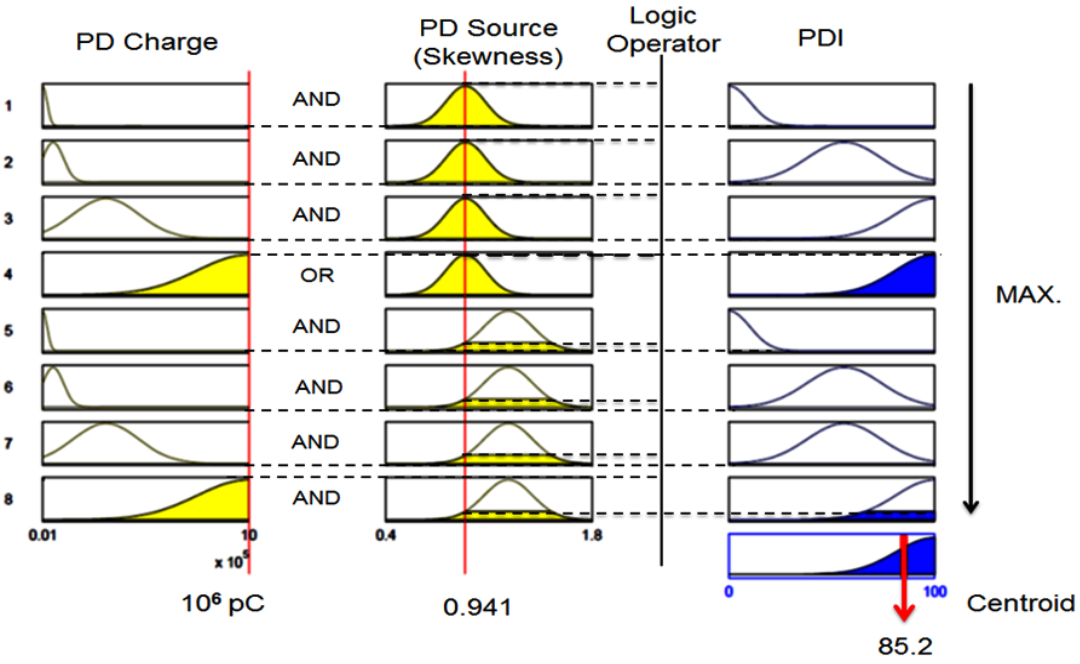

Figure 6.22: PDI value related to a dangerous condition

6.4 Including PDI in THI Calculations

Transformer health index (THI) calculation process involves:

- selecting the transformer factors to be used in the calculation,
- representing each factor by a numerical value (score) based on the factor's associated data,
- weighting each factor according to its importance, and
- combining the weighted scores.

Most of the research conducted in the area of THI emphasizes that partial discharge test in a transformer is a very important test. However, it is usually implicitly considered in THI calculations using the dissolved gas analysis test [9]. The fact that there is not a single number that represents the results of the transformer PD testing limits including the PD test in the THI calculations. The only number that is accepted by the researchers to represent the PD severe effects is the PD charge, which is hard to be measured in the transformer environment. Also, PD charge provides incomplete information to the classification of the transformer health without the knowledge of the source type.

In this research, I designed the PDI as a numeric value (score) that combines multiple important PD characteristics, including PD source and PD internal injected charge into a transformer winding. The PDI (score) ranges from ranges from 0 to 100, with 0 representing a very good condition and 100 representing a dangerous condition. However, this scoring system can be modified to suit any THI scoring system. The PDI can be then weighted and combined with other transformer tests in order to calculate the THI.

6.5 Summary

In this chapter, I have developed a technique to assess transformer winding insulation condition based on PD activity. In this technique, multiple PD characteristics, source and charge, were combined and mapped into one quantitative value called the PDI. A Mamdani fuzzy logic system was used to calculate the PDI, using the MATLAB fuzzy logic toolbox. The inputs to the fuzzy system were the skewness value of the measure leakage current pulse, which was an indication of the PD source type, and the PD charge value. The output was the PDI, which reflected the winding condition. The fuzzy MFs and the fuzzy rules were determined based on laboratory experiments and the existing literature. A transformer winding insulation condition classification was also provided based on the PDI values obtained for different PD cases. Furthermore, the PDI in this form can be used in THI calculations.

Chapter 7
Summary

7.1 Conclusions

The main objectives of this research were to develop online PD detection and PD severity assessment modules for transformer winding insulation so that insulation condition can be assessed and correctly maintained. To achieve these objectives, modules for determining the PD source, location, and charge were developed. Depending on the detected features, PD severity can thus be assessed using the designed severity assessment module, and the transformer winding insulation condition can be evaluated. Among various detection techniques, the electrical PD detection method is the most suitable method for detecting PD in power transformer windings. Therefore, it was used in this thesis to provide the database required for all modules.

The PD detection module has three distinct modules: PD source classification, PD localization, and PD charge determination. The PD localization module is used in the PD charge determination process.

In developing the PD source classification modules, neural network classifiers were designed using the statistical features extracted from the leakage current corresponding to different PD sources. Various PD sources, such as an air bubble, a sharp edge, and a surface discharge, were simulated and injected into different locations along the windings of a transformer under test. The leakage current signals, corresponding to each PD source and location, were measured at the transformer neutral. Statistical features such as variance, skewness, and kurtosis were then extracted from the measured signals.

Statistical features corresponding to the air bubble were completely separable from the features corresponding to the other two PD sources. The features corresponding to the sharp edge and surface discharge overlapped and their variance values were nearly in the same range. Different combinations of the extracted statistical features were used to train and test feedforward neural networks with different topologies. Using the variance alone resulted in a very low recognition rate, whereas combining the skewness and kurtosis for the neural network testing and training resulted in the best recognition rate (97%).

For the PD localization module, combinations of features extracted from the PD signals corresponding to tap locations were used to train and test feedforward neural networks that localized the signals coming from taps of the same phases or the same tap locations in different phases. Combining the three features produced a very high recognition rate to localize the PD within the same phase or three phases, reaching 100% in some cases.

To avoid underestimating the PD charge and corresponding insulation damage, I calculated the charge from the PD current injected into the winding during a PD event. The PD current was obtained using the developed transformer winding transfer function and the leakage current measured at the transformer neutral. Transformer windings were modeled using frequency response and transfer function techniques, and the sweep frequency response method was used to obtain the current frequency responses of all the accessible locations (taps) along the transformer winding by applying an end-to-end short circuit configuration. Transfer functions approximations were calculated from the measured frequency responses obtained using the MATLAB toolbox function “rationalfit”.To verify the PD charge calculation module, PD signals were injected into the different tap locations of the transformer under study, and the input and output PD currents were measured. The percentage error between the charge calculated from the measured and calculated input current by integration for the test PD signals was 10% or less.

The ultimate goal of any PD detection in transformer windings is to estimate the damage PD cause to to insulation systems. The fact that the winding insulation system is complex and cannot be visually examined significantly complicates this estimation process. To overcome the problem of overlapping ranges for PD characteristics that cause certain levels of insulation damage, a Mamdani fuzzy logic system was used to develop the PD severity assessment module, using the MATLAB fuzzy logic toolbox. The inputs to the fuzzy system are the skewness value of the measured leakage current pulse, which is an indication of the PD source type and the PD charge level. The output is the PDI, which is an indication of the number of damaged insulation papers.

For the transformer under test, the fuzzy MFs and rules were determined based on laboratory experiments and the existing literature. PD charge attenuation factors, between the input and output signals, were calculated for multiple PD sources. The maximum attenuation was then used to correlate the damage caused to the insulation papers, PDI, and a transformer classification based on the terminal apparent charge in the transformer main insulation. With this correlation, the transformer insulation system condition can be classified into one of five categories (i.e., normal, questionable,

harmed, critical or dangerous) and the quantitative PDI can be used in transformer health index calculations.

7.2 Contributions

For PD inside transformer winding:

- I have developed online, non-destructive and easy-to-use techniques for PD detection in transformer winding insulation. For each class of transformers, developing these techniques requires constructing a knowledge base of the transformer winding signatures on various PD types and the current frequency response measurement from all possible accessible locations to the transformer neutral. Once these modules are created, they require an online leakage current measurement to determine the PD source type, location, and charge level. The availability of these PD data may assist in the detection of 21% of transformer vessel problems [10].
- I have created a PD charge calculation technique to replace conventional PD detectors, which are very hard to use in a transformer environment. To avoid underestimating transformer insulation damage, the PD charges calculated using the developed technique are the PD charges injected into the transformer winding during a PD event and not the terminal PD charges, avoiding the attenuation effect of the PD propagation path through the transformer winding.
- I have correlated the conclusions drawn from experimenting on transformer insulation components and the transformer condition using the attenuation factor concept. The PD charges measured at transformer terminals are lower than those injected into the transformer winding during a PD event. The attenuation factors calculated in this thesis for different PD sources can be used to relate PD charge terminal measurements and internal PD charges.
- Alternative to the use of the dissolved gas analysis method (which is an offline method and does not provide any details about the PD characteristics), I have developed in this thesis a winding condition assessment tool that is directly related to PD features. Moreover, instead of considering only the PD charge to evaluate insulation condition, the PD source type was also considered in this severity assessment technique. The developed severity assessment technique combines PD charge level and source type into one index, called the PDI. This index is related directly to the transformer insulation classification.

- I have provided a technique to consider PD test results explicitly in transformer health index calculations. As the PDI is in quantitative form, it can be scored and weighted for THI calculations.
- I have developed an algorithm for functional representation of the winding frequency response, providing an easier method for fault interpretation. The algorithm developed for calculating the current transfer functions from the frequency response can be used for the calculation of any other transfer function type. Moreover, the calculated transfer functions can be used for winding fault interpretation directly.

7.3 Future Work Suggestions

To build on the work presented in this thesis, suggestions for possible future work are as follow.

7.3.1 Using Other PD Features and Pattern Recognition Classifiers

The PD location and source classifiers presented in this thesis use statistical features extracted from the leakage current to train and test neural networks. Features such as waveform shape characteristics and frequency content can also be used for the training and testing of the neural networks. Other classification techniques can be used as well, such as fuzzy logic and wavelet transform. In [86, 87], a fuzzy logic system is used to categorize PD sources into four types: air voids, surface discharges, oil-coronas, and coronas. The wavelet transform is a powerful tool that allows multi-resolution signal analysis. It has been widely used in pattern recognition, signal de-noising, and image processing. In [95], the resulting insulation degradation caused by PD voids was investigated by decomposing PD acoustic waveforms using Mexican hat and Gaussian wavelets. In [96], the wavelet packet transform was used to study four types of PD: coronas in air, internal discharges in oil, floating discharges in oil, and surface discharges in air, using the Symmlet and Daubechies wavelets.

7.3.2 Simulating More PD Sources and Injecting Them Simultaneously

More PD sources, such as a floating particle, can be considered in the assessment module. To simulate the existence of multiple PD sources in a transformer insulation system, various sources can be injected simultaneously into multiple locations. Because PD sources are characterized by different features, pattern separation techniques can be used to extract different PD patterns. A variety of techniques can be employed to separate PD signals, such as using phase-resolved features, along with

neural networks or a support vector machine, Fourier transform, wavelet analysis, and time-frequency mapping [58].

7.3.3 PD Localization Using Winding Transfer Functions

A bank of transfer functions from each tap to its phase bushing can be constructed. Using this bank together with the one constructed in this thesis, PD can be localized, as in [64, 97]. For PD sources existing in the winding insulation, PD signals can be calculated and compared using the corresponding signals measured at the transformer bushing and neutral, and then used with all the corresponding transfer functions from different locations along the winding to the bushing and neutral, respectively. The PD signal occurring at a certain location should be calculated correctly from both ends. In [85], the PD is localized using a sectional winding transfer function calculated to the bushing and neutral of a disk-type transformer. The PD is simulated by a current source, and the output signal is detected from the bushing and the neutral via detection impedances. Two transfer functions are calculated at different locations along the winding, from the PD injection point to the bushing and to the neutral. By comparing the PD current calculated using these transfer functions, the PD location can be determined. In [64], a similar technique is used, but the ratio of the transfer function from the PD source to the bushing to the transfer function to the neutral is calculated. This ratio is used to train and test one hidden-layer neural network for location recognition.

7.3.4 PD and Dissolved Gas Analysis

The dissolved gas analysis (DGA) is one of the most extensively employed techniques for fault detection in power transformers. The main disadvantages of using the DGA for PD detection and severity assessment is that it is an offline method and does not provide any details about PD characteristics, such as the PD charge and source type. A comprehensive laboratory experiment exploring the relationship between different PD sources with different charge levels would be beneficial for confirming the usefulness of the DGA as an assessment tool for PD activity. Few studies have investigated the correlation between certain PD characteristics and gases generated in the oil. In [98], a canonical correlation between various PD sources and dissolved gases in oil was established. Different PD sources were simulated using transformer insulation oil and pressboard. This study, however, investigated only dissolved gases associated with pressboard and oil, not insulation paper. Also, the effect of PD intensity on the amount of dissolved gases is not clear.

7.3.5 PD Detection Module for Whole Transformer

The PD detection and assessment modules presented in this thesis are for oil-impregnated paper winding insulation. If a transformer is divided into various internal zones, similar modules can be developed for each zone. Combining the results for all transformers' zones can provide an assessment of PD activity inside the whole transformer, leading to correct maintenance-action selection and better transformer design.

7.3.6 Transformer Winding Fault Interpretation Techniques Using Transfer Functions

Winding faults are usually interpreted from the frequency response by experts in the field. Different faults have different effects on the winding structure and hence result in changes in magnitude and the shifting of poe and zero locations in the frequency response. Establishing a database of the effects of various faults on the transfer function of the winding can provide a useful fault interpretation technique. This database can be constructed by applying various faults and correlating the coefficients of before-fault and after-fault transfer functions.

Bibliography

[1] A. E. B. Abu-Elanien, M. M. A. Salama, and M. Ibrahim, "Determination of Transformer Health Condition using Artificial Neural Networks," in International Symposium on Innovations in Intelligent Systems and Applications (INISTA), Istanbul , 2011 .

[2] Z. Wang, L. Pang, T. Wang, and H. Yang, "Breakdown Characteristics of Oil-paper Insulation under Lightning Impulse Waveforms with Oscillations," IEEE Transactions on Dielectrics and Electrical Insulation, vol. 22, no. 5, pp. 2620 - 2627, 2015.

[3] S. N. Rotby, A. H. El-Hag, M. M. A. Salama, and R. Bartnikas, "Partial Discharge Detection and Localization inside the Winding of Power Transformer," in Annual Report Conference on Electrical Insulation and Dielectric Phenomena (CEIDP), Montreal, QC, 2012.

[4] F. H. Kreuger, Partial Discharge Detection in High-Voltage Equipment, London, UK: Butterworth, 1989.

[5] A. Bossi, J. E. Dind, J. M. Frisson, U. Khoudiakov, and H. F. Light, "An International Survey of Failures in Large Power Transformers in Service," Final Report of the CIGRE Working Group, Electra, vol. 88, pp. 21-48, 1983.

[6] N. H. Ahmed and N. N. Srinivа, "On-Line Partial Discharge Detection in Transformer," in Conference Record of the IEEE International Symposium on Electrical Insulation, Arlington, Virginia, USA, 1998.

[7] J. L.Roldan, T. Tang, and M. Gaskin, "Design and Testing of UHF Sensors for Partial Discharge Detection in Transformers," in International Conference on Condition Monitoring and Diagnosis, Beijing, China, 2008.

[8] A. Naderian, S. Cress, R. Piercy, F. Wang, and J. Service, "An Approach to Determine the Health Index of Power Transformers," in Conference Record of the IEEE International Symposium on Electrical Insulation,, Vancouver, BC, 2008.

[9] Y. Z. Y. Ghazali, M. A. Talib, and H. A. Rosli, "TNB Experience in Condition Assessment and Life Management of Distribution Power Transformers," in International Conference and Exhibition on Electricity Distribution (CIRED), Prague, 2009.

[10] S. M. Strachan, S. Rudd, S. D. J. McArthur, M. D. Judd, S. Meijer, and E. Gulski, "Knowledge-

Based Diagnosis of Partial Discharges in Power Transformers," IEEE Transactions on Dielectrics and Electrical Insulation, vol. 15, no. 1, pp. 259-268, 2008.

[11] N. Izeki, A. Kurahashi, and K. Matsuura, "Behavior of Oil Corona and Damage of Transformer," IEEE Transactions on Power Apparatus and Systems, vol. 90, no. 5, pp. 2330 - 2338, 1971.

[12] A. Rodrigo, P. Llovera, V. Fuster, and A. Quijano, "Influence of High Frequency Current Transformers Bandwidth on Charge Evaluation in Partial Discharge Measurements," IEEE Transactions on Dielectrics and Electrical Insulation, vol. 18, no. 5, pp. 1798-1802, 2011.

[13] S. Venkatesan, B. G. Stewart, M. D. Judd, A. J. Reid, and R. A. Fouracre, "Analysis of PD in Voids Using Correlation Plots of RF Radiated Energy and Apparent Charge," in IEEE International Conference on Solid Dielectrics, Inchester, UK, 2007.

[14] S. Okabe, G. Ueta, H. Wada, and H. Okubo, "Partial Discharge-Induced Degradation Characteristics of Insulating Structure Constituting Oil-Immersed Power Transformers," IEEE Transactions on Dielectrics and Electrical Insulation, vol. 17, no. 5, pp. 1649 - 1656, 2010.

[15] IEEE Guide for Failure Investigation, Documentation, Analysis, and Reporting for Power Transformers and Shunt Reactors.

[16] A. Franzén and S. Karlsson, "Failure Modes and Effects Analysis of Transformers," Royal Institute of Technology, KTH, Stockholm, Sweden, 2007.

[17] M. Wang, A. J. Vandermaar, and K. D. Srivastava, "Review of Condition Assessment of Power Transformers in Service," IEEE Electrical Insulation Magazine, vol. 18, no. 6, pp. 12-25, 2002.

[18] P.A. Venikar, M. S. Ballal, B.S. Umre, and H.M. Suryawanshi, "Condition Assessment of Transformer by Park's Vector and Symmetrical Components to detect Inter Turn Fault," in IEEE International Conference on Condition Assessment Techniques in Electrical Systems (CATCON), Kolkata, 2013.

[19] Z. Husain, H. Malik, and M. A. Khan, "Recent Trends in Power Transformer Fault Diagnosis and Condition Assesment," Bulletin of Electrical Engineering and Informatics, vol. 2, no. 2, pp. 95-104, 2013.

[20] A. E. B. Abu Elanien, Transformer Health Index Assesment and Techno-Economic End of Life Evaulaution, PH.D. Thesis, University of Waterloo, Ontario, Canada, 2011.

[21] D. Arvind, S. Khushdeep , and K. Deepak, "Condition Monitoring of Power Transformer: A Review," in IEEE/PES Transmission and Distribution Conference and Exposition, Chicago,

Illinios, 2008.

[22] M. Duval, "Dissolved Gas Analysis and the Duval Triangle," in AVO New Zealand Conference, 2006.

[23] C. Guo-wei, P. Chao, W. Yan-tao, and Y. De-you, "A New Method Based on Fuzzy TOPSIS for Transformer Dissolved Gas Analysis," in International Conference on Sustainable Power Generation and Supply, Nanjing, China, 2009.

[24] T. K. Saha, "Review of Modern Diagnostic Techniques for Assessing Insulation Condition in Aged Transformers," IEEE Transaction on Dielectric and Electric Insulation, vol. 10, no. 5, pp. 903-917, 2003.

[25] A. M. Emsely and G. C. Stevens, "Review of Chemical Indicators of Degradation of Cellulosic Electrical Paper Insulation in Oil-Filled Transformers," Science, Measurement and Technology, vol. 141, no. 5, pp. 324 - 334, 1994.

[26] M. Ali, C. D. Eley, A. M. Emsley, R. J. Heywood, and X. Xaio, "Measuring and Understanding the Ageing of Kraft Insulating Paper in Power Transformers," vol. 12, no. 3, pp. 28 - 34, 1996.

[27] P.J. Baird, H. Herman, and G. C. Stevens, "Non-Destructive Measurement of the Degradation of Transformer Insulating Paper," IEEE Transactions on Dielectrics and Electrical Insulation, vol. 13, no. 1, pp. 309-318, 2006.

[28] L. Cheim, D. Platts, T. Prevos, and S. Xu, "Furan Analysis for Liquid PowerTransformers," IEEE Electrical Insulation Magazine, vol. 28, no. 2, pp. 8 - 21, 2012.

[29] A. D. Pablo, "Furfural and Ageing: HowAre They Related," in IEE Colloquium on Insulation Liquid, 1999.

[30] A. De Pablo and B. Pahlayanpoul, "Furanic Compounds Analysis: A Tool for Predictive Maintenance of Oil-Filled Electrical Equipment," Electra, vol. 174, pp. 9-18, 1997.

[31] B. D. Malpure and K. Baburao, "Failure Analysis and Diagnostics of Power Transformer using Dielectric Dissipation Factor," in International Conference on Condition Monitoring and Diagnosis, Beijing, China, 2008.

[32] B. García, J. C. Burgos,A. M. Alonso , and J. Sanz, "A Moisture-in-Oil Model for Power transformer Monitoring - Part I: Theoretical Foundation," IEEE Transaction on Power Delivery, vol. 20, no. 2, pp. 1417 - 1422, 2005.

[33] A. B. A. Ghani, Z. A. A. Zarim , J. A. Majeed, and H. Osman, "Diagnostic Criteria Based on the

Correlation of the Measurement of DGA, Moisture Contents with PD & tan δ in MV Oil-Filled Underground Cable," in IEEE International Conference on Dielectric Liquids, Trondheim, Norway, 2011.

[34] B. Pahlavanpour, "Transformer Oil Condition Monitoring," in IEE Colloquium on Transformer Life Management, London, UK, 1998.

[35] I. s. 60270, "High-Voltage Test Techniques- Partial Discharge Measurements," International Electrotechnical Commission, 2000.

[36] H. Ma, J. Seo, T. Saha, J. Chan, and D. Martin, "Partial Discharge Sources Classification of Power Transformer Using Pattern Recognition Techniques," in Annual Report Conference on Electrical Insulation and Dielectric Phenomena, Shenzhen, China, 2013.

[37] G. J. Paoletti and A. Golubev, "Partial Discharge Theory and Technologies Related to Medium-Voltage Electrical Equipment," IEEE Transactions on Industry Applications, vol. 37, no. 1, pp. 90-103, 2001.

[38] E. Kuffel, W. S. Zaengl, and J. Kuffel, High Voltage Engineering Fundamentals, United Kingdom: Butterworth-Heinemann, 2000.

[39] R. J. V. Brunt and M. Misakian, "Mechanisms for Inception of DC and 60-Hz AC Corona in SF6," IEEE Transactions on Electrical Insulation, vol. 17, no. 2, pp. 106-120, 1982.

[40] A. K. Lazarevich, "Partial Discharge Detection and Localization in High Voltage Transformer Using an Optical Acoustic Sensor," Master's Thesis of Science, Virginia Polytechnic Institute and State University, Virginia, 2003.

[41] G. Luo and D. H. Zhang, "Study on Performance of Developed and Industrial HFCT Sensors," in Australasian Universities Power Engineering Conference, Christchurch, New Zealan, 2010.

[42] S. Birlasekaran and W. H. Leong, "Comparison of Known PD Signals With the Developed and Commercial HFCT Sensors," IEEE Transaction on Power Delivery, vol. 22, no. 3, pp. 1581 - 1590, 2007.

[43] Z.Tang, C. Li, X. Cheng, W. Wang, and J. Li, "Partial Discharge Location in Power Transformers Using Wideband RF Detection," IEEE Transactions on Dielectrics and Electrical Insulation, vol. 13, no. 6, pp. 1193-1199, 2006.

[44] L. E. Lundgaard, "Partial Discharge - Part XIII: Acoustic Partial Discharge Detection - Fundamental Considerations," IEEE Electrical Insulation Magazine, vol. 8, no. 4, pp. 25 - 31,

1992.

[45] S. M. Markalous, S. Tenbohlen, and K. Feser, "Detection and Location of Partial Discharges in PowerTransformers Using Acoustic and Electromagnetic Signals," IEEE Transactions on Dielectrics and Electrical Insulation, vol. 15, no. 6, pp. 1576 - 1583, 2008.

[46] J. Fuhr, "Benefits and Limits of Advanced Methods Used for Transformer Diagnostics," in IEEE Electrical Insulation Conference, Montreal, Quebec, Canada, 2009.

[47] H. Malik, A. Azeem, and R. K. Jarial, "Application Research Based on Modern Technology for Transformer Health Index Estimation," in International Multi-Conference on Systems, Signals and Devices, Chemnitz, 2012.

[48] A. E. B. Abu-Elanien, M. M. A. Salama, and M. Ibrahim, "Calculation of a Health Index for Oil-Immersed Transformers Rated Under 69 kV Using Fuzzy Logic," IEEE Transactions on Power Delivery, vol. 27, no. 4, pp. 2029 - 2036, 2012.

[49] A. E. B. Abu-Elanien and M. M. A. Salama, "Survey on the Transformer Condition Monitoring," in Large Engineering Systems Conference on Power Engineering, Montreal, Quebec, 2007.

[50] Z. Zheng, Y. Yang, C. Li, S. Liu, and J. Ma, "Characteristics of Partial Discharge during its Evolution in Transformer Winding," in Conference Record of the 2010 IEEE International Symposium on Electrical Insulation , San Diego, CA, 2010.

[51] G. C. Stone, "Partial Discharge Diagnostics and Electrical Equipment Insulation Condition Assessment," IEEE Transactions on Dielectrics and Electrical Insulation, vol. 12, no. 5, pp. 891-904, 2005.

[52] A. Cavallini, G. C. Montanari, and M.Tozzi, "PD Apparent Charge Estimation and Calibration: A Critical Review," IEEE Transactions on Dielectrics and Electrical Insulation, vol. 17, no. 1, pp. 198-205, 2010.

[53] X. Zhang , J. Tang , and Y. Xie, "Investigation of the relationship between PD measured with RF techniques and apparent charge quantity of metal protrusion in air," in International Conference on High Voltage Engineering and Application (ICHVE), New Orleans, Louisiana, 2010.

[54] Q. Shaozhen and S. Birlasekaran, "The Study of Propagation Characteristics of Partial Discharge in Transformer," in Annual Report Conference on Electrical Insulation and Dielectric Phenomena, 2002.

[55] A. Rodrigo, P. Llovera, V. Fuster, and A. Quijano, "Study of Partial Discharge Charge

Evaluation and the Associated Uncertainty by Means of High Frequency Current Transformers," IEEE Transactions on Dielectrics and Electrical Insulation, vol. 19, no. 2, pp. 434-442, 2012.

[56] M. S. Abd Rahman, "Identification of Partial Discharge Sources and Their Locations withing High Volatge Transfomer Windings," Thesis for the degree of Doctor of Philosophy, University of Southhampton, Southampton, UK, 2014.

[57] M. Florkowski and B. Florkowska, "Wavelet-Based Partial Discharge Image Denoising," IET Generation, Transmission & Distribution, vol. 1, no. 2, pp. 340-347, March 2007.

[58] J. C. Chan, H. Ma, and T. K. Saha, "Time-frequency Sparsity Map on Automatic Partial Discharge Sources Separation for Power Transformer Condition Assessment," IEEE Transactions on Dielectrics and Electrical Insulation, vol. 22, no. 4, pp. 2271-2283, 2015.

[59] E. Gulski and F. H. Kreuger, "Computer-Aided Recognition of Discharge Sources," IEEE Transactions on Electrical Insulation, vol. 27, no. 1, pp. 82 - 92, 1992.

[60] N. Pattanadech and P. Nimsanong, "Partial Discharge Classification Using Learning Vector Quantization Network Model," in IEEE Region 10 Conference TENCON, Bangkok, Thailand, 2014.

[61] P. H. Chen, H. C. Chen, and L. M. Chen, "Pattern Recognition for Partial Discharge Diagnosis of Power Transformer," in International Conference on Machine Learning and Cybernetics, Qingdao, 2010.

[62] X. Jin and L. Jiang, "Partial Discharge Pattern Recognition of Power Transformer with Neural Network Applications," in IEEE Annual Report Conference on Electrical Insulation and Dielectric Phenomena, Austin, Texas, 1999.

[63] F. O. Karray and C. W. De Silva, Soft Computing and Intelligent Systems Design Theory, Tools and Applications, Pearson/Addison Wesley, 2004.

[64] P. Werle, A. Akbari, H. Bors, and E. Gockenbach, "Partial Discharge Localization in Power Transformers Using Neural Networks Combined with Sectional Winding Transfer Function as Knowledge Base," in Proceedings of International Symposium on Electrical Insulating Materials , Himeji, Japan, 2001.

[65] M. Heindl, S. Tenbohlen, A. Kraetge, M. Krüger, and J. L. Velásquez, "Algorithmic Determination of Pole-Zero Representations of Power Transformers' Transfer Functions for Interpretation of FRA Data," in International Symposium on High Voltage Engineering, Innes

House, Johannesburg, South Africa, 2009.

[66] M. F. M. Yousof, T. K. Saha, and C. Ekanayake, "Investigating the Sensitivity of Frequency Response Analysis on Transformer Winding Structure," in IEEE PES General Meeting Conference & Exposition, National Harbor, Maryland, 2014.

[67] M. F. M. Yousof, C. Ekanayake, T.K. Saha, and H. Ma, "A Study on Suitability of Different Transformer Winding Models for Frequency Response Analysis," in IEEE Power and Energy Society General Meeting, San Diego, California, 2012.

[68] G. B. Gharehpetian, H. Mohseni, and K. Moller, "Hybrid Modelling of Inhomogeneous Transformer Winding for Very Fast Transient Overvoltage Studies," IEEE Transactions on Power Delivery, vol. 13, no. 1, pp. 157 - 163, 1998.

[69] D. A. K. Pham, T. M. T. Pham, V. N. C. Ho, and E. Gockenbach, "Duality-Based Lumped Transformer Equivalent Circuit At Low Frequencies Under Single-Phase Excitation," in International Conference on High Voltage Engineering and Application, Shanghai, China, 2012.

[70] H. Tavakoli, D. Bormann, and G. Engdahl, "Localization of Mechanical Deformations In Transformer Windings Using Time-Domain Representation of Response Functions," International Transactions on Electrical Energy Systems, vol. 24, no. 1, pp. 16-29, 2012.

[71] M. Bagheri, B. T. Phung, and T. Blackburn, "Transformer Frequency Response Analysis: Mathematical and Practical Approach to Interpret Mid-frequency Oscillations," IEEE Transactions on Dielectrics and Electrical Insulation, vol. 20, no. 6, pp. 1962-1970, 2013.

[72] P. Werelius, M. Öhlen, L. Adeen, and E. Brynjebo, "Measurement Considerations using SFRA for Condition Assessment of Power Transformers," in International Conference on Condition Monitoring and Diagnosis, Beijing, China, 2008.

[73] E. AlMurawwi, R. Mardiana, and Q. Su, "Effect of Terminal Connections on SFRA Results of Three-Winding Power Transformers," in International Conference on Electric Power and Energy Conversion Systems (EPECS), Sharjah, UAE, 2011.

[74] S. Tenbohlen and S. A. Ryder, "Making Frequency Response Analysis Measurements: A Comparison of the Swept Frequency and low Voltage Impulse Methods," in International Symposium on High Volatge Engineering, Rotterdam, The Netherlands, 2003.

[75] M. Shaohua and R. He, "Method for Detecting System on PowerTransformer Winding Deformation," in International Conference on Electrical Machines and Systems, Tokyo, Japan,

2009.

[76] M. F. M. Yousof, "Frequency Response Analysis for Transformer Winding Condition Monitoring," Ph.D. Thesis, The University of Queensland, Brisbane, Australia, 2015.

[77] A. Abu-Siada, N. Hashemnia, S. Islam, and M. A. S. Masoum, "Understanding Power Transformer Frequency Response Analysis Signatures," IEEE Electrical Insulation Magazine, vol. 29, no. 3, pp. 48 - 56, 2013.

[78] S. D. Mitchell and J. S. Welsh, "Modeling Power Transfomers to Support the Interpretation of Frequency-Response Analysis," IEEE Transactions on Power Delivery, vol. 26, no. 4, pp. 2705-2717, 2011.

[79] G. M. Kennedy, A. J. McGrail, and J. A. Lapworth, "Using Cross-Correlation Coefficients to Analyze Transformer Sweep Frequency Response Analysis (SFRA) Traces," in IEEE Power Engineering Society Conference and Exposition in Africa, Johannesburg, South Africa , 2007.

[80] B. Gustavsen and A. Semlyen, "Rational Approximation of Frequency Domain Responses by Vector Fitting," IEEE Transactions on Power Delivery, vol. 14, no. 3, pp. 1052-1061, 1999.

[81] L. Yunpeng, L. Fangcheng, and L. Chengrong, "The Transfer Characteristic of Partial Discharge Propagation Along Power Transformer WindingBased on Vector Fitting," in IEEE International Conference on Electric Utility Deregulation, Restructuring and Power Technologies, 2004.

[82] D. Zheng, D. Zhao, L. Zhang, and X. Chen, "Research on PD Locating Method of Dry-Type Transformer with Subsection and Layer Windings Based on Transfer Functions," in IEEE International Conference on the Properties and Applications of Dielectric Materials, Harbin, China, 2009.

[83] M. A. Eldery, E. F. El-Saadany, and M. M. A. Salama, "Parameters Identification of Sectional Winding High Frequency Trransfornmer Model Using Neural Network," in IEEE Midwest Symposium on Circuits and Systems, Cairo, Egypt, 2003.

[84] A. Akbari, P. Werle, H. Borsi, and E. Gockenbach, "Transfer Function Based Partial Discharge Localization in Power Transformer: A Feasibility Study," IEEE Electrical Insulation Magazine, vol. 18, no. 5, pp. 22 - 32, September- October 2002.

[85] A. M. Jafari, A. Akbaril ,and M. Kharezi, "Partial Discharge Localization in Transformers Using Detailed Modeling," in International Conference on Solid Dielectrics, Winchester, UK, July 2007.

[86] S. Gopal, B. Karthikeyan, and D. Kavith, "Partial Discharge Pattern Classification using Fuzzy Expert System," in Proceedings of IEEE International Conference on Solid Dielectric, Toulouse, France, 2004.

[87] A. Cavallini, M. Conti, A. Contin, and G.C.Montanari, "Inferring Partial Discharge Identification Through Fuzzy Tools," in Annual Report Conference on Electrical Insulation and Dielectric Phenomena, 2002.

[88] M. M. A. Salama and R.Bartnikas, "Fuzzy Logic Applied to PD Pattern Classification," IEEE Transactions on Dielectrics and Electrical Insulation, vol. 7, no. 1, pp. 118-123, 2000.

[89] A. Vladimirov, E. R. Kyrtselin, G. T. Velev, and V. Cozma, "Condition Assessment of Power Transformers Through Monitoring of Partial Discharges and Gasses Dissolved in Insulating Oil," Annals of the Constantin Brancusi University of Targu Jiu, Engineering Series, no. 3, pp. 44-49, 2013.

[90] V. Jeyabalan and S. Usa, "Frequency Domain Correlation Technique for PD Location in Transformer Winding," IEEE Transactions on Dielectrics and Electrical Insulation, vol. 16, no. 4, pp. 1160-1167, 2009.

[91] N. C. Sahoo, M. M. A. Salama, and R. Bartnikas, "Trends in Partial Discharge Pattern Classification: A Survey," IEEE Transactions on Dielectrics and Electrical Insulation, vol. 12, no. 2, p. 248–264, 2005.

[92] S. N. Hettiwatte, P. A. Crossley, Z. D. Wang, A. Darwin, and G. Edwards, "Simulation of a Transformer Winding for Partial Discharge Propagation Studies," in IEEE Power Engineering Society Winter Meeting, 2002.

[93] MATLAB, "MAthWorks," http://www.mathworks.com/help/rf/rationalfit.html. [Online].

[94] J. Fuhr, "Procedure for Identification and Localization of Dangerous PD Sources in Power Transformers," IEEE Transactions on Dielectrics and Electrical Insulation, vol. 12, no. 5, pp. 1005-1014, 2005.

[95] M. Masanori, T. Okano, S. Nishimoto, I. Kitani, and K. Ani, "Study on Application of Wavelet Analysis for Degradation Diagnosis of Partial Discharge in A Void," in IEEE International Conference on Conduction and Breakdown in Solid Dielectrics, Leicester, UK, 1995.

[96] L. Zhao and Y. Son, "Noise Elimination in Partial Discharge On-line Monitoring for Transformer Based on Wavelet Transform," in International Conference on E-Product E-Service

and E-Entertainment , Henan, China, 2010.

[97] P. Werle, Gockenbach,and H. Borsi, "Partial Discharge Measurements on Power Transformers using Transfer Function for Detection and Localisation," in Proceedings of the 7th International Conference on Properties and Applications of Dielectric Materials, Nagoya, 2003.

[98] W. Chen , X. Chen, S. Peng, and J. Li, "Canonical Correlation Between Partial Discharges and Gas Formation in Transformer Oil Paper Insulation," Energies, vol. 5, no. 4, pp. 1081-1097, 2012.